THE EFFECT OF BIOFILM FORMATION ON THE SETTLING VELOCITY OF MICROPLASTICS IN FRESHWATER AND SEAWATER

A THESIS SUBMITTED TO
THE GRADUATE SCHOOL OF NATURAL AND APPLIED SCIENCES
OF
MIDDLE EAST TECHNICAL UNIVERSITY

BY

BAHAR EVREN

IN PARTIAL FULFILLMENT OF THE REQUIREMENTS
FOR
THE DEGREE OF MASTER OF SCIENCE
IN
ENVIRONMENTAL ENGINEERING

JANUARY 2022

Approval of the thesis:

THE EFFECT OF BIOFILM FORMATION ON THE SETTLING VELOCITY OF MICROPLASTICS IN FRESHWATER AND SEAWATER

submitted by **BAHAR EVREN** in partial fulfilment of the requirements for the degree of **Master of Science in Environmental Engineering, Middle East Technical University** by,

Prof. Dr. Halil Kalıpçılar

Dean, Graduate School of **Natural and Applied Sciences**

Prof. Dr. Bülent İçgen

Head of the Department, **Environmental Engineering**

Assist. Prof. Dr. Zöhre Kurt

Supervisor, **Environmental Engineering, METU**

Examining Committee Members:

Prof. Dr. F. Dilek Sanin

Environmental Engineering, METU

Assist. Prof. Dr. Zöhre Kurt

Environmental Engineering, METU

Prof. Dr. Ayşegül Aksoy

Environmental Engineering, METU

Assist. Prof. Dr. Hale Demirtepe

Environmental Engineering, Izmir Institute of Technology

Assist. Prof. Dr. Cüneyt Baykal

Civil Engineering, METU

Date: 27.01.2022

I hereby declare that all information in this document has been obtained and presented in accordance with academic rules and ethical conduct. I also declare that, as required by these rules and conduct, I have fully cited and referenced all material and results that are not original to this work.

Name, Last name: Bahar Evren

Signature:

ABSTRACT

THE EFFECT OF BIOFILM FORMATION ON THE SETTLING VELOCITY OF MICROPLASTICS IN FRESHWATER AND SEAWATER

Evren, Bahar
Master of Science, Environmental Engineering
Supervisor: Assist. Prof. Dr. Zöhre Kurt

January 2022, 110 pages

Microplastics (MPs) are plastic pieces smaller than 5 mm. They find their way into freshwater, sea, or wastewater treatment plants during their life cycle, and eventually, they have adverse impacts on ecosystems. Since they have a high surface area/volume ratio and are a good carbon source, they provide a suitable attachment surface for microorganisms. As a result, biofilm formation appears on the surface of microplastics. This formation increases the weight and volume of the microplastics. For this reason, their settling velocity in the water columns, and therefore their transport behaviour in the vertical direction in water bodies, changes. In this study, biofilm formation by *Escherichia coli*, *Enterococcus faecalis,* and *Pseudomonas aeruginosa* cultures on common MPs, polystyrene (PS), polypropylene (PP), thermoplastic polyurethane (TPU), polyethylene terephthalate (PET), polyethylene (PE), high-density polyethylene (HDPE), low-density polyethylene (LDPE), and its effects on the settling velocity of the MPs in freshwater and seawater are investigated. The settling velocity measurements were carried out by using MATLAB Image Processing Algorithm. Thus far, this is the very first study measuring settling velocities of biologically weathered MPs using image processing algorithm. Initially buoyant MPs did not settle down after biofilm formation in contrast to the hypotheses in the literature. Yet, settling velocity of initially settling MPs changed after biofilm formation, Colonization of *E. coli* on PS surface increased its settling velocity by 8.2%, *E. faecalis* on PS by 10.1% and *E. faecalis* on TPU by 5.6% in freshwater whereas P. aeruginosa colonization lowered PS by 12%, TPU by 1% and PET by 22%. In seawater, biofilm formation by all bacteria species enhanced the settling velocities of TPU particles but slowed down PS and PET particles.

Keywords: Microplastics, settling velocity, biofilm, image processing

ÖZ

BİYOFİLM OLUŞUMUNUN MİKROPLASTİKLERİN TATLI SU VE DENİZ SUYUNDAKİ ÇÖKME HIZINA ETKİSİ

Evren, Bahar
Yüksek Lisans, Çevre Mühendisliği
Tez Yöneticisi: Dr. Ögr. Üyesi Zöhre Kurt

Ocak 2022, 110 sayfa

Mikroplastikler (MP'ler), 5 mm'den küçük plastik parçalardır. Yaşam döngüleri boyunca tatlı su, deniz veya atık su arıtma tesislerine girerler ve sonunda ekosistemler üzerinde olumsuz etkileri olur. Yüksek yüzey alanı/hacim oranına sahip oldukları ve iyi bir karbon kaynağı oldukları için mikroorganizmalar için uygun tutunma yüzeyi sağlarlar. Sonuç olarak, MPlerin yüzeyinde biyofilm oluşumu görülür. Bu oluşum MPlerin ağırlığını ve hacmini arttırır. Bu nedenle su kolonlarında çökme hızları ve buna bağlı olarak su kütlelerinde düşey doğrultuda taşınma davranışları değişmektedir. Bu çalışmada, ortak MP'ler, polistiren (PS), polipropilen (PP), termoplastik poliüretan (TPU), polietilen tereftalat (PET), polietilen (PE), yüksek yoğunluklu polietilen (HDPE), düşük yoğunluklu polietilen (LDPE) üzerinde *Escherichia coli, Enterococcus faecalis* ve *Pseudomonas aeruginosa* kültürleri tarafından biyofilm oluşumu ve bu oluşumun MPlerin tatlı su ve deniz suyundaki çökme hızları üzerindeki etkileri araştırılmıştır. Çökme hızı ölçümleri MATLAB Görüntü İşleme Algoritması kullanılarak gerçekleştirilmiştir. Şimdiye kadar, bu çalışma, görüntü işleme algoritmasını kullanarak biyolojik olarak yıpranmış MPlerinin yerleşme hızlarını ölçen ilk çalışmadır. Literatürdeki hipotezlerin aksine, başlangıçta çökmeyen MPler biyofilm oluşumundan sonra da çökmemiştir. Bununla birlikte, biyofilm oluşumundan sonra başlangıçta çöken MPlerin çökme hızı değişmiştir, *E. coli*'nin PS yüzeyinde kolonizasyonu çökme hızını %8,2, *E. faecalis*'in PS üzerinde kolonizasyonu %10,1 ve *E. faecalis*'in TPU üzerinde kolonizasyonu tatlı sudaki hızlarını %5.6 artırmıştır ancak *P. aeruginosa* kolonizasyonu PS çökme hızını %12, TPUyu %1 ve PET'i %22 düşürmüştür. Deniz suyunda, tüm bakteri türleri tarafından biyofilm oluşumu, TPU parçacıklarının çökme hızlarını artırmış, ancak PS ve PET parçacıklarını yavaşlatmıştır.

Anahtar Kelimeler: Mikroplastik, çökme hızı, biyofilm, görüntü işleme

To my beloved family

ACKNOWLEDGMENTS

I would like to thank my supervisor Assist. Prof. Dr. Zöhre Kurt for standing open to new ideas. I would like to express my gratitude to Assist. Prof. Dr. Cüneyt Baykal, Dr. Gökhan Güler and Koray Deniz Göral for their unconditional guidance, experience share and help in image tracking studies.

I would like to present thanks to METU Molecular Microbiology Laboratory for providing pure cultures of the bacteria species used in this study.

I would like to present my gratitude to Supervising Committee Members for their participation and valuable contribution.

I would like to thank to my family in the lab, Rayaan Harb, Ertan Hoşafçı, Irmak Subaşı and Aslı Onursal for sharing their valuable laboratory experiences and brainstorming with me whenever I needed guidance.

I am also thankful to my one and only comrade, Mert Erkanlı, for his wisdom and always standing by me no matter what the situation is. I am very grateful to my sweetheart, Cansu Polat for her superior support and help at all times; without her existence, I would certainly falter. They have been more than a friend along the whole way.

I would also like to present my thanks to my dear roommates, Tercan Çataklı and Naz Zeynep Şimşek who always kept the home-like atmosphere in the best office ever.

I would like to express my special thanks to my family, my mother, Çiğdem Evren my father, Sabri Mehmet Evren, my brother, Oktay Meriç Evren and Ali Orhon who were always there in my whole education life, who supported me in all conditions and kept believing in me all the time.

Last but not least, I am heartedly thankful to my dear partner Batuhan Şahin for his endless encouragement and compassion, and to our fluffy friends, Duomo, Kivi and Mercan for comforting me whenever I felt overwhelmed.

TABLE OF CONTENTS

LIST OF TABLES

TABLES

LIST OF FIGURES

FIGURES

LIST OF ABBREVIATIONS

ABS: acrylonitrile butadiene styrene

AnMBR: anaerobic membrane bioreactor

BOD: biochemical oxygen demand

BOD_7: biochemical oxygen demand within 7 days

CAS: conventional activated sludge

CFU: colony-forming unit

COD: chemical oxygen demand

DOC: dissolved organic carbon

EPDM: ethylene propylene diene monomer

EPS: extracellular polymeric substances

Fps: frames per second

FPA: focal plane array

FTIR: fourier-transform infrared spectroscopy

HD: high definition

HDPE: high-density polyethylene

HOC: hydrocarboxyl

LB: Luria Broth

LED: light emitting diode

LDPE: low-density polyethylene

LSCM: laser scanning confocal microscopy

MBR: membrane bioreactor

MP: microplastics

N_R: Reynold’s number

PA: polyamide

PAC: powdered activated carbon

PAH: polycyclic aromatic hydrocarbon

PBAT: polybutylene adipate terephthalate

PBS: phosphate buffer saline

PCB: polychlorinated biphenyl

PCL: polycaprolactone

PDBE: polybrominated diphenyl ether

PE: polyethylene

PET: polyethylene terephthalate

PEVA: poly (ethylene-vinyl acetate)

PLA: polylactic acid

POP: persistent organic pollutant

PP: polypropylene

PS: polystyrene

PTFE: Polytetrafluoroethylene

PVC: polyvinyl chloride

Re: Reynold’s number

SAN: styrene-acrylonitrile resin

SBB: starch-based bioplastic

SEM: scanning electron microscopy

SS: suspended solids

TPU: thermoplastic polyurethane

OD_{600}: optical density measured at a wavelength of 600 nm

WWTP: wastewater treatment plant

UV: ultraviolet

VAC: vinyl acrylic copolymer

VSS: volatile suspended solids

WW: wastewater

WWTP: wastewater treatment plant

WwTW: wastewater treatment works

CHAPTER 1

INTRODUCTION

Microplastics (MPs) are defined as plastic materials that are smaller than 5 mm in size (Barnes et al., 2009; Duis & Coors, 2016; Peng et al., 2018). It is also possible to classify MPs as large and small according to their particle size. MP particles between 1-5 mm are large MPs , while small MPs size range is defined as 20 μm-1mm. MPs are composed of PP, PET, PE, PS, PVC, PA, nylon, HDPE, LDPE, PES, PEVA, PTFE , ABS, expanded PS, EPDM (Fauziah et al., 2018).

Primary MPs are plastics manufactured by the industry as microbeads, and initially, their size is in the range of pollutant MPs (Andrady, 2017). They are present in personal care products as exfoliants and abrasives. They can also be used as industrial abrasive materials, drilling fluids (oil and gas exploration) (Duis & Coors, 2016), virgin plastics pellets (Andrady, 2017). Any leakage of pellets during manufacturing, transportation, or use results in MPs pollution (Andrady, 2017). A model developed by International Union for Conservation of Nature and Natural Resources suggests a portion of 15-31% plastics in oceans are due to primary sources with an annual release of 1.5 million tons. In other words, 212 grams per capita per week account for the world equivalent. Primary MPs are known to reach water bodies primarily by road run off 66%, wastewater treatment plants (WWTPs) 25%, and wind transfer 7% (Boucher and Friot, 2017).

On the other hand, secondary MPs result from the fragmentation of large plastic debris due to degradation by solar UV radiation, physical forces, and microorganisms (Peng et al., 2018). The result of such interactions is the formation of MPs from larger plastic particles. Fibres from clothing materials and cleaning products, car tires, plastic waste dumping, and discarded or lost materials from fishing vessels are the primary sources of secondary MPs pollution (Duis and Coors, 2016).

A significant increase in concentrations of MPs in marine environment have been detected in the last four decades (UNEP, 2016). MPs are found in high concentrations close to the areas where they have been produced, likewise, they are populated highly in central places (UNEP, 2016.They have been detected in atmospheric fallout in Paris, urban dust in Tehran metropolis, atmospheric dry & wet deposition in Pyrenees mountains, urban snow in Helsinki, supraglacial debris in Italian Alps, suspended in atmosphere in open ocean West Pacific, wet deposition in Arctic snow (Y. Zhang et al., 2020). Analysis of sediment cores from an estuary in Tasmania, in an urban lake in London, in Dongting Lake in China and in deep sea sediments in Atlantic Ocean, Mediterranean Sea and Indian Ocean have revealed the abundance of MPs in the sediments (Willis et al., 2017; Turner et al., 2019; Jiang et al., 2018; Woodall et al., 2020). According to the identification of plastic type in 79 samples, PE, PP and PS are the most possible MP particles to encounter in marine and sea samples (Hidalgo-Ruz et al., 2012).

Although the scientific world has begun to orient attention towards this emerging pollutant, the studies mainly focus on MP detection in environmental compartments and its effects on the ecosystem. The research on MPs' transport mechanisms, especially those that have gone under weathering processes, is limited. For the modelling of microplastic transport in water column, their settling velocity parametrization is a gap to be filled in current literature (Khatmullina and Isachenko, 2017). Likewise, lack of knowledge in the area of biofilm formation, a weathering process, on microplastic particles and its effects on fate of MPs have been addressed in the literature so far (Tu et al., 2020; Waldschläger et al., 2020; Waldschläger & Schüttrumpf, 2019; Miao et al., 2019).

Objectives of the study are given as,

- ❖ Estimation of time dependent biofilm formation on different MPs,
- ❖ Estimation of biofilm formation amount on different MPs by pure cultures of 3 different bacteria species *Escherichia* coli, *Enterococcus Faecalis* and *Pseudomonas aeruginosa,*
- ❖ Implementation of a MATLAB based image tracking algorithm for detecting settling velocities of MPs in vertical column,
- ❖ Estimation of effect of biofilm formation on the settling behavior of MPs in vertical direction in freshwater and seawater.

The outline of the thesis is presented below.

- Chapter 1 commences as an introductory section including problem statement, objective of the study and the methods used.
- Chapter 2 is composed of literature review, where problems arising from MP accumulation in ecosystem, transport mechanisms as a link between MP sources to sinks, transformation mechanisms affecting MPs nature, occurrences of MPs both in environment and WWTPs are reviewed as well as research done on settling velocity and biofilm formation of MPs.
- Chapter 3 reveals the materials used and methodology implemented. Biofilm formation assays and settling velocity measurement protocol are given. Experiments conducted in METU Environmental Engineering laboratories as well as METU Central Laboratory are explained in detail.
- Chapter 4 presents the results and discusses upon the findings with the information available in the literature.
- Chapter 5 summarizes the outcomes of the thesis and serve recommendations based on the knowledge gained by this particular study and literature research.

CHAPTER 2

LITERATURE REVIEW

2.1 Ecologic Impact of Microplastics

The abundance of MPs in the environment is a concern due to its ingestion by aquatic organisms, accumulation within the food chain, and hence reaching humans (Cole et al., 2015). MPs can accumulate in living organisms (Jiang et al., 2018). MPs within 32–63 µm size range were found ingested by amphipods (Straub et al., 2017).PE litters within 10–27 µm size range, PP fibers of 20–75 µm length, and particles with a diameter of 20 µm were ingested by freshwater amphipod *Hyalella azteca* (Au et al., 2015). MPs were proven to lower growth kinetics of *Nephrops norvegicus* (Welden and Cowie, 2016), *Arenicola marina*, lugworm, and shore crabs, *Carcinus maenas* . MPs were also detected in the guts of fish species, *Gobio gobio* (Sanchez et al., 2013), bivalve *Mytilus edulis* (van Cauwenberghe and Janssen, 2014).

Apart from aquatic species, MPs have been identified in marine birds such as fulmars, *fulmaris glacialis*, shearwater, *Procellaridae*, and gull, *Laridae*. Other bird species in terrestrial and freshwater ecosystems, including the buzzard *Buteo buteo*, the large hawk cuckoo *Culculus sparverioides*, and the little grebe *Tachybaptu sruficolis* contained MPs in the digestive system (Mahon et al., 2017). When upper levels of the food chain are examined, the results are exemplary of MP transport in the food chain. MP intake of invertebrates continues with vertebrates like birds and fish and further reaching up to mammal species. According to a study, MPs are detected in harbour seals, and *Phoca vitulina* stomach (Mahon et al., 2017). Size, type and source of plastics and corresponding affected organisms are summarized in Table 1.

Table 1 Size, type, source of plastics and corresponding affected organisms (Essel et al., 2015; Galgani et al., 2013; STAP, 2011)

Size of Plastic	**Type of Plastic**	**Source of Plastic**	**Affected Organism**
>25 mm	secondary	manufactured products	vertebrates, birds
5-25 mm	secondary	manufactured products and pellets	birds, fish
1-5 mm	primary	pellets	fish, crustaceans
< 1 mm	primary	personal care products and cosmetics	mussels, plankton

Although the studies concerning the health effects due to microplastic consumption are limited, there has been an increase in the amount of literature on this topic. Several studies have discussed the adverse effects of microplastic exposure on human health. For instance, Prata et al. (2020) concluded in their study that microplastics may lead to inflammatory lesions. Similarly, the study by Ragusa et al. (2021) was the first study that revealed microplastic existence in the human placenta.

Moreover, MPs accumulation has been proven for salts (Peixoto et al., 2019). Based on this study 550-681, 43-364, 7-204 MP particles/kg of salt have been accumulated on sea salt, lake salt, and rock salt, respectively. Even though the study concluded that MPs are more accumulated in the oceans and seas, obtaining MPs in other types of salts suggested that freshwater sources are also contaminated.

Considering the possible threats by MPs on food security, well-being of water resources and agricultural activities, identification of extend of pollution becomes crucially important in environmental compartments.

2.2 Transport Mechanisms of Microplastics

MPs accumulate in the environment and pollute marine, freshwater, and terrestrial habitats (Thompson et al., 2009). An illustration of transport mechanisms of MPs from sources to sinks is given in Figure 1. The MPs originated from urban and industrial sources find their ways into oceans, lake and river sediments, agricultural soils through pathways. Urban runoff, effluent discharge and direct inputs from lands are the processes where the MPs are being transported into main channels, river and WWTPs. With the further processes taking place, MPs end up in the sinks.

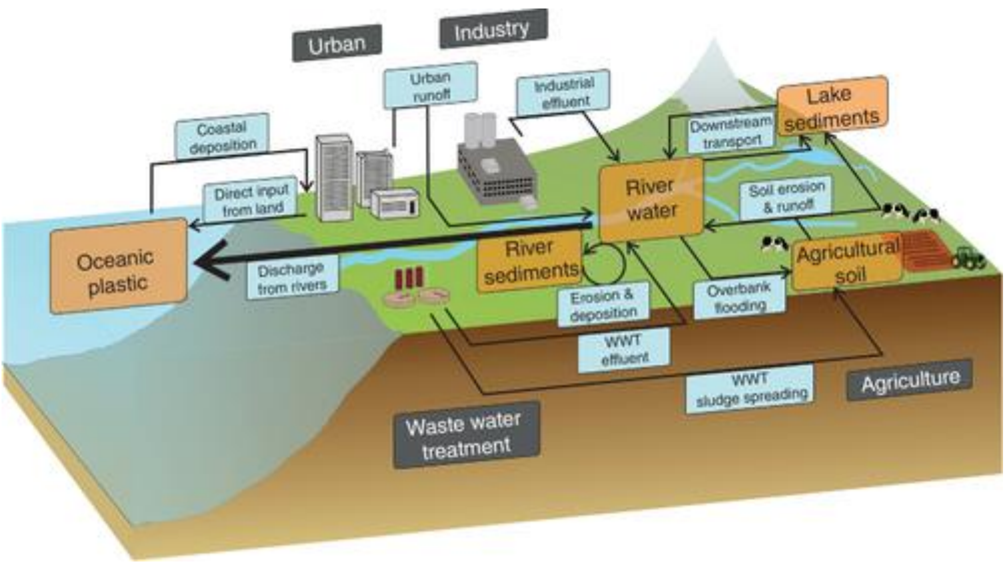

Figure 1 Plastic cycle concept introduced by Horton et al. (2017)

As plastics enter marine environments, they are subject to biofouling (Kubowicz & Booth, 2017). Microbead density increases by biofouling. Consequently, they are transported into sediments. However, as in the case of cold and anaerobic sediments, the rate of the biodegradation process is low. Also, biofouling affects sorption of MPs as they increase surface polarity. Metal-like substances that can ionize are adsorbed by such surfaces (Wardrop et al., 2016). Biofouling has adverse impacts on photooxidation, providing a shield to suppress UV light. Likewise, mechanical degradation is lowered. As a result, the material resists the buoyancy force less and sinks into deep sediments more easily (Kubowicz and Booth, 2017). A representative scheme regarding MP transport affected by biofouling is given in Figure 2.

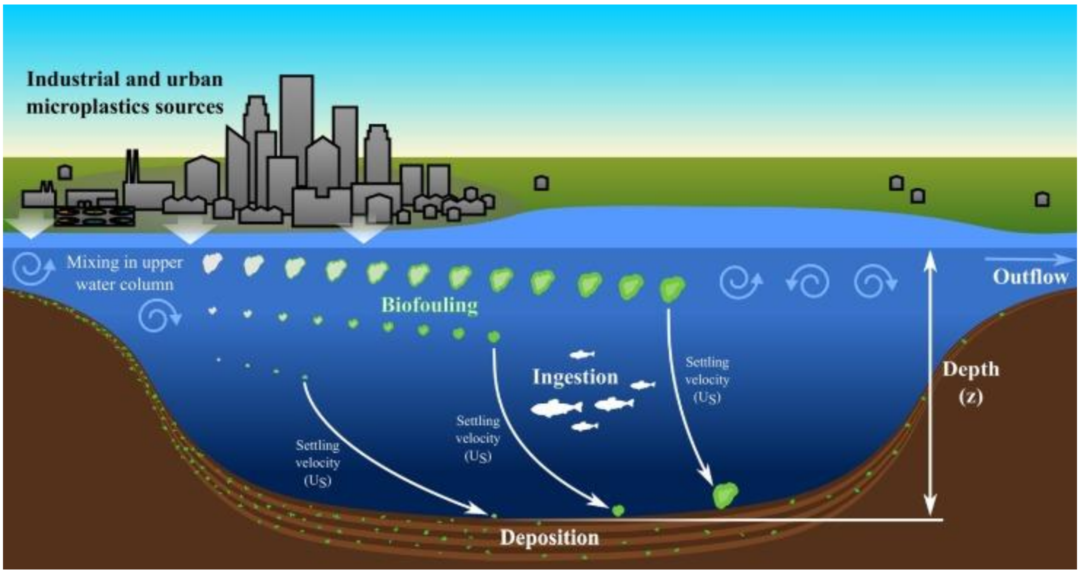

Figure 2 Scheme of MP transport from sources to water sink with biofouling effect (Semcesen and Wells, 2021)

2.3 Transformation Mechanisms of MPs

Abundance of MPs, synthetic polymers, in environment is attributed to their property of being highly resistant under environmental conditions. Hence, once they find their way into environment, they can retain for long residence times, and they show extremely low degradability. Their degradation in environment is divided into two categories: biotic and abiotic. Each category is driven by factors, being physical, chemical, or biological (Klein et al., 2018). There is another terminology, describing a similar trend of alteration of MPs in environment, which is weathering. It basically refers to the loss of physical integrity of the material, including degradation (Rummel et al., 2017).

In general, physical degradation is caused by abrasive forces, wetting and drying, heating and cooling and freezing and melting, whereas photodegradation is mostly driven by UV light. Synthetic polymers may also be oxidized or hydrolyzed and consequently, chemically altered. Bacteria fungi and algae are organisms that cause microplastic degrade biologically. These factors act on polymers and start their fragmentation into smaller polymers so called oligomers, dimers and monomers, followed by biomass activity which eventually end up in mineralization of the polymers and yielding CO_2, H_2O H_2S and NH_3, as final products (Klein et al., 2018)**.** These processes are explained in detail in the following sections.

2.3.1 Physical Transformation

Physical transformation is one of the initial steps of weathering processes. It is the fragmentation of plastic debris into smaller size particles, and it has significant impacts on the proceeding of further degradation processes (Hepsø, 2018).

Harsh conditions along shorelines, e.g., exposure to sunlight and abrasive mechanical forces acting on, plastic particles in various sizes –millimeter to micrometer range- and chemical characteristics are present in these areas blended with sand (Ceccarini et al., 2018). Each MP type experiences transformation processes at different levels. MPs with lower density are mainly distributed along shorelines and water surfaces and subject to physical degradation rather than deposition (Graca et al., 2017). Hebner and Jones (2020) state that motion in waterbodies enhance formation of smaller size microplastics which have previously been exposed to UV radiation of 254 nm than the ones in stationary water. Type of the polymer affected the number of microplastics generated because each polymer type shows different reaction characteristics and products when exposed to sunlight, but all types of microplastics studied revealed similar turbulent to stationary particle generation trend. Thicker PP films show more resistance to light degradation and therefore, their availability to degrade under physical stress is reduced. (Hebner and Maurer-Jones, 2020).

Followingly, physical degradation should not be considered apart from other weathering processes. For example, photodegradation, mentioned in detail below, result in embrittlement of MP and consequently the particles become more available to mechanical degradation. In addition, physical forces acting on MPs alters the chemical structure of MPs, breaking the polymeric chains and formation of radical fragments. In presence of oxygen, peroxide radicals may form, and particle will experience oxidation and chemically transformed (Hepsø, 2018)

2.3.2 Chemical Transformation

Internal and external factors affect the photodegradation process. Internal factors, as the name implies, refer to the structural properties of the polymer. Molecular defects, morphology, additives present, impurities, and chromophore groups available are the main contributors of this group. On the other hand, external factors relate to ambient conditions, such as changes in temperature, humidity or water content, availability of oxygen, energy radiation, microorganisms present and associated enzymes, acidic or basic solvents and external loading (Tofa, 2018).

MPs have a shortened polymer backbone in comparison with larger plastics. As a result of this structural change, MPs become more prone to chemical degradation than their mother fragments. Also, followed by surface erosion, they become more oxidizable and crystalline in structure (ter Halle et al., 2017).

Most of the plastic material such as PE, PP, PET, PS available are water-insoluble, therefore their hydrolysis is hindered. Members of polyolefin group e.g., PE and PP have alkyl backbone which provides high resistance against hydrolysis, but still these polymers are subject to transformation by oxidation (Wagner and Lambert, 2018a).

Low molecular weight intermediate products are formed during photocatalytic reactions of microplastics, these intermediates are then converted during organic synthesis (Bratovcic, 2019).

Due to varying photochemical properties of polymers, their exposure to sunlight differs. For example, the study shows that microplastics of origin PET has the most absorbency of UV light photons then PE and PP respectively (Hebner and Maurer-Jones, 2020). Also, photodegradation of commercialized plastic products is slower than the virgin nurdles as during manufacturing processes, UV stabilizers are added to the plastics. Such additives prevent oxygen from diffusing into the material (Andrady, 2011).

Photocatalytic degradation is mostly driven by photo-oxidation process as air and sunlight are present. As a result of this process, hydroxyl, peroxide, carbonyl groups are produced along the chain, yielding decrease in molecular weight (Tofa, 2018). As the common plastics HDPE, LDPE, PP and nylons enter in marine environment, UV-B radiation stars the photo-oxidation firstly. Followed by this initiation, thermo-oxidative degradation may proceed where further UV radiation is no longer needed. Light driven degradation is known to be the fastest mechanism among others which are comparably much slower in orders of magnitude. However, photodegradation is much more efficient for airborne plastics and plastics on shorelines when compared to the ones on the sea surface. This retardation is due to lower temperatures and oxygen concentrations in waterbodies. In addition, microplastics may be subject to fouling in water environment, for this reason, penetration of light on material surface is lowered and photodegradation is retarded. As for microplastics suspended in water columns or sinking down to sediments, their degradation through light irritation is less likely to occur, as UV-B is already attenuated, and lower temperatures and oxygen concentrations are present than on surfaces of waterbodies.(Andrady, 2011)

According to the study by Zhu et al. (2020), simulated sunlight irradiation on MPs which are collected from sea surface resulted in fragmentation, oxidation and change in color of the polymer. The study also yielded that DOC is the main byproduct of the plastic photodegradation under sunlight. DOC formed is further used by bacteria in the marine environment readily. Yet, photodegradation products may cause release of organics or co-polymers that hinder microbial activity. Therefore, individual processes and their combined effects must be studied thoroughly. They may either boost their function or act as a barrier on the action of another.

Thermal degradation is another process involved in chemical transformation mechanisms. Nevertheless, it requires high temperatures, above 100 °C, closer to melting point of the polymers, therefore it is not a dominating process determining fate of MPs in environment. At ambient temperatures, this thermal reaction would proceed very slowly. Also, during manufacturing, some additives having antioxidant properties are added to plastics, which provide further stability under thermal conditions (Booth et al., 2017).

A study investigating weathering of PE pellets in artificial seawater has shown that microcracking on pellet surfaces is mostly resulted from salinity rather than UV light for prolonged time periods. Also, thermal degradation profile revealed that PE pellets incubated in artificial seawater without washing showed a different profile than the ones incubated in deionized seawater and the virgin PE. (Da Costa et al., 2018)**.**

In addition to these, one interesting study is carried out by Kataoka et al. has found a direct relationship between MP mass concentration and river pollution in river environment in Japan. According to the study, the pollution of MP showed similar trend in water quality profile when compared to other conventional pollutants. A strong correlation is observed among BOD, DO, total-N and total-P. Increase in BOD, being a water pollution indicator, and decrease in DO is attributed to increase in numerical and mass concentrations of MPs (2019). Considering this information, it can be deduced that presence of MPs at certain level in water bodies would have an impact on water chemistry parameters.

2.3.3 Biological Transformation

As plastics enter marine environments, they are subject to biofouling (Kubowicz and Booth, 2017). Microbead density increases by biofouling. Consequently, they are transported into sediments. However, as in the case of cold and anaerobic sediments, the rate of the biodegradation process is low. Also, biofouling affects sorption of MPs as they increase surface polarity. Metal-like substances that can ionize are adsorbed by such surfaces (Wardrop et al., 2016).

MPs are prone to biofilm formations on their surface by colonization of microorganisms in benthic and pelagic zones (Rummel et al., 2017).This formation is strongly influenced by several factors, such as type of MP, surface characteristics, geographic location, and environmental pressures of salinity, solar radiation, hydrodynamics and temperature (Kesy et al., 2019). Contributors to plastispheres are known to have important effects on transfer of pathogens, alteration of MP buoyancy, biodegradation of the polymers and associated contaminants (Harrison et al., 2018).

McGivney et al. (2020) revealed that biofilm formation has caused changes in physicochemical characteristics of tested MPs in short term exposure. Such changes have been detected the most as increased crystallinity in PE beads, decreased stiffness in PP beads and increased maximum compression in PS beads. Cross-correlated physicochemical characteristics in virgin MPs have been vanished away upon biofilm formation, hence, weathering due to biological formations caused convergence of such properties in time.

Having biofilm on MPs has a derivative effect on these tiny materials other than degradation processes. As previously mentioned, MPs may be a conveyor of pollutants. In case of sorption of HOCs and biofilm formation take place on the same MPs, kinetics and persistence of these pollutants are affected by this interaction. Transport and transformation of these pollutants between polymeric bulk phase and the environment surrounding through biofilm interface need to be further investigated to allocate the role of biological formations on MPs being a source of contaminant release and transport (Rummel et al., 2017).

Plastic biodegradation takes place following four consecutive steps of bio-deterioration, bio-fragmentation, assimilation and finally mineralization. The first step, bio-deterioration describes the pattern of microbial activity which results in external degradation modifying the mechanical, chemical and physical features of the plastic. It is then followed by bio-fragmentation, the term addressing reduction of size by enzymatic activities occurring and with the help of secretion of free radicals by biota. Next step, assimilation take place, where molecules are transported in cytoplasm and being metabolized. The last process is oxidation of the molecules yielding ultimate degradation products of CH_4, N_2, CH_4, H_2O (Lucas et al., 2008).

Yet, complete degradation and mineralization of MPs is limited in number. Aliphatic polyesters, bacterial biopolymers and some bio-derived polymers are among the group of plastics which are readily biodegradable (GESAMP, 2015) whereas complete degradation of plastics into CO_2 and H_2O, known as biomineralization, is very rare. Even under most suitable laboratory conditions, only 0.1% per year of the carbon in polymers is biomineralized (Gewert et al., 2015).

There are three considerations that have a significant role on the extent of biodegradation.

1. Presence of certain microorganisms that can depolymerize the substance in proper metabolic pathway using specific enzymes yielding mineralization of the compound
2. Maintaining suitable environmental conditions for biodegradation, for example, temperature, pH, moisture, and salinity
3. Appropriate morphology of the polymer which should support attachment of the microorganisms and biofilm formation as well as polymer structure which should not interfere biological activity. Such structural characteristics are

chemical bonding, degree of polymerization, degree of branching, also physical properties of hydrophobicity and crystallinity affect the activities mentioned above (Klein et al., 2018).

Some additives and alterations in biodegradation production processes of plastics are enhanced. Yet, it causes the formation of MPs as intermediates (Wagner and Lambert, 2018). Therefore, control of factors influencing biodegradation should be handled properly.

Plastics with higher molecular weight are not susceptible to biodegradation at required reaction rates as only a rare portion of microbial species can utilize these compounds metabolically. (Andrady, 2011)**.** Also, many of the synthetic polymers present in the aquatic environment are water insoluble, as in case of PE, PP, PS, and PET that degrade very slowly or not at all. Both abiotic and biotic factors affect the extent of the biodegradation process (Wagner and Lambert, 2018b).

Still, there are several studies in the literature which reveals MP biodegradation in environment. Degradation of PE by *Pseudomonas* sp and *R. ruber* (Klein et al., 2018; Mor et al., 2018) and marine fungus *Zalerion maritimum,* plastic resin pellets by *Mycobacterium*, PP beads in thermophilic anaerobic digestors, LDPE by *Aspergillus versicolor, Aspergillus* sp., PCL by *Shewanella*, *Moritella* sp., *Psychrobacter* sp., *Pseudomonas*sp., *Clonostachysrosea*, *Trichoderma* sp., *Rhodococcus*sp., PBAT by soil microorganisms including filamentous fungi have been studied previously (Paço et al., 2017; Nielsen et al., 2019; Sekiguchi et al., 2011; Urbanek et al., 2017; Urbanek et al., 2018; Wilkes and Aristilde, 2017; Zumstein et al., 2018; De Tender, 2017). Additionally, plastic polymer degrading species include *B. Cereus*, *B. Gottheilii* (Auta et al., 2017), HDPE degrading species include *Arthrobacter sp,* LDPE degrading species include *K. Palustris, B.pumilis, B. Subtilis* (Sangale, 2012).

2.4 Occurrence of Microplastics in Environment

Plastic cycle concept is introduced (Horton and Dixon, 2018) to better see the fluxes and retention of MPs between environmental compartments. In this concept, MPs are ending up in oceans via coastal deposition and direct release from urban areas. Urban runoff, industrial effluents, effluents from WWTPs brings MPs into river system where they may be subject to sedimentation in rivers or in lakes through downstream transport or relocate into oceans through river discharges. Also, flooding of the rivers and land application of wastewater sludge brings MPs to agricultural soil matrices.

Also, as a secondary contamination threat, MPs are associated with chemical pollution in the environment. Having large surface area to volume ratios, MPs are becoming a suitable sorbent for toxic chemicals, e.g., heavy metals and organic pollutants. In this way such contaminants may get mobilized by sorption on MP surfaces and become readily available to organisms and in different environmental compartments (Verla et al., 2019). According to U.S National Library of Medicine, there are some pollutants listed as the significant concerns regarding MPs, which are dioxins, POPs, PDBEs, PCBs and PAHs (National Institutes of Health, 2019).

2.5 Occurrence of Microplastics in Wastewater Treatment Plants

WWTPs are considered as one of the freshwater MPs polluters. The types of MPs observed in the effluents of WWTPs include PE, PET, and nylon, mostly in terms of fibers or microbeads (Ziajahromi et al., 2017). WWTPs are known to contribute to MP pollution in the forms of plastic fibers from synthetic clothes and primary resources, usually downstream of the plants (Gewert et al., 2017; Murphy et al., 2016b; Ziajahromi et al., 2017). As previously mentioned in section 2.2, after MPs are discarded or unintentionally lost, they find their ways into water bodies where WWTPs act as an intermediate step for MP transport into environment.

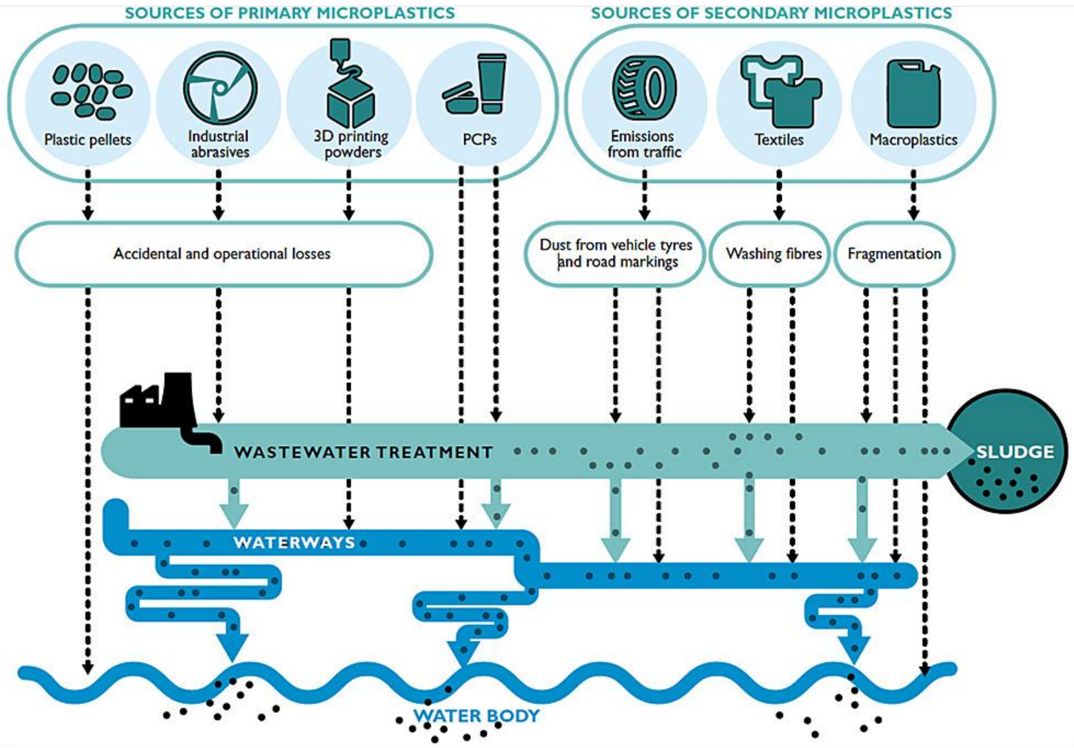

Figure 3 MP pathway from sources to sinks
(Setälä et al., 2017; modified from UNEP, 2016)

Understanding how MPs are removed is a relevant point to modify or understand their removal capacities and the conditions that can affect the removal performance since the MPs removal rate in the WWTPs changes based on the process used. This section aims to provide a detailed review of WWTP processes to understand if MPs are effectively treated in the WWTP by critically synthesizing the data available for different treatment technologies. Gathering the data available in the literature can help understand the fate of MPs in the WWTPs.

Most of the studies covering MPs in WWTPs so far were focused on the concentration and classification of MPs, not on the treatment processes with their operational characteristics that are affecting the removal of MPs (Rajala et al., 2020).

Physical processes are defined as processes with no chemicals are involved. Those processes can be classified as screening, comminution, settling, filtering, and skimming. In a WWTP, during primary, secondary, and tertiary treatment steps, removal is achieved even though the removal efficiency differs greatly from one unit to another, as can be seen below in Table 2 and Table 3.

Various parameters can affect the removal of microplastics. For instance, analyzing the data from Table 2, it can be observed that the removal rate changes even though the same physical treatment was applied. Similar findings were reported by (Long et al., 2019), stating that MPs abundance is higher in overloaded WWTPs since overloaded operation decreases the hydraulic detention time with the increased flow rate of the wastewater (Hamidian et al., 2021).

WWTPs are known to emit plastic fibers from synthetic clothes and primary resources. They are mostly found in form of fibers at downstream of the plants (Gewert et al., 2017).Tertiary treatment provides 90% removal for particles in the size of 10 µm, yet the efficiency declines down to 10% as the size is approaching 1 µm (Hale, 2016). Micro-screening is a new trend to adopt in WWTPs, instead of primary sedimentation tank, promising excellent removal for particles smaller than 100 µm (Hale, 2016). A basic mass balance equation would yield a result that most of the MP retain untreated in sewage sludge. Annual 44,000-430,000-ton MP input via is foreseen in European and North American terrestrial area Carsten et al. (2015) and Sundt, (2014). Therefore, MP retaining in sludge must be handled attentively for prevention of spreading in food chain.

A detailed study (Murphy et al., 2016a) discussed the fate of MPs at different treatment steps in a wastewater treatment plant. It was concluded that a significant portion of MPs was removed during grease removal with the skimming process. In addition, the preliminary and primary treatment could achieve a removal efficiency of 78.34% for the MPs in the liquid fraction. However, the effluent flow being constantly discharged from the WWTP is significantly large. This constant discharge is a potential source of MPs in the aquatic environment (Talvitie et al., 2015; Talvitie et al., 2017). Another study in two WWTPs of Turkey revealed that the removal rates of microplastics were ranging from 73% to 79%. The influent of the two WWTPs contained from 1 million to 6.5 million particles of MPs per day. In contrast, the effluent contained 220,000 to 1.5 million particles of MPs per day, which indicated that the effluent still contained a high number of MPs. This supports the idea of WWTPs as a potential source of MPs for the aquatic environment (Gündoğdu et al., 2018). On the other hand, mechanical and chemical pretreatment methods reached a removal efficiency in the range of 97.4 - 98.4% for most of the microliter particles in the largest WWTP in Finland, with a contribution from approximately 800.000 people (Talvitie et al., 2017).

However, biofilm may fall as film and flow out with treated water after exhaustion. In the case of backwashing, the MPs attached or fixed in the biofilm might be released into the wastewater which was generated during the backwash. This situation means that re-suspended MPs are retreat by returning to the main treatment stream (Zhang et al., 2020). On the other hand, the degradation of MPs during biological treatment is complex considering the short retention time of biological reactors such as 4 h-12 h (Zhang et al., 2020).

Table 2 summarizes the removal rate of microplastics with the type of physical treatment applied, wastewater characteristics, shapes, size range, units, and the identification method of various WWTP worldwide.

Biological treatment of microplastics generally includes two types, activated sludge-related process and biofilm-related process. Activated sludge consists of microorganisms that use contaminants in the wastewater as a food source; these microorganisms release extracellular polymeric substances (EPS) to adsorb the contaminants. The main removal of MPs during the activated sludge process occurs with adsorption and aggregation with sludge flocs. The Biofilm method also consists of aerobic, anoxic, and anaerobic microorganisms; hence EPS is secreted. The MPs are adsorbed by EPS and play a role as an attachable carrier for supporting biofilm growth. Then, they are fixed in the biofilm, which is another pathway of MP's removal. However, biofilm may fall as film and flow out with treated water after exhaustion. In the case of backwashing, the MPs attached or fixed in the biofilm might be released into the wastewater which was generated during the backwash. This situation means that re-suspended MPs are retreat by returning to the main treatment stream (Zhang et al., 2020). Table 3 summarizes the removal rate of microplastics with the type of biological treatment applied, wastewater characteristics, shapes, size range, units, and the identification method of various WWTP worldwide.

Table 2 MP Removal Efficiencies in Physical Treatment Processes in WWTPs

Type of treatment applied	MP Removal (%)	WWTP	WW characteristics given	Shapes identified	Size range studied	Units expressed	Method of Identification	Reference
Primary settlement tanks	33.75	A large secondary WwTW located on the River Clyde, Glasgow	PE, wastewater flow	Flake, fiber, film, bead, foam	>11 µm	MP/L	FTIR	(Murphy et al., 2016a)
Aeration and clarification	20.07	A large secondary WwTW located on the River Clyde, Glasgow	PE, wastewater flow	Flake, fiber, film, bead, foam	>11 µm	MP/L	FTIR	(Murphy et al., 2016a)
Rapid sand filtration	73.8	Daegu, South Korea, WWTP C	Average effluent flow rate, PAC	Microbead, fiber, sheet (except some samples), fragment	>1.2 µm	MP/L	a Leica DM 750 microscope combined with IMT iSolution Lite analysis software	(Hidayaturrahman and Lee, 2019)

Type of treatment applied	MP Removal (%)	WWTP	WW characteristics given	Shapes identified	Size range studied	Units expressed	Method of Identification	Reference
Primary treatment	56.8	Daegu, South Korea, WWTP B	Average effluent flow rate, PAC	Microbead, fiber, sheet, fragment	>1.2 µm	MP/L	a Leica DM 750 microscope combined with IMT iSolution Lite analysis software	(Hidayaturrahman and Lee, 2019)
Primary treatment	64.4	Daegu, South Korea, WWTP C	Average effluent flow rate, PAC	Microbead, fiber, sheet (except some samples), fragment	>1.2 µm	MP/L	a Leica DM 750 microscope combined with IMT iSolution Lite analysis software	(Hidayaturrahman and Lee, 2019)
Rapid sand filtration as an additional polishing step	99.7	One of the ten largest WWTPs in Denmark	COD	Acrylate, SAN, VAC, PE, PP, PE-PP copolymer, Pest, PS, PU, PVC	10-500 µm	Item/L µg/L	FPA-based FTIR	(Simon et al., 2018)

Type of treatment applied	MP Removal (%)	WWTP	WW characteristics given	Shapes identified	Size range studied	Units expressed	Method of Identification	Reference
Grit and grease treatment	44.59	A large secondary WWTP located on the River Clyde, Glasgow	PE, wastewater flow	Flake, fiber, film, bead, foam	>11 µm	MP/L	FTIR	(Murphy et al., 2016a)

Table 3 MP Removal Efficiencies in Biological Treatment Processes in WWTPs

Type of treatment applied	MP Removal (%)	WWTP	WW characteristics given	Shapes identified	Size range studied	Units expressed	Method of Identification
Biofilter (advanced polishing step for treated wastewater)	79 by particle number 89 by particle mass	Biofilter fed with secondary effluent from a conventional WWTP in Denmark.	Not reported	100-300 µm	Item/m^3 µg/ m^3	FPA based FTIR	(Liu et al., 2020)
Secondary treatment	83.1	Daegu, South Korea, WWTP A	Average effluent flow rate, PAC	>1.2 µm	MP/L	Leica DM 750 microscope combined with IMT iSolution Lite analysis software	(Hidayaturrahman and Lee, 2019)
Secondary treatment	75.0	Daegu, South Korea, WWTP B	Average effluent flow rate, PAC	>1.2 µm	MP/L	Leica DM 750 microscope combined with IMT iSolution Lite analysis software	(Hidayaturrahman and Lee, 2019)

Type of treatment applied	MP Removal (%)	WWTP	WW characteristics given	Shapes identified	Size range studied	Units expressed	Method of Identification
Secondary treatment	91.9	Daegu, South Korea, WWTP C	Average effluent flow rate, PAC	>1.2 µm	MP/L	Leica DM 750 microscope combined with IMT iSolution Lite analysis software	(Hidayaturrahman and Lee, 2019)
Activated sludge + secondary clarifiers	85.2±6.0	Rifle Rang WWTP, South Carolina, USA	Service composition, population served, Plant Capacity, Avg. Volume Treated	>418µm,178-418µm, and 60-178µm	MP/L	Visual counting using stereomicroscope and micro-FTIR for MPs showing digestion	(Conley et al., 2019)
Activated sludge + secondary clarifiers	85.5±9.1	Center Street WWTP, South Carolina, USA	Service composition, population served, Plant Capacity, Avg. Volume Treated	>418µm,178-418µm, and 60-178µm	MP/L	Visual counting using stereomicroscope and micro-FTIR for MPs showing digestion	(Conley et al., 2019)

Type of treatment applied	MP Removal (%)	WWTP	WW characteristics given	Shapes identified	Size range studied	Units expressed	Method of Identification
Secondary treatment	89.96	HC WWTP in Xiamen, China	SS	63-43 µm 125-63 µm 355-125 µm 5000-355 µm	Item/L	The light microscopic and micro-Raman spectroscopic analysis	(Long et al., 2019)
Secondary treatment	94.89	XL WWTP in Xiamen, China	SS	63-43 µm 125-63 µm 355-125 µm 5000-355 µm	Item/L	The light microscopic and micro-Raman spectroscopic analysis	(Long et al., 2019)
Secondary treatment	89.38	JM WWTP in Xiamen, China	SS	63-43 µm 125-63 µm 355-125 µm 5000-355 µm	Item/L	The light microscopic and micro-Raman spectroscopic analysis	(Long et al., 2019)

Type of treatment applied	MP Removal (%)	WWTP	WW characteristics given	Shapes identified	Size range studied	Units expressed	Method of Identification
Secondary treatment	97.84	TA WWTP in Xiamen, China	SS	63-43 μm 125-63 μm 355-125 μm 5000-355 μm	Item/L	The light microscopic and micro-Raman spectroscopic analysis	(Long et al., 2019)
Secondary treatment	91.71	XA WWTP in Xiamen, China	SS	63-43 μm 125-63 μm 355-125 μm 5000-355 μm	Item/L	The light microscopic and micro-Raman spectroscopic analysis	(Long et al., 2019)
Secondary treatment	92.45	QP WWPT in Xiamen, China	SS	63-43 μm 125-63 μm 355-125 μm 5000-355 μm	Item/L	The light microscopic and micro-Raman spectroscopic analysis	(Long et al., 2019)

Type of treatment applied	MP Removal (%)	WWTP	WW characteristics given	Shapes identified	Size range studied	Units expressed	Method of Identification
Secondary treatment	79.33	YD WWPT in Xiamen, China	SS	63-43 µm 125-63 µm 355-125 µm 5000-355 µm	Item/L	The light microscopic and micro-Raman spectroscopic analysis	(Long et al., 2019)
Secondary treatment	90.52	Average of seven WWPTs above in Xiamen, China	SS	63-43 µm 125-63 µm 355-125 µm 5000-355 µm	Item/L	The light microscopic and micro-Raman spectroscopic analysis	(Long et al., 2019)
Activated sludge	99.3 by item/L 98.3 by µg/L	Average of nine of the largest WWTPs in Denmark	COD	10-500 µm	Item/L µg/L	FPA based FTIR	(Simon et al., 2018)
CAS + disinfection or MBR (pilot)	99.9	Kenkaveronniemi WWTP, located in city of Mikkeli, South-East of Finland.	SS, BOD_7, total P, total N, population equivalent, Efflux	>300 µm, 100-300 µm and 20-100 µm	MP/L	Stereo microscope with an integrated HD camera and imaging FTIR spectroscopy	(Talvitie et al., 2017).

The particle removal depends on the physical retention of particles in filters with the sludge cake formation in the filter panels (Talvitie et al., 2017). In the case of raw-high-solid influent, microplastics with a lower density float or settle if they are trapped in solid flocs and can easily be removed by skimming or settling. Nevertheless, the removal of microplastics may be affected by factors such as the trapping of MPs in unstable flocs that might not settle properly. This effect results in the escape of some microplastics in the skimming and settling (Carr et al., 2016). Furthermore, extensive biofilms on discharged solids in the secondary effluent may also affect the MP particles by changing their physical properties. (Carr et al., 2016) stated that bio-coatings might modify the surface properties of hydrophobic polyethylene fragments or biofilm that might change the relative densities of plastics compared to clean or uncoated, which impact the removal efficiencies of MPs at municipal treatment plants. In fact, a portion of microplastics found in secondary discharges may result from biological surface deposits. In addition, longer contact times of solids may lead to effluents with higher MPs concentration (Carr et al., 2016).

Magni et al., (2019) estimated that 3,400,000,000 MPs accumulate daily in sewage sludge of one of the biggest WWTPs of Northern Italy. This number of MPs resulted from the processing of 30 tons/dry weight of sludge. Also, they concluded that the removal of MPs probably happened during the grease and sedimentation process.

However, advanced final stage treatments, which included sand filters, also greatly contributed to the MP removal. Nevertheless, future research is needed to understand the distribution, removal, and release of MPs in the aquatic environment by WWTPs. The connections between the physical/chemical behavior of these pollutants and the effectiveness of various treatment stages are still being clarified (Magni et al., 2019).

The contaminants attached to the MPs are transported into the sludge at the same time as the MPs themselves. As a result, they may affect the microorganisms involved in digestion. The most commonly mentioned contaminants include antibiotics, POPs, and heavy metals, all of which have a major influence on anaerobic digestion. MPs are extremely difficult to biodegrade, especially over a short period of time, considering a retention duration of 4–12 hours of a typical biological reactor. As a result, MPs are transferred from wastewater to sludge during the wastewater treatment process. The main pathways of the transfer of MPs include settling, adsorption, flotation, entrapment, and interception.

Although MPs do not affect anaerobic digestion, they can carry various toxic substances that inhibit the digestion process. This inhibitory impact mainly depends on the desorption of toxic substances out of MPs.

Furthermore, since most MPs are retained in the sludge, sludge land application may release more microplastics to the receiving bodies than the direct discharge of wastewater. Up to this date, a particular treatment process focused on removing microplastics has not yet been implemented in a full-scale WWTP. Additionally, microplastic-targeted treatment technology is still in its early stages of development (Sun et al., 2019).

Assuming that microplastics that are not in the effluent will be detected in the sewage sludge is reasonable and the fact that 99% of the microplastics retained in a WWTP with 12000 population equivalent that they examined indicates that more research into the fate of microplastics in sewage sludge is needed (Magnusson and Norén, 2014).

CHAPTER 3

MATERIALS AND METHODS

3.1 Microplastics

Anhydride modified PE pellets from Fusabond® E MB-226DE supplied by DuPont, having a density of 0.93 g/cm^3 (Dow, n.d.), PS pellets from BASF Polystyrol® 165 H, 1.05 g/cm^3 of density (D.S., 1997); ethylene terpolymer resin Elvaloy® PTW which is promoter toughening of PET with a density of 0.94 g/cm^3 (DuPont, 2013), TPU resin from Epaflex EL 392 A 25 from Interplast, with a density of 1.19 g/cm^3, HDPE resins from Sadara Chemical Company, with 0.95 g/cm^3 density (Sadara, 2019), LDPE resins from ExxonMobil with 0.924 g/cm^3 density (ExxonMobil, 2017), PET resins from Indorama Ventures with 1.40 g/cm^3 density (IDES, 2014), PP resins from LyondellBasell with 0.90 g/cm^3 density (LyondellBasell, 2019) were purchased. Weight measurements have been done for 20 particles for each MP type by using analytical balance with an accuracy of 0.0001. The physical properties of selected MPs are listed in Table 4. The images of MPs are shown in Figure 4.

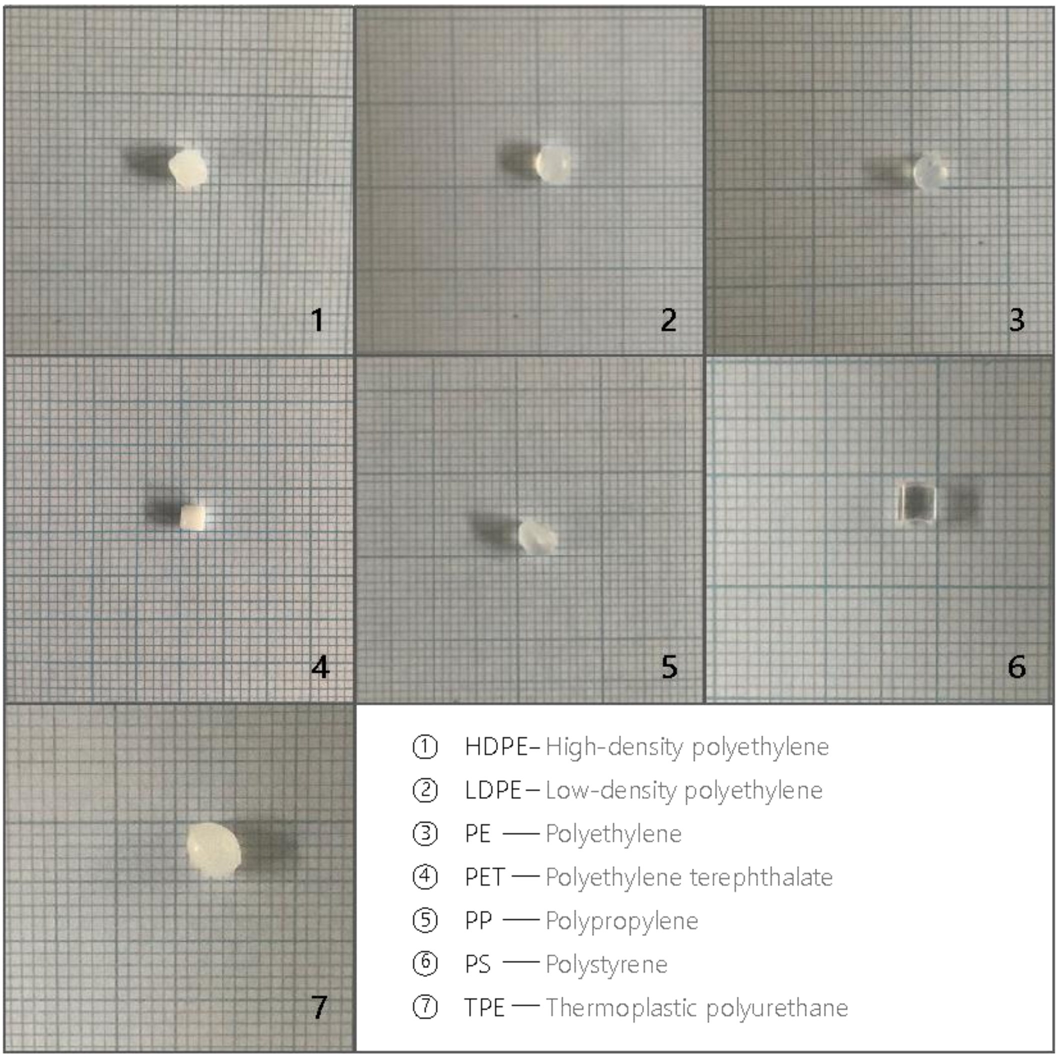

Figure 4 Images of MPs on millimetre paper

Table 4. Physical Properties of MPs studied

Microplastic Type	**Density (g/cm^3)**	**Size (mm)**	**Mass/particle ()**	**Shape**	**Colour**
HDPE	0.95	3	0.0292± 0.0022	Sphere	white-opaque
LDPE	0.924	2.5	0.0265± 0.0012	Sphere	white-transparent
PE	0.93	2.5	0.0131± 0.0017	Cylinder	white-transparent
PET	1.40	2	0.0143± 0.0011	Cylinder	white-opaque
PP	0.9	3	0.0224± 0.0058	Sphere	white-transparent
PS	1.05	3	0.0223± 0.0020	Cylinder	transparent & white opaque
TPU	1.19	3	0.0350± 0.0100	Sphere	white-opaque

All MPs were sterilized with %70 (v/v) ethanol solution, shaking at 130 rpm for 15 min, and further rinsed three times by ultrapure water as mentioned in (Rosato et al., 2020).

3.2 Bacteria Species

Three different bacteria species were chosen for this study, which are *Enterococcus faecalis, Escherichia coli*, *Pseudomonas aeruginosa*, bacteria commonly detected in wastewater (Rodríguez-Chueca et al., 2013) and polluted freshwater.

Non-pathogenic strains of these bacteria were obtained from Middle East Technical University Molecular Microbiology Laboratory in streaked nutrient agar plates. The visuals of bacteria species are available in the following figures.

Figure 5 *E. coli* culture on nutrient agar

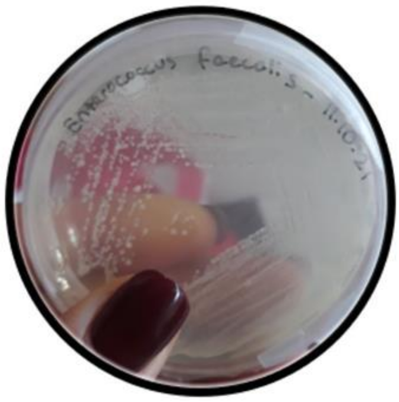

Figure 6 *E. faecalis* culture on nutrient agar

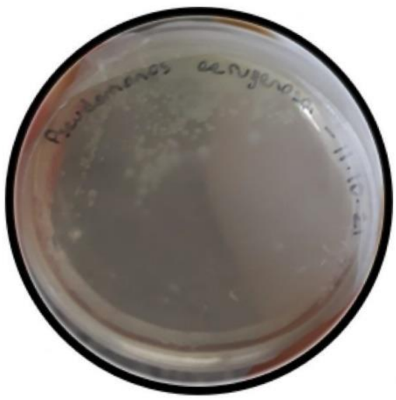

Figure 7 *P. aeruginosa* culture on nutrient agar

For negative control, microcosm without bacteria inoculations was set and run under the same conditions.

Single colonies from each bacteria sample was taken and transferred to LB broth using aseptic technic and incubated at 37°C for 24 hours. Further, streak plating was done on LB agar plates periodically to maintain active pure cultures. Stock cultures of bacteria were prepared by adding 0.5 mL overnight cultures in LB broth and 0.5 mL 50% v/v autoclaved glycerol solution in Eppendorf tubes and pipetting the solution. Then, the Eppendorf tubes were kept in -20°C for any possible further experimentation and keeping as backup.

Morphology and some biochemical properties of the bacteria species chosen for the study are tabulated in .

Table 5 Morphological and Biochemical Properties of the Bacteria Species Studied

Bacteria Specie	Phylum	Shape	Gram Reaction	Presence of Flagella	Motility	Presence of Capsule	Oxygen Requirement	Sporulation	Reference
E. coli	Proteobacteria	rod	negative	multiflagellated	motile	capsulated	facultative anaerobe	non-sporing	(Percival and Williams, 2014)
E. faecalis	Firmicutes	cocci	positive	non-flagellated	non-motile	non-capsulated	facultative anaerobe	non-sporing	(Flint, 2002)
P. aeruginosa	Proteobacteria	rod	negative	monoflagellated	motile	non-capsulated	facultative aerobe	non-sporing	(Wu et al., 2015)

3.3 Experimental Design

The medium consisting of bacteria, MP, and LB broth were prepared in a way that enables observation of biofilm formation by each bacterium on each MP individually. There were 7 MPs and 3 bacteria together with 1 blank as inoculum, yielding a total of 28 cases to be observed which are presented in Table 6.

Table 6 Experimental cases matching MPs and bacteria species studied

E. coli x HDPE	*E. faecalis* x HDPE	*P. aeruginosa* x HDPE	Blank x HDPE
E. coli x LDPE	*E. faecalis* x LDPE	*P. aeruginosa* x LDPE	Blank x LDPE
E. coli x PE	*E. faecalis* x PE	*P. aeruginosa* x PE	Blank x PE
E. coli x PET	*E. faecalis* x PET	*P. aeruginosa* x PET	Blank x PET
E. coli x PP	*E. faecalis* x PP	*P. aeruginosa* x PP	Blank x PP
E. coli x PS	*E. faecalis* x PS	*P. aeruginosa* x PS	Blank x PS
E. coli x TPU	*E. faecalis* x TPU	*P. aeruginosa* x TPU	Blank x TPU

Sampling was done on the 24th, 36th and 72nd hours of incubation to examine the time-dependency of biofilm formation, as previously studied by Colón-González et al. (2004).

For the sake of practicality in the analysis, 7 glass tubes with above mentioned content were set for each case. 3 of them were used for dry weight analysis at 24th 48th and 72nd hours, 3 crystal violet staining at 24th, 48th and 72nd hours and 1 for SEM analysis. The details of the analysis are explained in detail in Section 3.6. None of the cases with blank samples were subjected to SEM analysis. Therefore, a total of 213 glass tube were set. Each glass tube was labelled with the bacteria name, type of MP, sampling time and the corresponding analysis, for example, *Escherichia coli,* PE, =24th hour, dry weight analysis.

The glass tubes were incubated under darkness to prevent material transformation due to photodegradation, at 37 º C, and the rpm was set to 80.

3.4 Biofilm Formation Experiments

3.4.1 Preparation of Bacteria Cultures

Single colonies from streaked LB agar plates were taken and incubated in 80 mL LB broth tube at 37˚ C at 130 rpm overnight. Then, 200 µL of the overnight culture was transferred into 200 mL LB broth in 500 mL Erlenmeyer flask, yielding a dilution ratio of 1/1000. The inoculated LB broth was incubated at 37°C at 120 rpm until the OD_{600} reached~0.1. 50 µL of the bacterium culture was taken and added into each corresponding glass tube with a total filling volume of 5 mL The glass tube was filled with LB broth resulting in a total bulk volume of 2 mL and a dilution ratio of 25/1000. 3 MP particle of same type were added into the tubes.

The same steps were followed for preparation of biofilm formed MPs for settling velocity analysis. Yet, since the sample number is different for biofilm measurement and settling velocity measurements, which is explained thoroughly in 3.7.3, the volume of the medium and amount of bacteria inoculated changed without altering the dilution ratio. Biofilm formation assay specific for settling velocity analysis was conducted in 100 mL Erlenmeyer flask having 20 mL fresh LB broth medium, 500 µL of the bacterium culture with OD_{600} ~0.1. 30 MP particle of same type were added into the flasks for biofilm formation assay.

3.4.2 Bacteria Growth Experiment

Single colonies from streaked LB agar plates were taken and incubated in 80 mL LB broth tube at 37° C at 130 rpm until OD_{600} reached to approximately 0.1. 50 µL was taken from each grown culture and transferred into 200 mL fresh LB broth medium individually and incubated for 72 hours. At the beginning of the experiment, initial pH of LB broth medium was measured as 7.02. At 12th, 24th, 36th, 48th, 60th and 72th hours, sampling was done in order to quantify bacteria growth spectrophotometrically by measuring absorbance at 600 nm (Hach DR3900 Laboratory Spectrophotometer) against blank sample.

3.5 Experimental Set-up for Biofilm Formation Assay

All laboratory glassware, pipettes and pipette tips were wrapped with aluminium foil an autoclaved at 121°C for 20 min prior to use. Racks were used for stabilization of glass tubes in the shaker incubator. Glass tubes were placed in the racks in inclined position for maintaining proper aeration for the cultures. The figure of the experimental set-up is represented in the Figure 8.

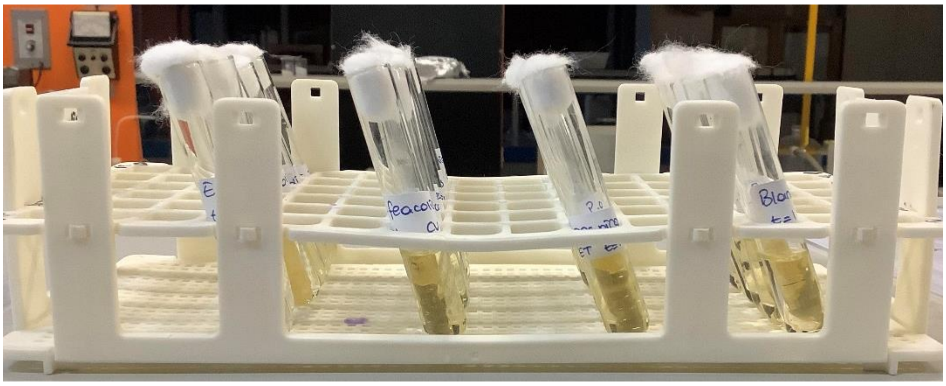

Figure 8 A Picture of The Experimental Set-Up

3.6 Biofilm Measurement

Biofilm measurements were done by both in METU Department of Environmental Engineering Laboratories and METU Central Laboratory. In the department laboratories, crystal violet staining and gravimetric analysis were conducted to quantify biofilm by measuring optical density and mass respectively. The biofilm formed MPs were also sent to METU Central Laboratory for visualization of biofilm morphology and structure formed.

3.6.1 Dry Weight Measurement

Dry weight measurement method was modified from (Leiser et al., 2021). At each sampling period, the growth medium in each tube was removed by pipetting. MPs were dried at 60ºC for 24 h in drying oven. The MPs were carefully taken away from the glass tube by using tweezers. The weight of each MP was measured by using analytical balance with an accuracy of 0.0001 g. The MPs were then soaked in 96% (v/v) ethanol solution overnight upon vortexing to remove all biofilm on MP surface, modified from Tarafdar et al. (2021). The ethanol solution was removed by pipetting and MPs were dried at 60ºC for 24 h in the drying oven. Finally, the MPs were weighted by using the same analytical balance. The weight of the biofilm formed was determined by calculating the difference between the two measurements.

3.6.2 Crystal Violet Staining

The method for crystal violet staining was modified from (Hchaichi et al., 2020.; Rodrigues et al., 2009 and; Rosato et al., 2020). At each sampling period, the growth medium in each tube was removed by pipetting. MPs were dried at 60ºC for 24 h in drying oven. Then, each MP was stained with 150 µL of crystal violet solution (0.1% in ultrapure water) for 15 min. After staining, MPs were rinsed with deionized water thoroughly to remove the unbound stain. Lastly, destaining was carried out by adding 2 mL of 96% (v/v) ethanol solution modified from Rosato et al. (2020), Hchaichi et al. (2020), Rodrigues et al. (2009) and Leiser et al. (2020).The obtained solution was vigorously shaken by vortexing to release all the bound stain and obtain a homogenized solution. Then the absorbance of the solution was measured spectrophotometrically at 570 nm wavelength as proposed by Rosato et al. (2020), by using Hach DR3900 Laboratory Spectrophotometer against blank sample. Experiments were done for triplicates of each sample. An exemplifying picture of the crystal violet staining analysis done is shown in Figure 9.

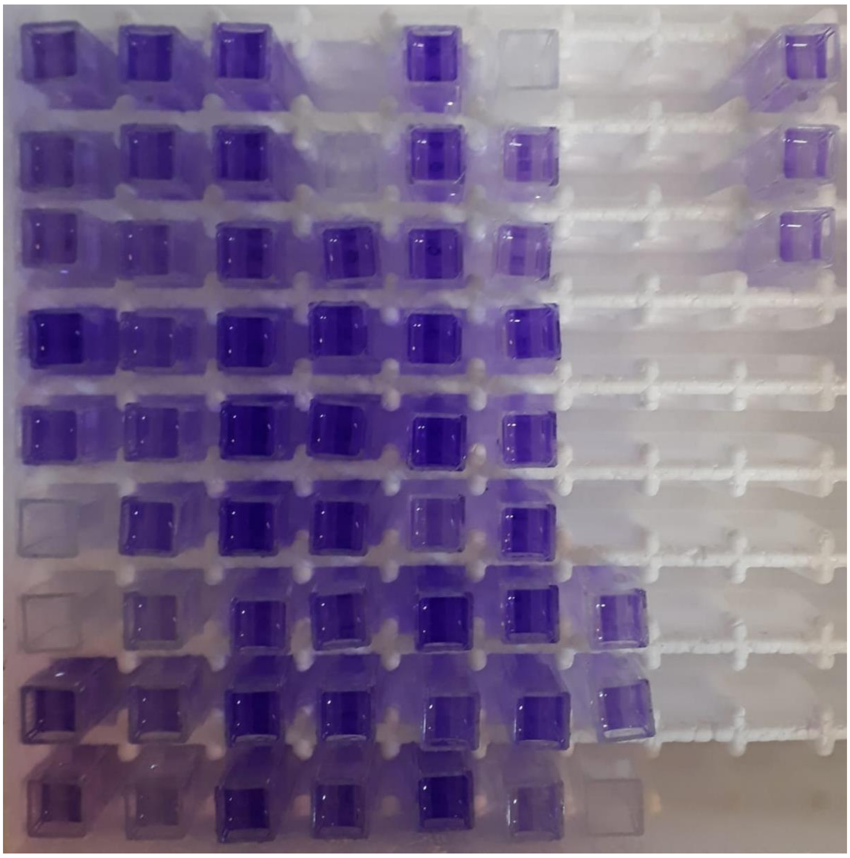

Figure 9 Picture of crystal violet staining experiment conducted in the laboratory

3.6.3 Scanning Electron Microscopy

Morphology of biofilm formation on MPs after 72 hours of incubation was visualized by using SEM in METU Central Laboratory as well as pristine MPs (without any biological treatment). The sample treatment was done based on the methodology presented by (Tarafdar et al., 2021). Immobilization of MP particles were performed by adding biofilm formed MPs in glutaraldehyde solution (2.50% in PBS, pH=7.2, the recipe is available in Table 7) in Eppendorf tubes for 4 hours. Dehydration of immobilized biofilm were done by keeping MPs in ethanol solutions of 30%, 50%, 70%, 80%, 90% (v/v) for 10 minutes in each solution serially. MPs were kept in absolute ethanol (>99.9 %) for 10 minutes, twice as the final step. Dehydrated MPs were then dried at room temperature under laminar flow for 16 hours prior to SEM analysis. Pristine MPs were also analysed by SEM imaging to compare the particle surfaces before and after the biofilm formation.

Table 7 Recipe of PBS (Chazotte, 2008)

Chemical	Amount added (g) in 1 ultra-pure water L
NaCl	8
KCl	0.2
Na_2HPO_4	1.44
KH_2PO_4	0.24

The SEM analysis was carried out by using Philips QUANTA 400F Field Emission SEM under high vacuum. The pre-treated MPs were covered with Au-Pd with 3 nm thickness.

3.7 Settling Velocity Measurement

The settling velocity measurements were done for pristine MPs in freshwater, seawater and wastewater, and for 72-hour grown biofilm formed on MPs in freshwater and seawater. Theoretical settling velocities of pristine MPs in freshwater, seawater and wastewater were calculated for validation of the code-based settling velocity measurement method.

3.7.1 Theoretical Settling Velocity Calculations

Theoretical settling velocities of pristine MP particles were calculated by Stoke's law expression which is presented in Equation 1.

$$v = \frac{(\rho_P - \rho_L) d_P^2 g}{\mu} \qquad \text{Equation 1}$$

In, v represents Stoke's velocity (cm/s), ρ_P particle density (g/cm^3), ρ_L liquid density (g/cm^3), g gravitational acceleration (cm^3/s^2), d_P particle diameter (cm) and μ absolute viscosity of the liquid (g/cm.s). However, there are limitations for Stoke's law implementation in environmental engineering practises. First of all, the Stoke's law is only applicable for spherical particles, and low Re where inertial terms are neglected. Also, it requires infinite liquid, meaning infinite distance, to extent the flow distance generated by the particle. Yet, these limitations are oftentimes minor, so that the Stoke's law becomes applicable. Moreover, in case of inapplicable conditions, Stoke's law still serves as a baseline to compare with the other results (Benjamin and Lawler, 2013).

Stoke's law is only valid for laminar flow conditions where N_R <1. (Fulford et al., 1997). The formulation for N_R is given in Equation 2.

$$N_R = \frac{v d_P \rho_L}{\mu} \qquad \text{Equation 2}$$

The physical properties of water columns used to calculate theoretical settling velocities of pristine MPs are given in Table 8. It should be noted that the water columns named as seawater and wastewater were water solutions prepared by dissolving NaCl and $C_6H_{12}O_6$ in deionized water in a way that the theoretical densities of these columns are maintained. The detailed information regarding preparation of these solutions is given in section 3.7.2. In addition, all MPs were assumed as spherical particles, their diameters were considered as one half of their sizes, which have been presented previously in Table 4.

Table 8 Physical properties of water columns used in calculation of theoretical settling velocities by using Stoke's law

Physical properties	Freshwater	Seawater	Wastewater	Reference
Density at 20°C (g/cm^3)	0.998	1.025	1.05	(Weast, 1972;ITTC, 2011;Tchobanoglous et al., 2014)
Absolute viscosity at 20°C (g/cm.s)	1.002×10^{-2}	1.054×10^{-2}	1.003×10^{-2}	(Nayar et al., 2016;Tchobanoglous et al., 2014)

3.7.2 Experimental Set-Up for Settling Velocity Measurement

Settling experiments were done in Armfield Sedimentation Studies Apparatus-W2 with a length of 1 m and diameter 51 mm, immobilized vertically on a backboard. The picture of the experimental set up is represented in the following Figure 10. The background is covered with checkerboard with 2 cm x 2 cm squares for calibration of the image tracking code. The sedimentation column was filled with deionized water with a density of 1.0 g/cm^3 to simulate freshwater density, 0.998 g/cm^3, at 19°C (Weast, 1972), salty water prepared by dissolving 25 g NaCl in 1 L deionized water to simulate seawater density, 1.025 g/cm^3, at 19°C (ITTC, 2011) and synthetic wastewater prepared by dissolving 50 g $C_6H_{12}O_6$ in 1 L deionized water to simulate wastewater density 1.050 g/cm^3 (Tchobanoglous et al., 2014).The motion of MPs through the sedimentation column was recorded with iPad Air (3rd generation) camera , with 1080p HD video recording at 30 fps. The experiments were conducted at 18.6 °C, the column was lighted by red neon led lighting strips fixed along the long sides of the column. MPs were released individually by tweezers 1 cm below the water surface to eliminate water surface tension effect as proposed by Wang et al. (2021).

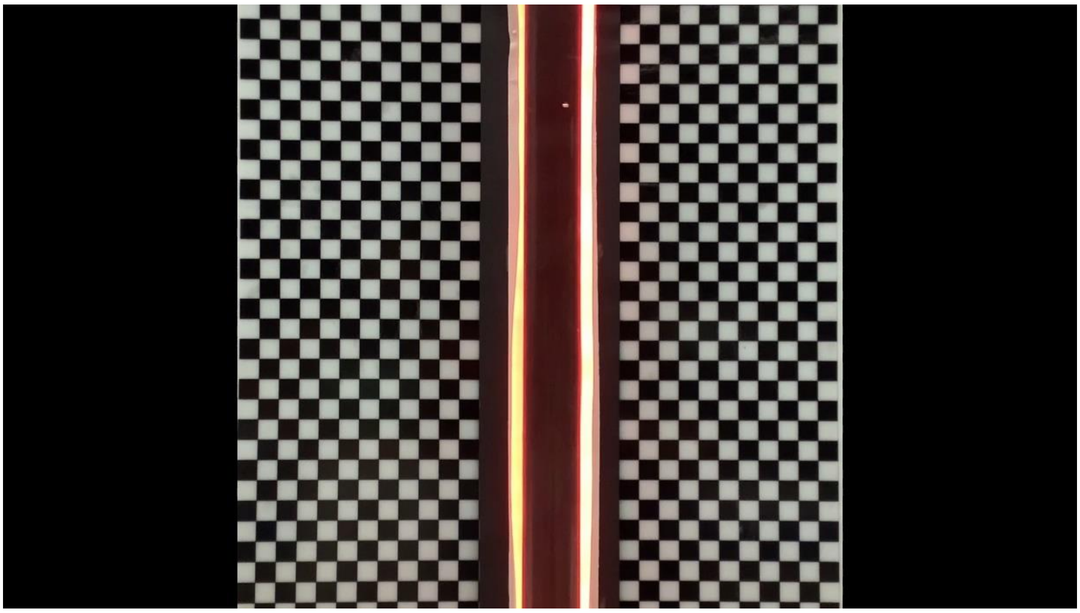

Figure 10 Settling Velocity Measurement Set Up

3.7.3 Description of MATLAB Image Tracking Code

Settling experiments were done by recording the free fall movement of the pristine MPs and MPs with biofilm formation in freshwater, wastewater and seawater filled in the column separately. A MATLAB code analysed the video recordings upon image processing algorithm modified from (Goral et al., 2021) and (Shafiei et al., 2016). Videos were prepared for code analysis by using video editing software tools. Videos were separated into frames by using the code cutCodeFun.m in Appendix A. Then, the code pre_RotDist.m in Appendix A was used for calibration. The mean calibration ratio for the transformation of pixel to meters was determined by marking the farthest points on the checkerboard both in horizontal and vertical directions. To illustrate, an example of the calibration process is given in Figure 11 and Figure 12. The calibration process was done for analysis of each case individually.

Next, SettlingVidAnlys_v1_Manual.m code in Appendix A measured the MP settling velocity through the column and the settling velocity profile. The mean calibration ratio was introduced. Frames created by cutCodeFun.m were entered into Settling Analysis code as initial and end number of the images. Manual tracking was performed on every 10 images by setting sampling division to 10. The particle's position versus time was determined and recorded as matrix, namely Repetition #.

As the final step, Repetition # matrix was analyzed by Settling Analysis.m code in Appendix A. The trial number was entered in the code and column height, 1m, camera fps, 30, confidence band limit for the graph, 95%, confidence band standard multiplier, 1.96, settling velocity measurement start and endpoints, which were adjusted manually for each measurement.

The number of repetitions was set to 10 based on the repetition analysis carried out by (Goral, 2020). According to the analysis, 10 repetitions would yield reliable results with a power of 80%. Frequency analysis was neglected, assuming it had a negligible effect on video analysis.

Figure 11 Calibration of the distance in horizontal direction

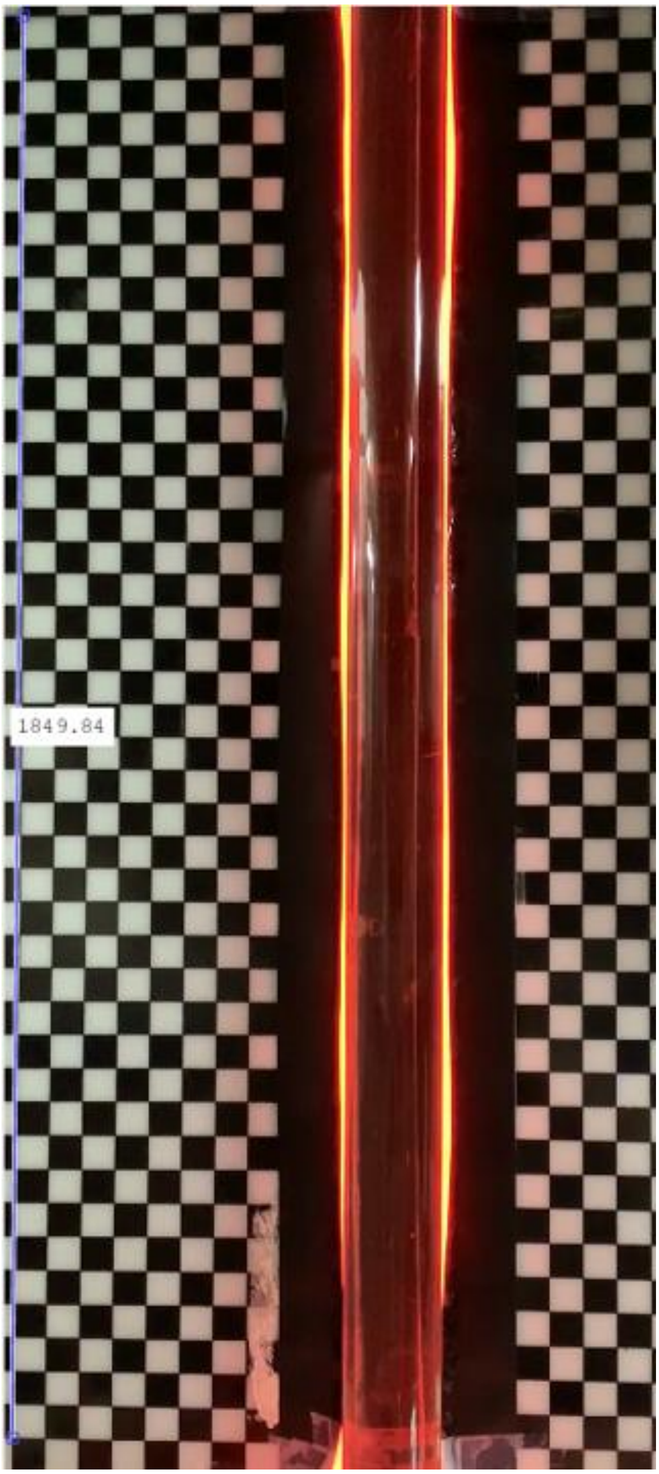

Figure 12 Calibration of distance in vertical direction

CHAPTER 4

RESULTS AND DISCUSSION

4.1 Bacteria Growth Mediums and Curves

Timewise change in bacteria growth mediums are given in Figure 13, Figure 14 and Figure 15 below. The appearance of the blank medium did not change, whereas growth medium with *E. coli* inoculation turned yellow with increasing turbidity with respect to time. *E. faecalis* growth medium had started to turn green by the 24^{th} hour, became nile green by the 72^{nd} hour and at the end of the experiment had a darker green colour. Likewise, *P. aeruginosa* growth medium became greenish which is expected as stated in (Labauve and Wargo, 2012), but not as much as *E. faecalis* culture medium.

Figure 13 Bacteria Growth Mediums at 24^{th} Hour
(Blank sample, *E. coli*, *E. faecalis*, *P. aeruginosa* cultures from left to right)

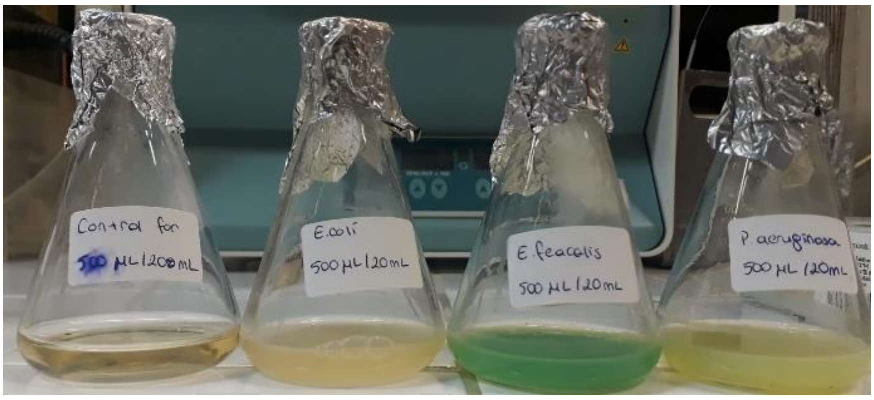

Figure 14 Bacteria Growth Mediums at 36th Hour
(Blank sample, *E. coli*, *E. faecalis*, *P. aeruginosa* cultures from left to right)

Figure 15 Bacteria Growth Mediums at 72th Hour
(Blank sample, *E. coli*, *E. faecalis*, *P. aeruginosa* cultures from left to right)

The growth curves of bacteria species in LB broth are displayed in Figure 16. *E. coli* culture reached to stationary phase where OD_{600} became stable around 1.8 at 12^{th} hour whereas *E. faecalis* and *P. aeruginosa* cultures did not go under a steady stationary phase. Rather, their OD_{600} values peaked at 48^{th} and 60^{th} hour respectively and switched to the death phase afterwards. It should be noted that the growth curve produced in this study was the growth curve of bacteria in bulk growth medium. To be able to fully assess timewise biofilm formation, biofilm growth must be measured as done by Kroukamp et al. (2010).

.

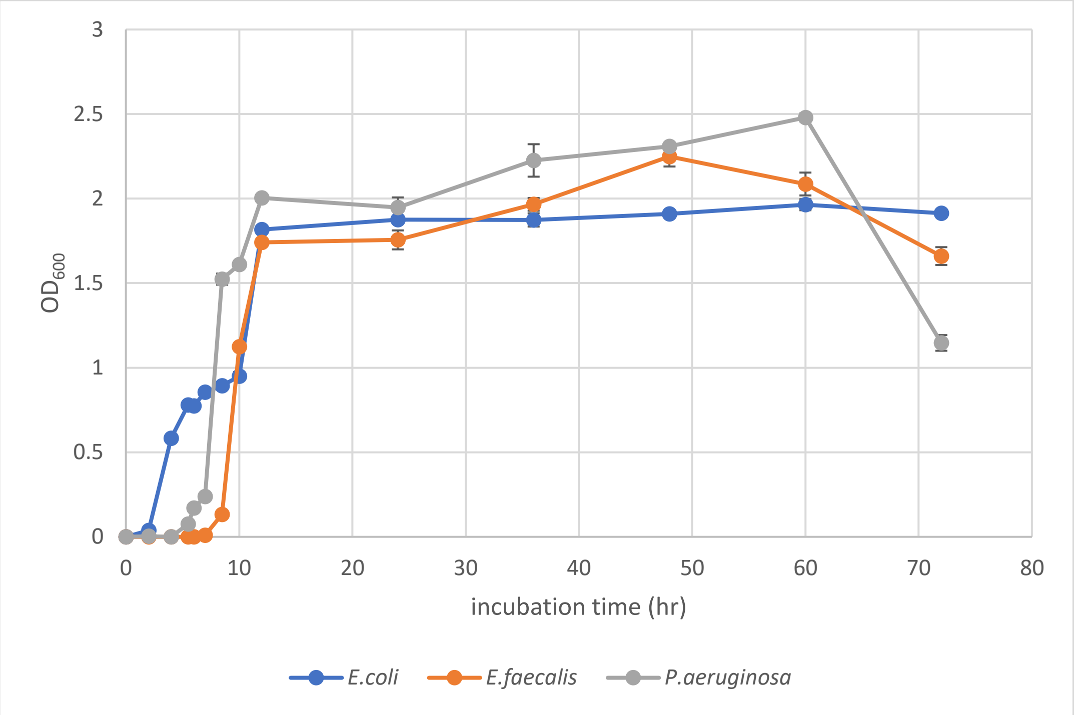

Figure 16 Growth curve of *E. coli*, *E. faecalis* and *P. aeruginosa* in LB Broth at 37°C, 80 rpm at different incubation times

4.2 Dry Weight Measurement Results

Results of dry weight measurements are given in

. The missing bars correspond to the MPs whose biofilm formation could not be detected using analytical balance. According to the available results, TPU had the highest biofilm formation in terms of dry weight at 24th and 48th hours. On the final day of the experiment, HDPE showed the highest biofilm formation by *E. faecalis* followed by *P. aeruginosa*. *E. coli* biofilm on LDPE showed an increasing trend from 24th hour to 72nd hour.

Biofilm formation on PP could only be detected at 48th hour by bacteria, *E. coli* and *P. aeruginosa.* Negligible amount of biofilm by *E. faecalis* on PP was detected.

Biofilm formation by *E. faecalis* on PET and PS particles could only be detected gravimetrically in the 24th hour.

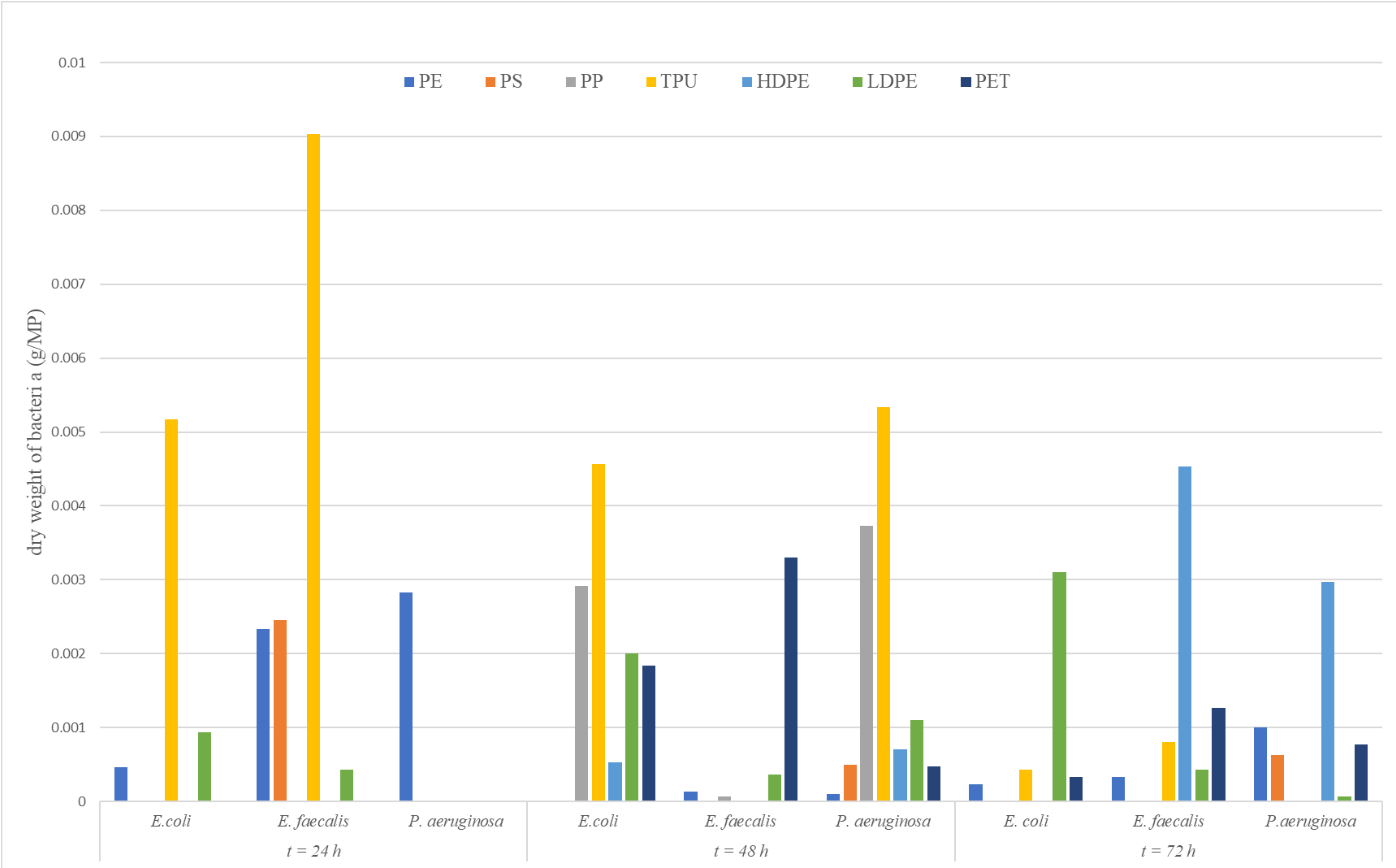

Figure 17 Dry weight measurements of biofilms at 24th, 48th and 72nd hours

4.3 Crystal Violet Staining Experiment Results

The crystal violet staining experiment results are shown in this section. The timewise biofilm formation on MPs by *E. coli*, *E. faecalis* and *P. aeruginosa* are presented in Figure 18, Figure 19 and Figure 20 respectively.

Colón-González et al. (2004) previously reported that highest biofilm formation by *E. coli* grown in LB broth occurred at 24^{th} hour in a 72-hour experiment. They explained this result by stating possible detachment of biofilm from the attached surface after incubation for a certain period of time. In this study, peak biofilm formation by *E. coli* at 24^{th} hour occurred only for biofilm grown on TPU, HDPE, PET and LDPE particles. For PS, biofilm formation peaked at 72^{th} hour, for PP, biofilm formation showed gradual increase with respect to time. Yet, biofilm formation assay in the study by Colón-González et al. (2004) was done on PVC dish surfaces. Since 7 different MPs were used as attachment surface in this study, the surface properties of these MPs could also affect the biofilm formation in addition to period of incubation. Zheng et al. (2021) listed the surface properties that influences biofilm formation as surface charge density, surface wettability, surface roughness, surface topography, surface stiffness and complex surface properties.

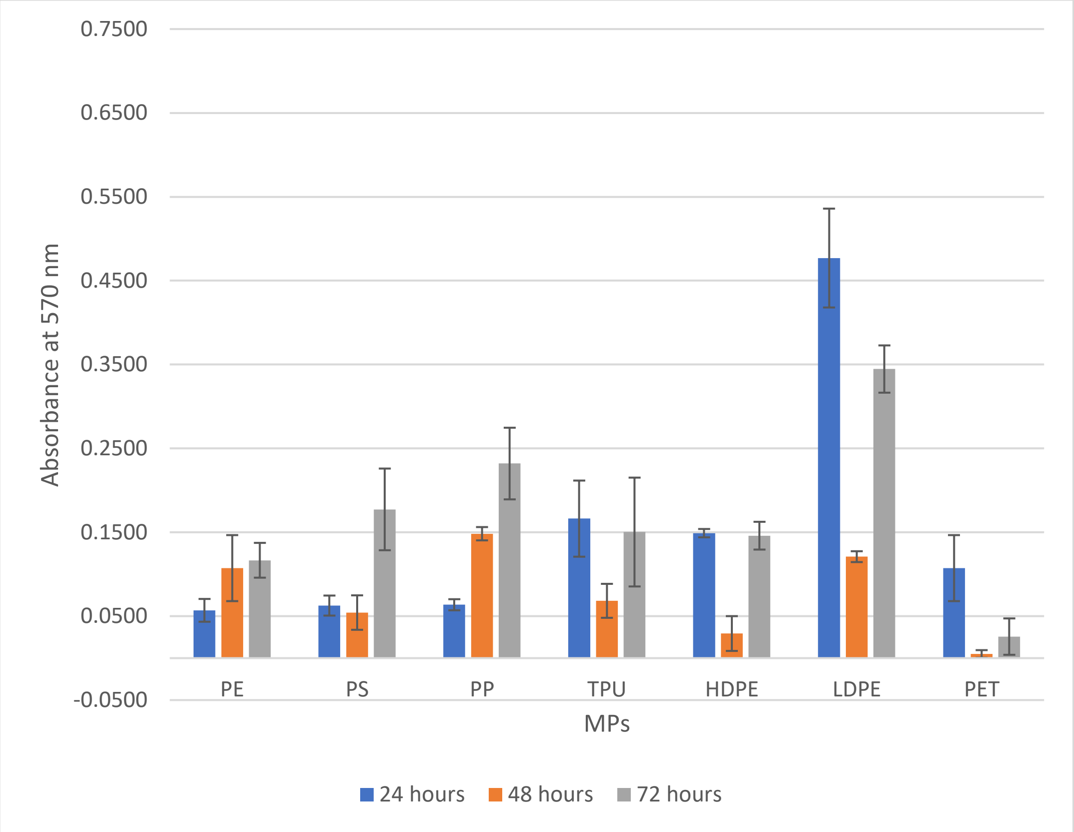

Figure 18 The Amount of *E. coli* biofilm formation on MPs in terms of absorbance measurement at 570 nm

High variances among replicates were observed in crystal violet staining of biofilm formed by *E. faecalis*. The highest biofilm formation *by E. faecalis* was observed on PP surface at 24^{th} hour. However, high standard deviations cause uncertainty in the results. Biofilm by *E. faecalis* on PS and HDPE surfaces at 24^{th} hour, and on PET at 24^{th} and 48^{th} hours could not be detected by using crystal violet staining.

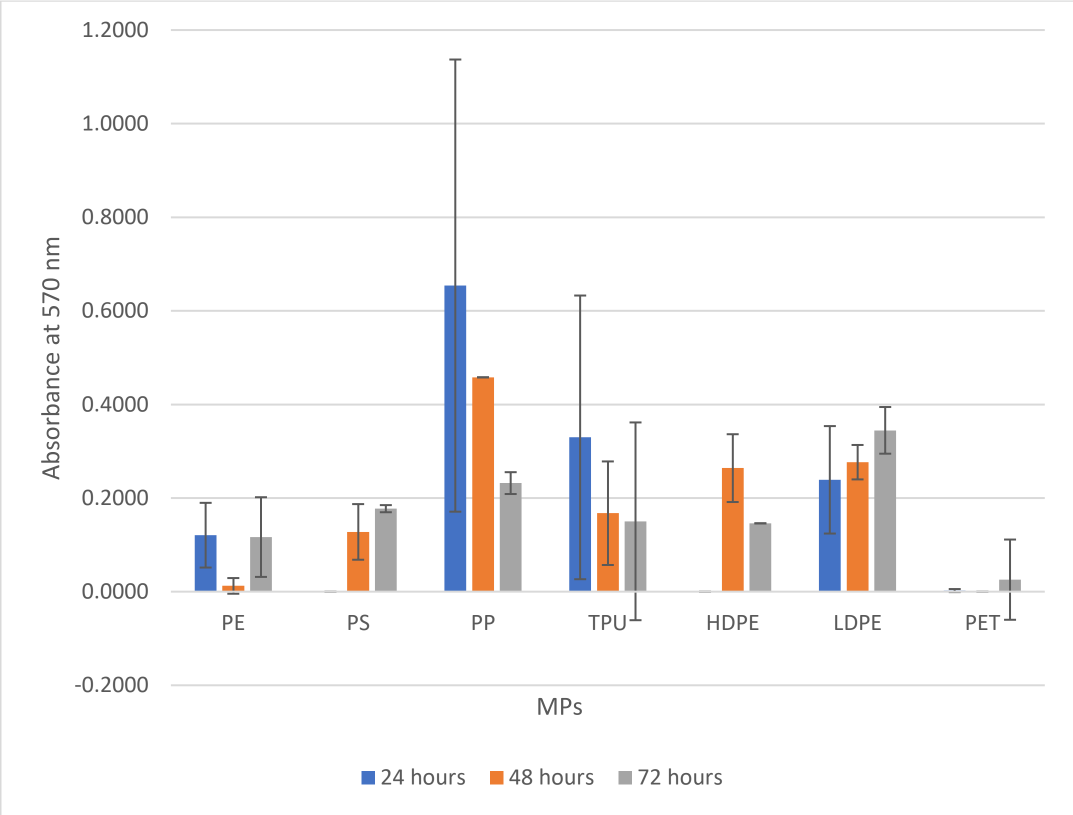

Figure 19 The amount of *E. faecalis* biofilm formation on MPs in terms of absorbance measurement at 570 nm

Although high variances among replicates are also valid for *P. aeruginosa* biofilms, biofilm amount on PE, PS and TPU particles followed a similar pattern, gradually increasing with respect to time. Highest biofilm formation was observed on LDPE, similar to the case in *E. coli*, except from the period of incubation, as the biofilm formation peaked at 48th hour.

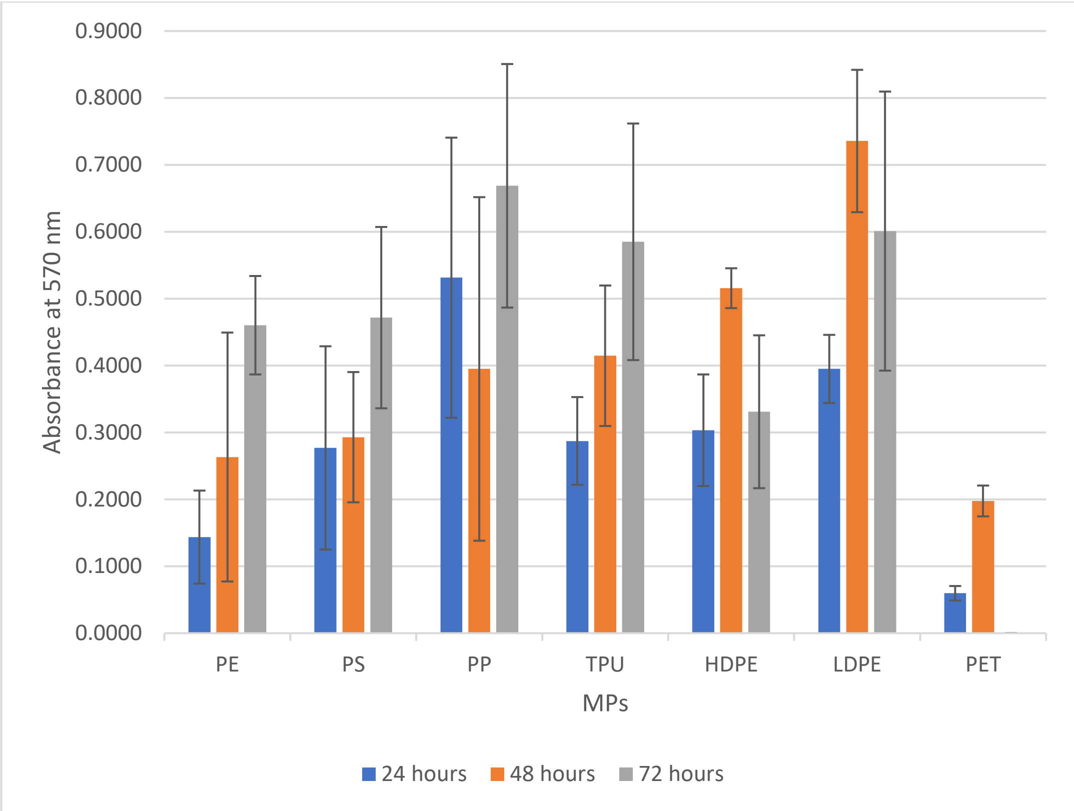

Figure 20 The amount of *P. aeruginosa* biofilm formation on MPs in terms of absorbance measurement at 570 nm

4.4 SEM Analysis Results

Surface morphological structure of pristine MPs' can be seen in Figure 21. Surface coverage by *E. coli* on HDPE surface can easily be detected by bacillus shape bacteria in Figure 22. Lower biofilm abundance was observed on LDPE, PE, PET, PP and PS surfaces. Rather than biofilm, single bacillus shape bacteria was detected on TPU surface. However, it should be considered that these images were taken on specific parts of the particle surfaces, they do not reflect the overall surface area.

E. faecalis biofilms showed higher coverage than *E. coli* on MPs especially on HDPE, LDPE and PET as visualised in Figure 23. The shapes of bacteria identified were coccus, diplococcus, and streptococcus.

Higher bacteria colonization on MP surface was also observed by *P. aeruginosa* on MPs as well. In Figure 24, on LDPE, PE and PET surfaces, biofilm formation by bacillus shape bacteria can be seen. In addition, biofilm entering the pores on the PP surface was captured, which might reveal that beyond changing surface characteristics, biofilm formation may also alter the internal structure of MPs.

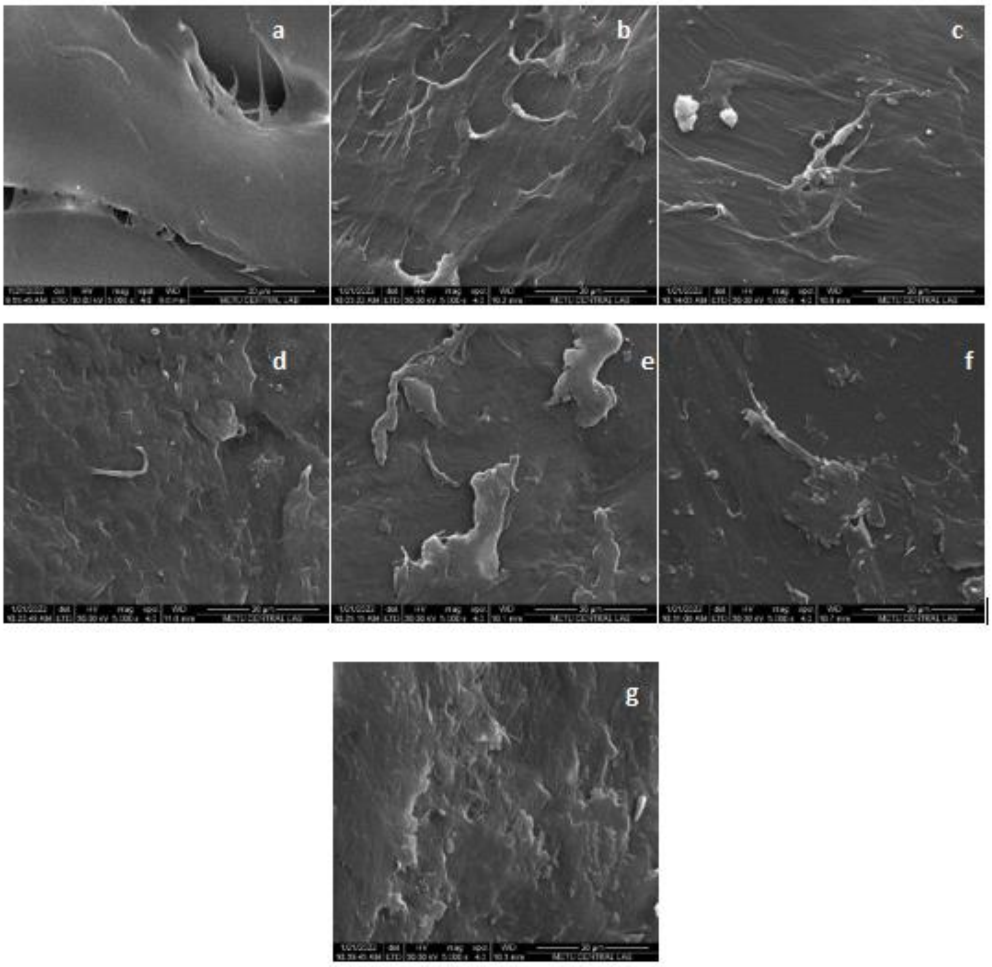

Figure 21 SEM pictures of pristine MPs
a) HDPE, b) LDPE, c) PE, d) PET, e) PP, f) PS, g) TPU

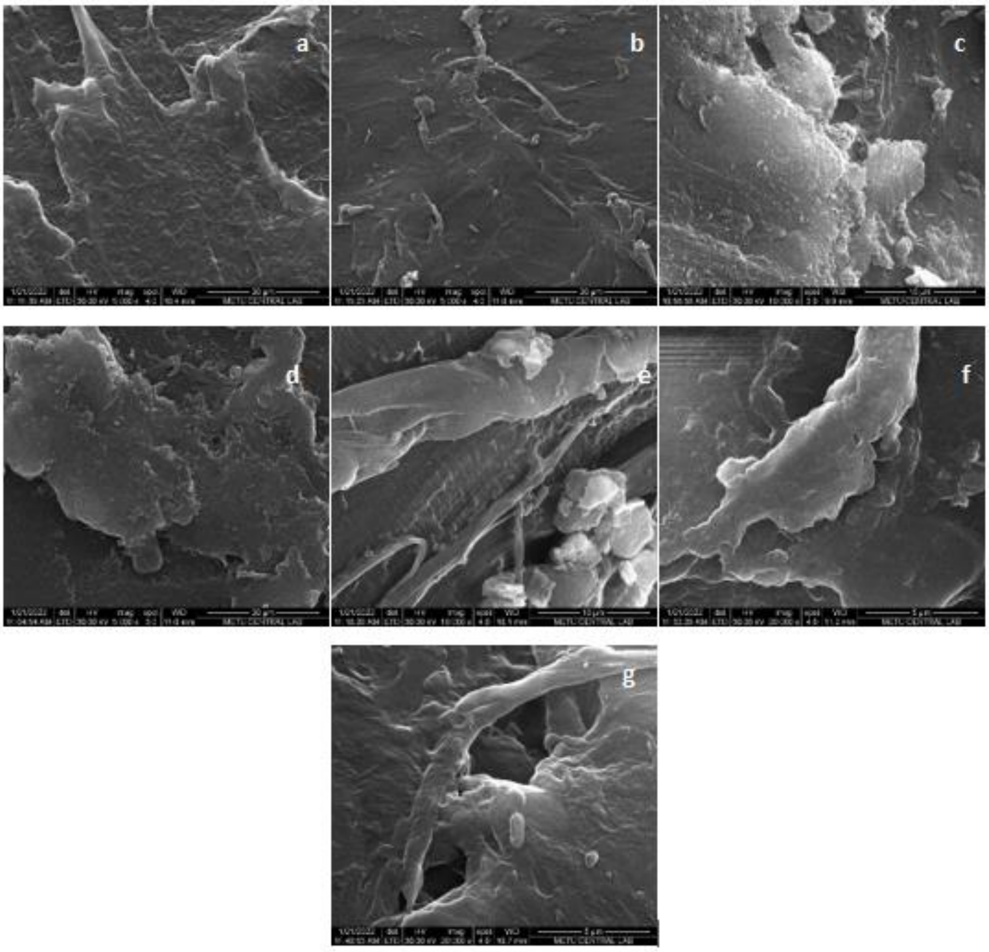

Figure 22 SEM pictures of MPs with biofilm formation by *E. coli*
a) HDPE, b) LDPE, c) PE, d) PET, e) PP, f) PS, g) TPU

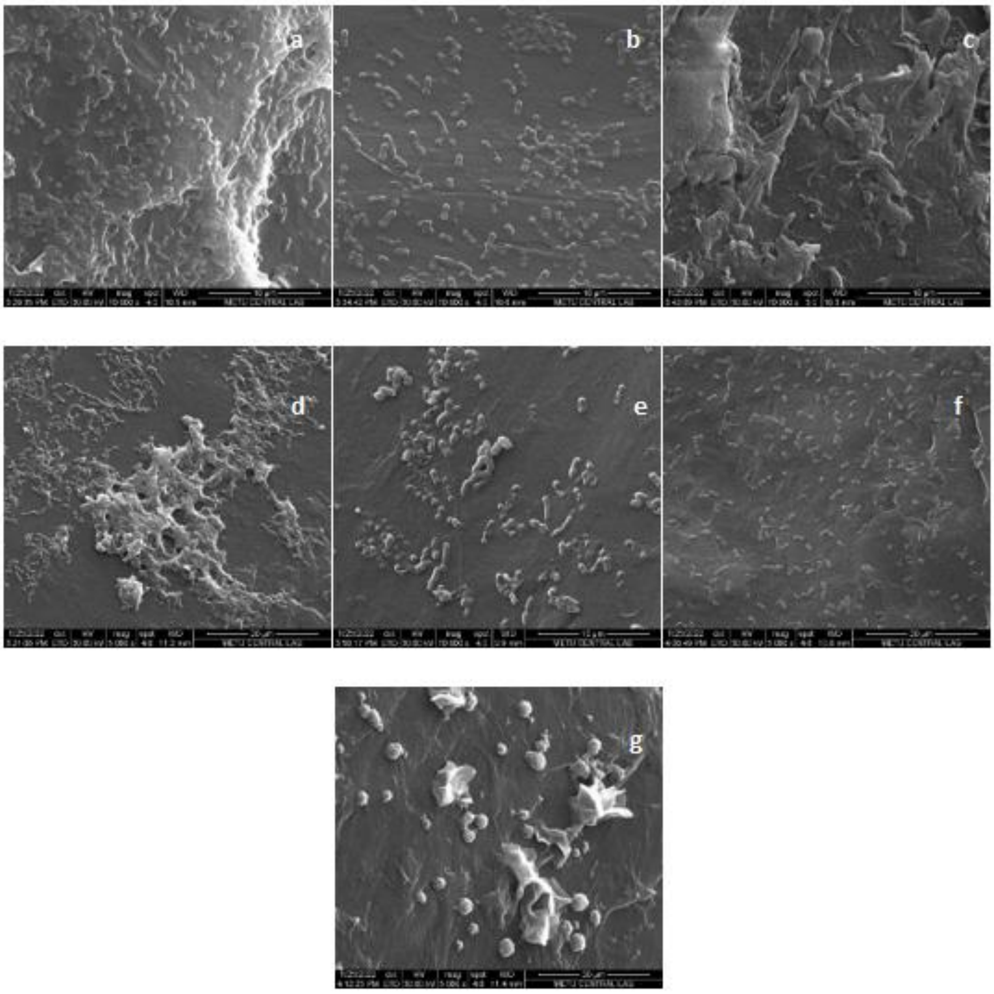

Figure 23 SEM pictures of MPs with biofilm formation by *E. faecalis*
a) HDPE, b) LDPE, c) PE, d) PET, e) PP, f) PS, g) TPU

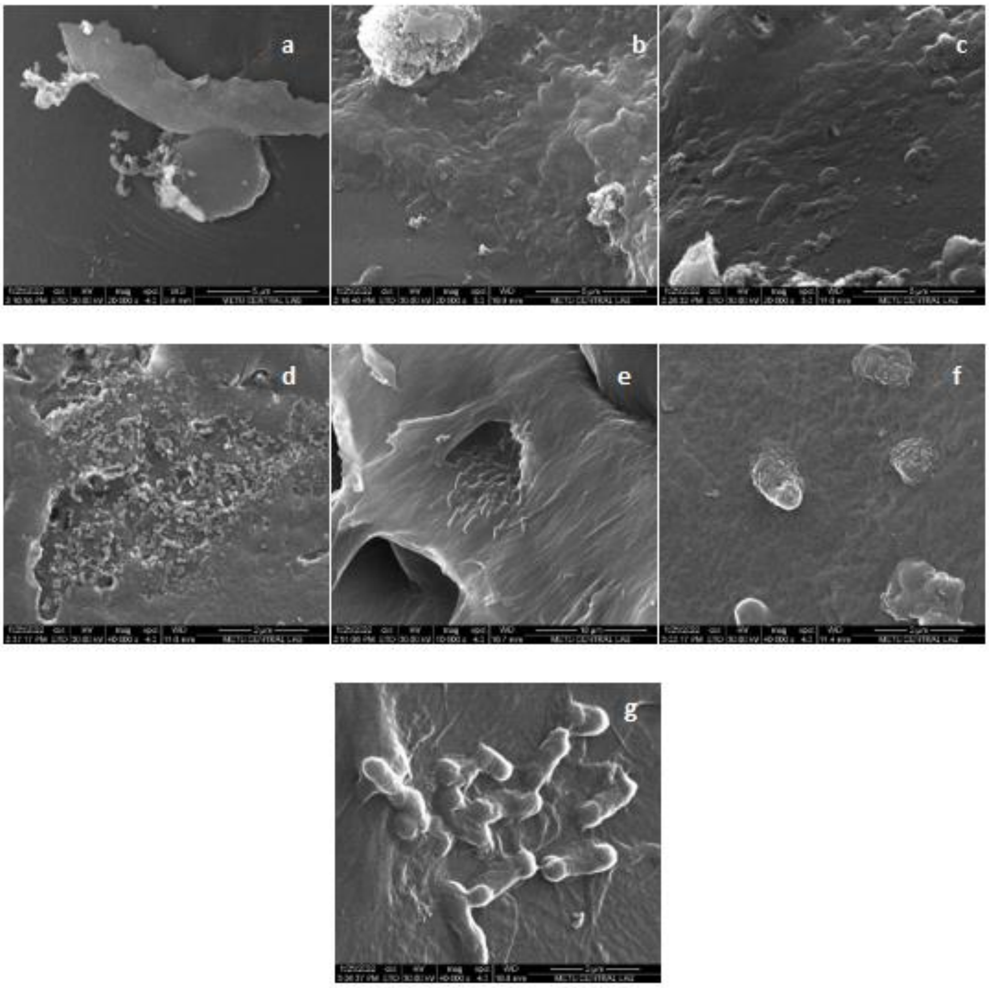

Figure 24 SEM pictures of MPs with biofilm formation by *P. aeruginosa*
a) HDPE, b) LDPE, c) PE, d) PET, e) PP, f) PS, g) TPU

4.5 Settling Velocity Measurement Results

4.5.1 Settling Velocity Measurement Results of Pristine MPs

Settling velocity profiles of pristine MPs are presented in this section. The settling velocities of each MPs are given by showing the mean of the repetitions and the 95% confidence bands for the mean line. The profiles for freshwater are available in Figure 25, seawater in Figure 26 and wastewater in Figure 27. The x axis, named as *y* indicates the column length (m), 0 meaning the location where MP was released. The y axis named as V_y indicates the settling velocity (m/s). Dashed red line represents the confidence interval (95%), grey lines demonstrate the settling velocity profiles of the repetitions, and the black line shows the mean settling velocity profile.

LDPE, HDPE, PE and PS MPs did not show settling behaviour due to their lower density than deionized water, and they floated on the water surface. Upon 10 measurements, pristine PET particles had a settling velocity of 1.1891 ± 0.0441 m/s. Wang et al. (2021) reported the settling velocity of near-spherical PET particles with an equivalent spherical diameter of 1.927 mm in 0.980 g/cm^3 water solution as 9.074 cm/s, much higher than the value found by this study. The same study reported the settling velocities of polygonal ellipsoid PS, equivalent spherical diameter of 1.195 mm, and near-spherical PS, equivalent spherical diameters, 1.16 mm as 1.323 cm/s, 1.317cm/s respectively, still higher values than 0.3296 cm/s that is found by this study.

Although the size and densities of the materials are similar in this study and (Wang et al., 2021), the density of the water used is different and the mechanism of establishing the settling velocity was not dependent on an image tracking code. The difference between the literature measured and obtained values is probably the settling velocity measurement method Wang et al., 2021 calculate settling velocity by simply dividing particle travel distance by travel duration. This basic technique neglects the acceleration period of the particle before the particle reaches terminal settling velocity. Therefore, estimating a methodology that could consider complex variables such is probably a more accurate way of describing the settling.

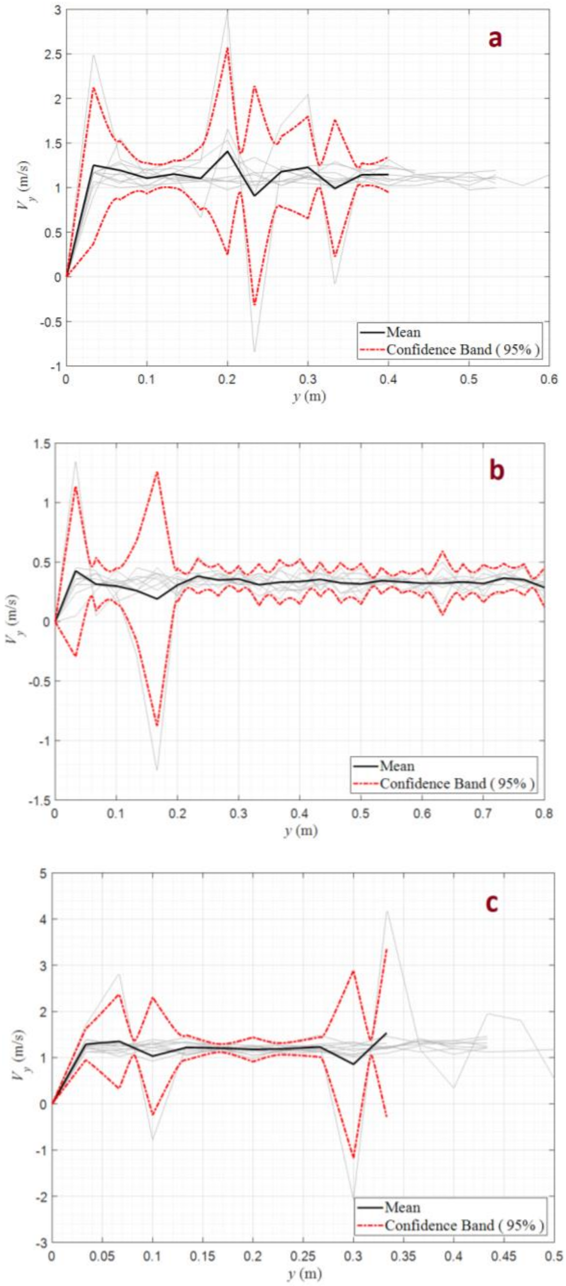

Figure 25 Settling velocity profiles of pristine MPs in deionized water column, a) PET, b) PS and c) TPU

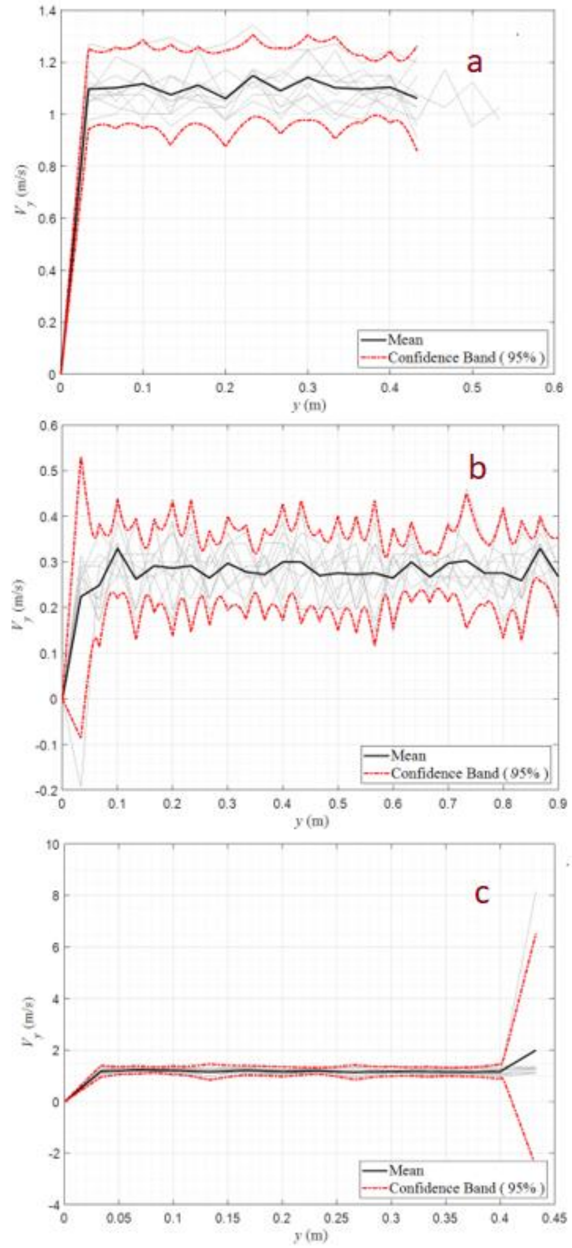

Figure 26 Settling velocity profiles of pristine MPs in seawater column,
a) PET, b) PS and c) TPU

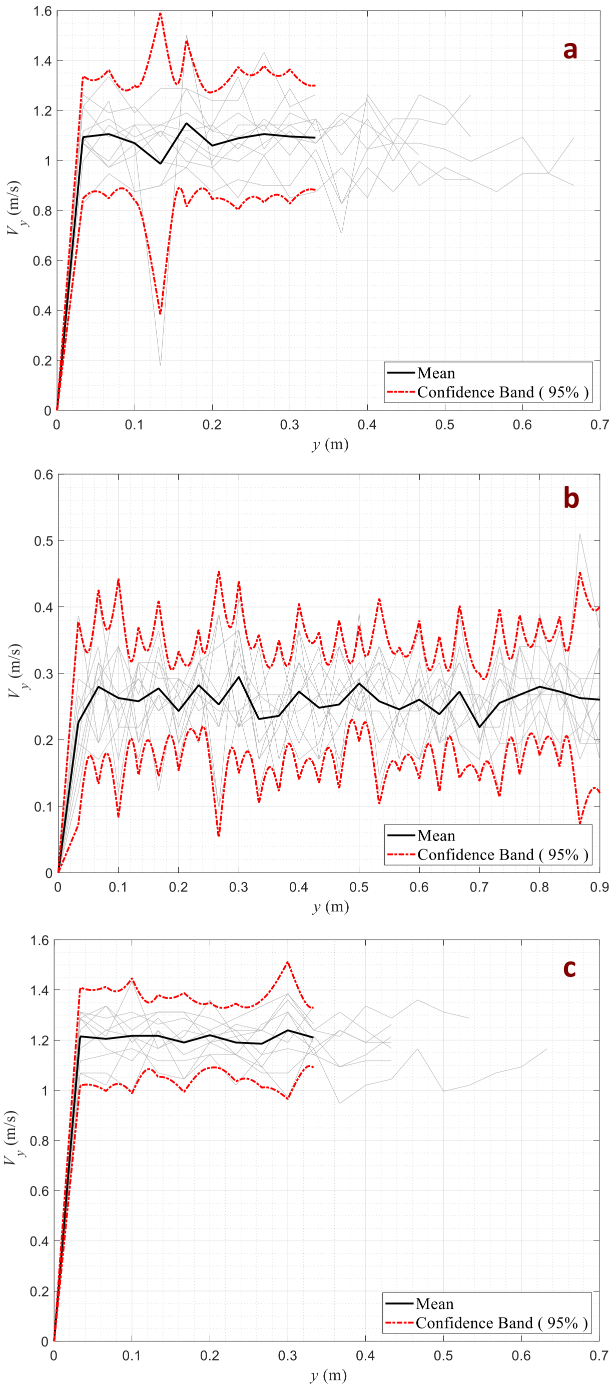

Figure 27 Settling velocity profiles of pristine MPs in wastewater column, a) PET, b) PS and c) TPU

Mean settling velocities of pristine MPs measured are given in Figure 28. Particles were expected to have the highest settling velocities in freshwater and lowest in wastewater due to densities of these liquids. This expectation was met for PS particle. However, PET and TPU particles had slightly lower settling velocity in seawater than wastewater column. This might be caused by not attaining well mixed conditions in seawater and wastewater columns.

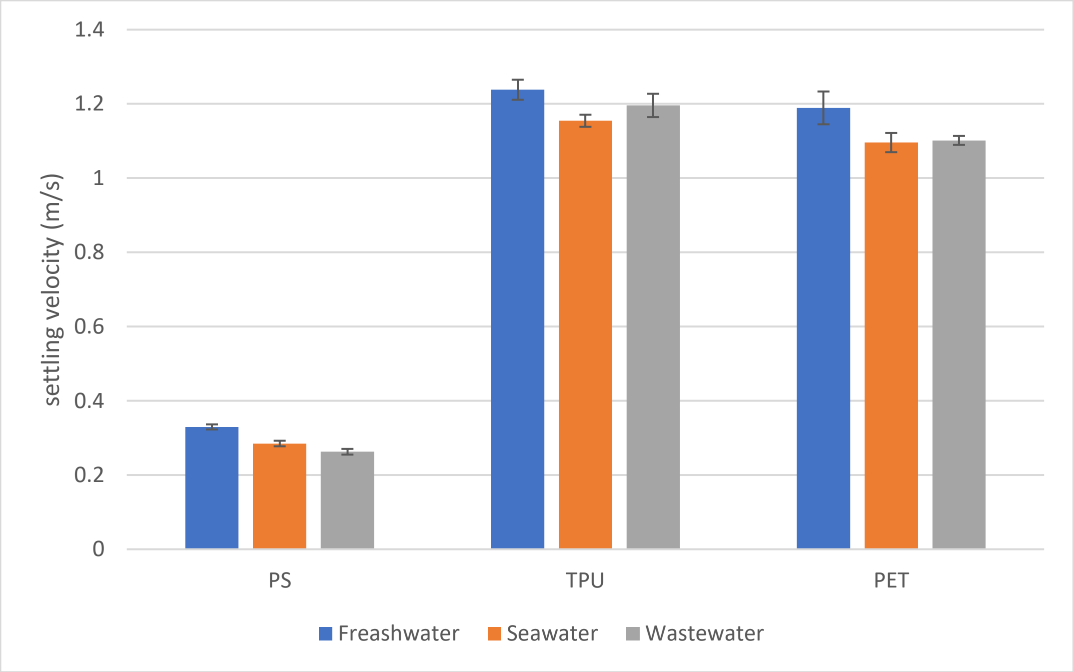

Figure 28 Mean settling velocities of pristine MPs in different water columns

4.5.2 Comparison Between Theoretical and Measured Settling Velocities of Pristine Microplastics

Theoretical settling velocities calculated by using Stoke's law and corresponding N_R values calculated are available in Table 9. N_R values were lower than 1 in all of the cases, meaning that laminar flow conditions were held and Stoke's law was applicable (Tchobanoglous et al., 2014).

Table 9 N_R values calculated for theoretical settling velocities

MPs	Theoretical Settling Velocity (m/s)			N_R (dimensionless)		
	Freshwater	Seawater	Wastewater	Freshwater	Seawater	Wastewater
PET	2.19	1.94	1.37	0.22	0.19	0.10
PS	0.64	0.29	0.00	0.10	0.04	0.00
TPU	2.35	1.92	1.24	0.35	0.28	0.14

Theoretical settling velocities were compared with the mean settling velocities measured by MATLAB image tracking code. The comparative figure showing theoretical and measured settling velocities are given in Figure 29. The percentage differences between theoretical and measured settling velocities are calculated by formula given as Equation 3. The results are tabulated in Table 10.

$$Percentage\ difference\ (\%) = \frac{(Theretical\ settling\ velocity - Measured\ settling\ velocity)}{Measured\ settling\ velocity}\ x\ 100 \quad \text{Equation 1}$$

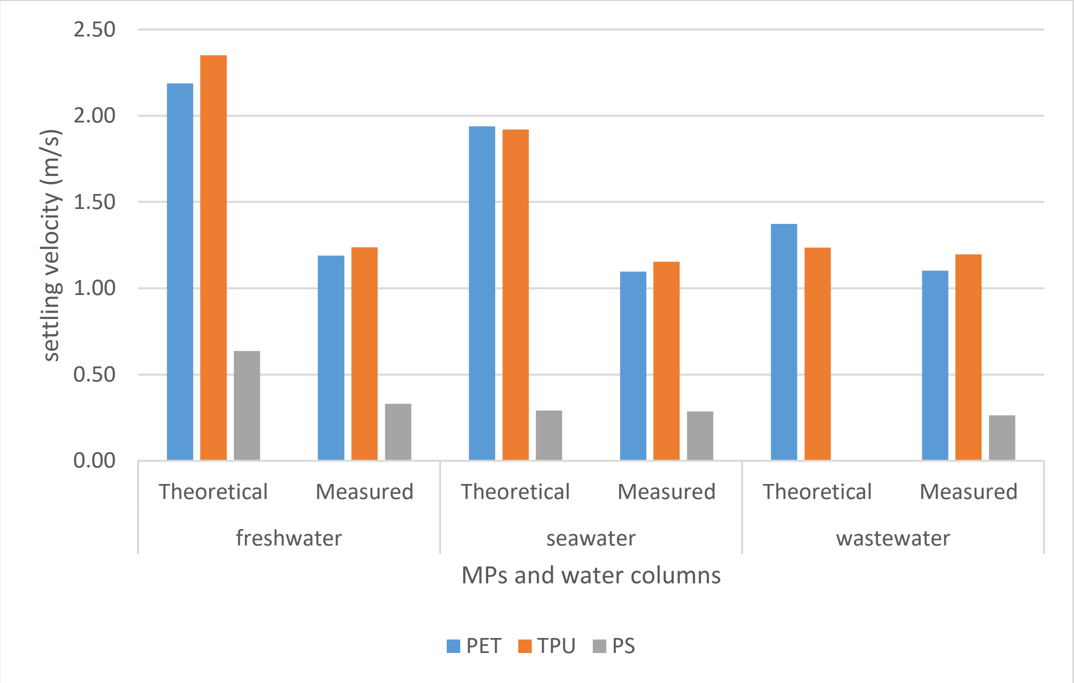

Figure 29 Comparison between settling velocities calculated by Stoke's law and measured by MATLAB code

Table 10 Percentage differences between theoretical and measured settling velocities of pristine MPs

MPs	Percentage Difference (%)		
	Freshwater	Seawater	Wastewater
PET	83.9	76.9	24.6
PS	93.0	2.1	-100.0
TPU	89.8	66.3	3.3

According to the comparative results, theoretical settling velocities were higher in almost all the cases except from PS in wastewater. The reason is, as the Equation 1 implies, theoretical settling velocity of PS particle in wastewater column is equal to zero as the particle density is equal to wastewater density, meaning the particle would not settle theoretically. In contrast, PS particle did settle in the wastewater column as visualized by the video recording with a mean settling velocity of 0.2628 m/s. This major difference could be attributed to the heterogeneous dispersion of glucose molecules in deionized water, although complete dissolution was maintained by mixing vigorously, yielding uneven water density throughout the column. As Figure 27 displays, PS particles showed oscillating pattern in settling velocity profile, meaning that the particle travelled along the column with altering velocities.

The variations between theoretical and measured settling velocities were the highest for all MPs travelling in freshwater column. The variations lowered in seawater and wastewater apart from PS in wastewater, which has been previously discussed. The reason was certainly that the Stoke’s law is valid for spherical particles whereas PET and PS particles were cylindrical and TPU was not perfectly sphere. The sphericity factor, the ratio of the surface area of a sphere having the same volume as a given particle to the surface area of the particle, must be implemented in Equation 1 for such cases. Yet, in this study, the surface areas of the MPs were not known of. Therefore, sphericity factor was neglected in calculations. On the other hand, MATLAB image tracking algorithm provided the mean settling velocities without the use of physical properties of the particles. Deviations from ideal cases, such as density, viscosity or temperature heterogeneity in water columns are not reflecting in Stoke’s law. Implementing a code-based measurement method would give more accurate and factual results.

4.5.3 Settling Velocity Measurement Results of Biofilm Formed MPs

Initially non-settling particles, LDPE, HDPE, PE and PP, did not settle after biofilm formation by bacteria species studied, although (Chubarenko et al., 2016) discussed that biofouling was the key factor for settling of slightly buoyant MPs such as PE and PP. In this study, biofilm formed in 72 hours was not heavy enough to sink down; they floated on the water surface. Expectedly, there had been changes in settling velocities of initially settling particles, PS, TPU and PET.

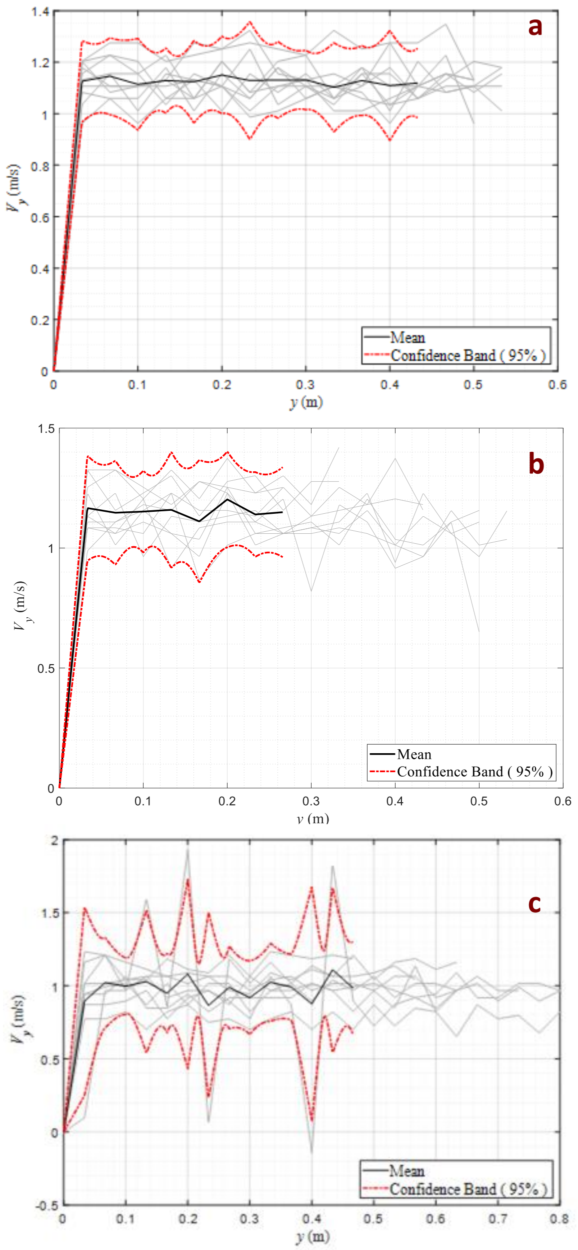

Figure 30 Settling velocity profile of PET MPs with biofilm formation by a) *E. coli*, b) *E. faecalis* and c) *P. aeruginosa* in deionized water column

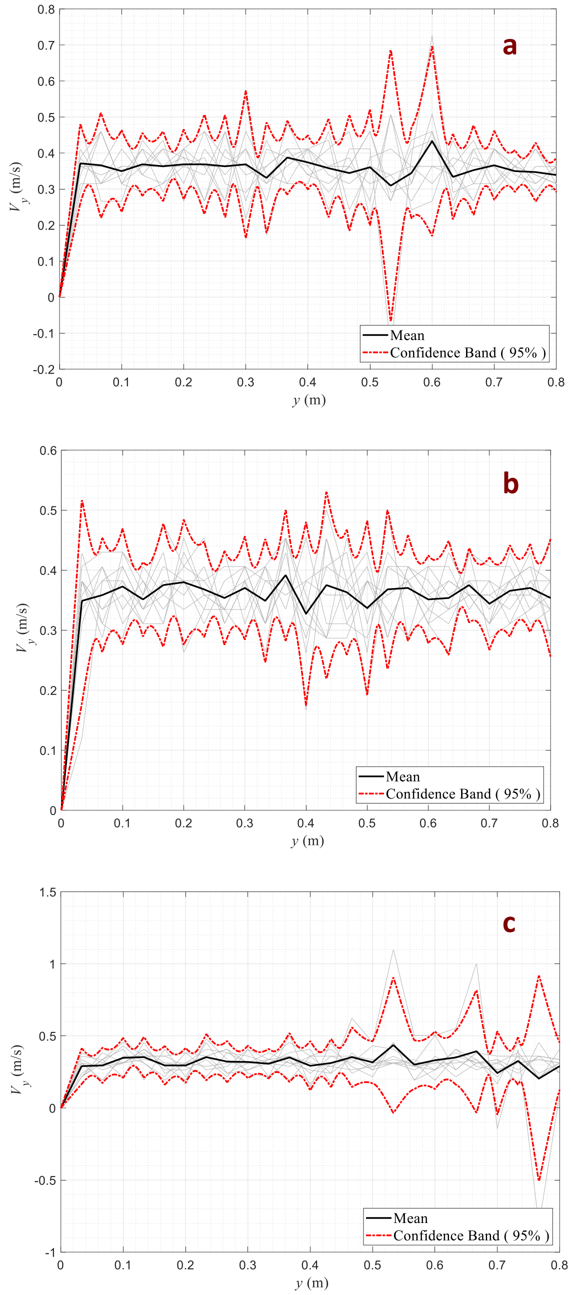

Figure 31 Settling velocity profile of PS MPs with biofilm formation by a) *E. coli*, b) *E. faecalis* and c) *P. aeruginosa* in deionized water column

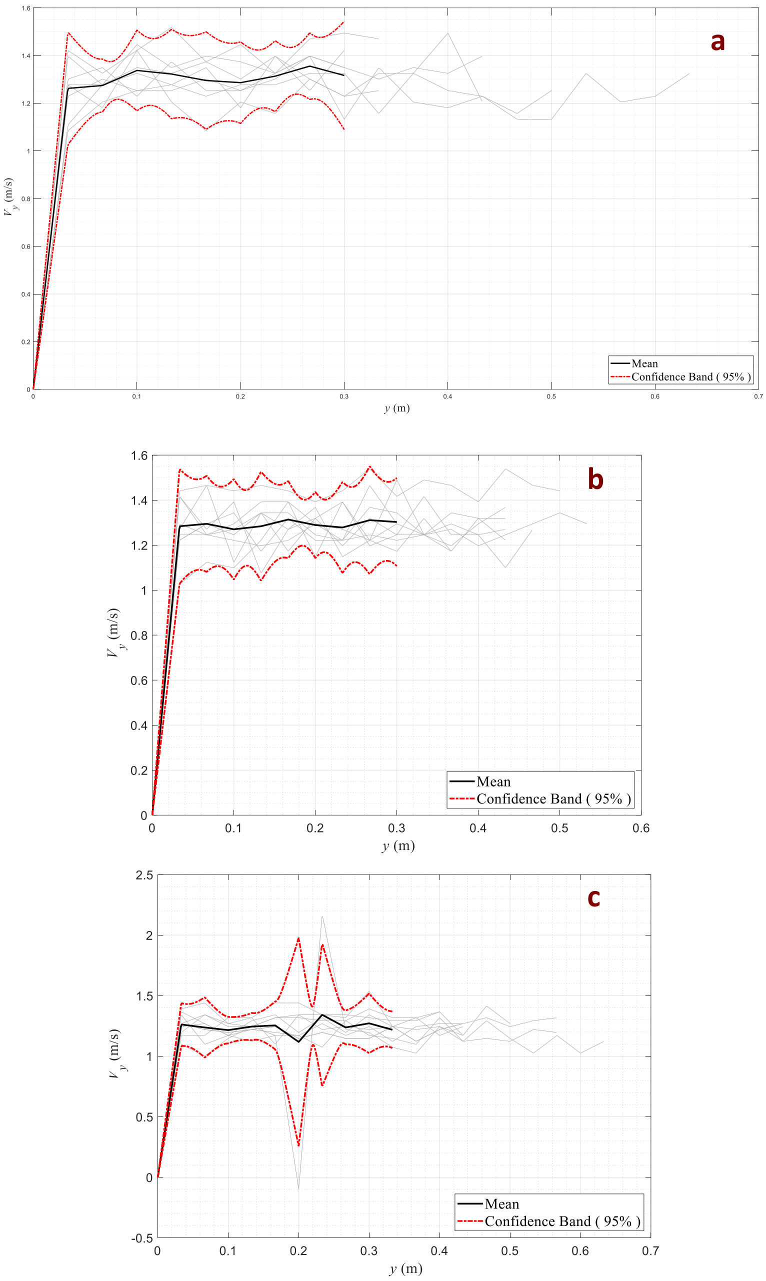

Figure 32 Settling velocity profile of TPU MPs with biofilm formation by a) *E. coli*, b) *E. faecalis* and c) *P. aeruginosa* in deionized water column

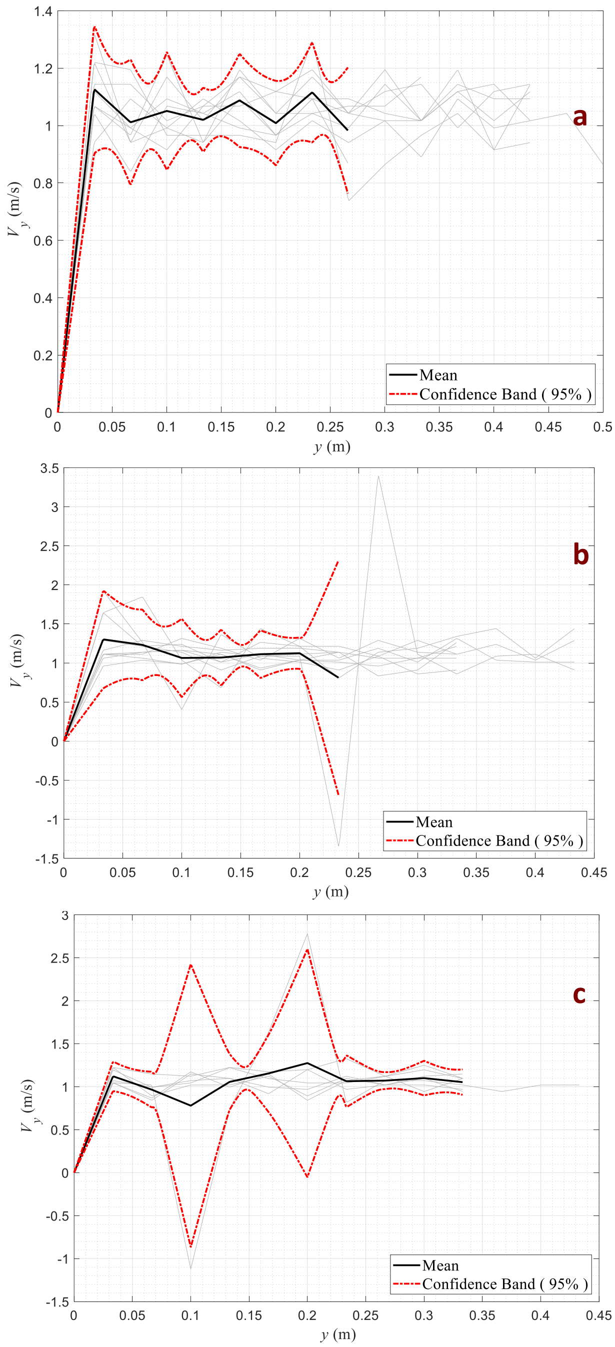

Figure 33 Settling velocity profile of PET MPs with biofilm formation by a) *E. coli*, b) *E. faecalis* and c) *P. aeruginosa* in seawater column

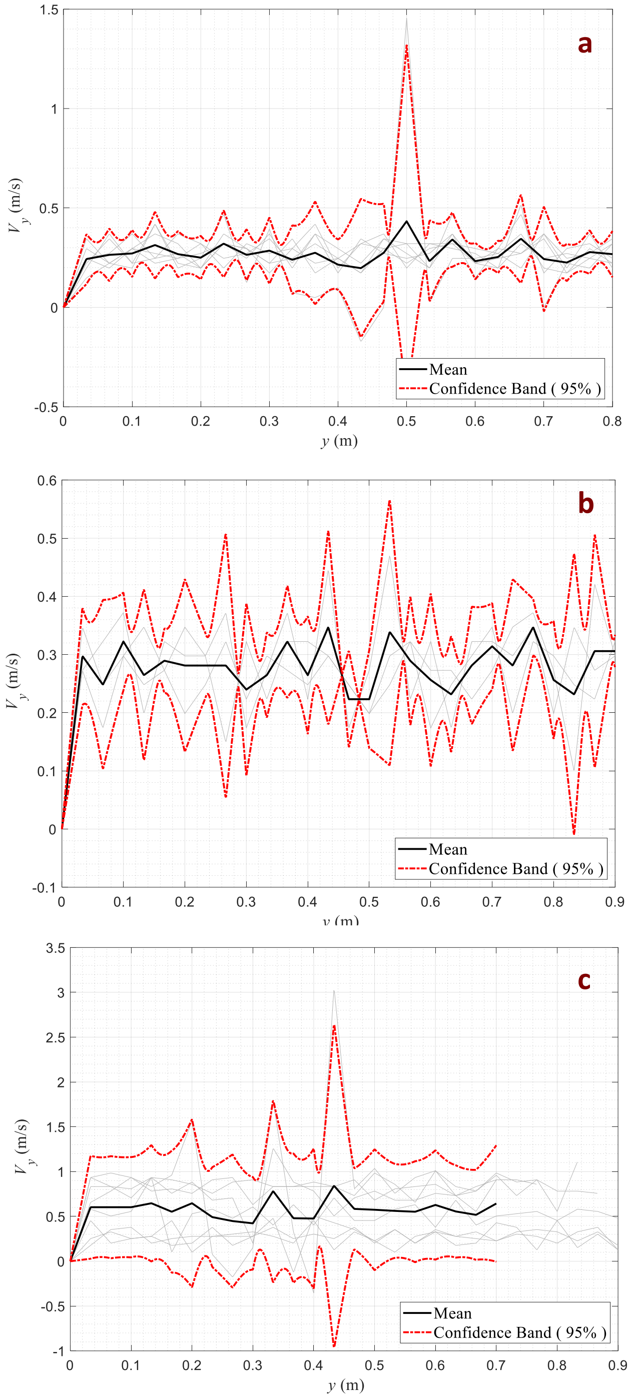

Figure 34 Settling velocity profile of PS MPs with biofilm formation by a) *E. coli*, b) *E. faecalis* and c) *P. aeruginosa* in seawater column

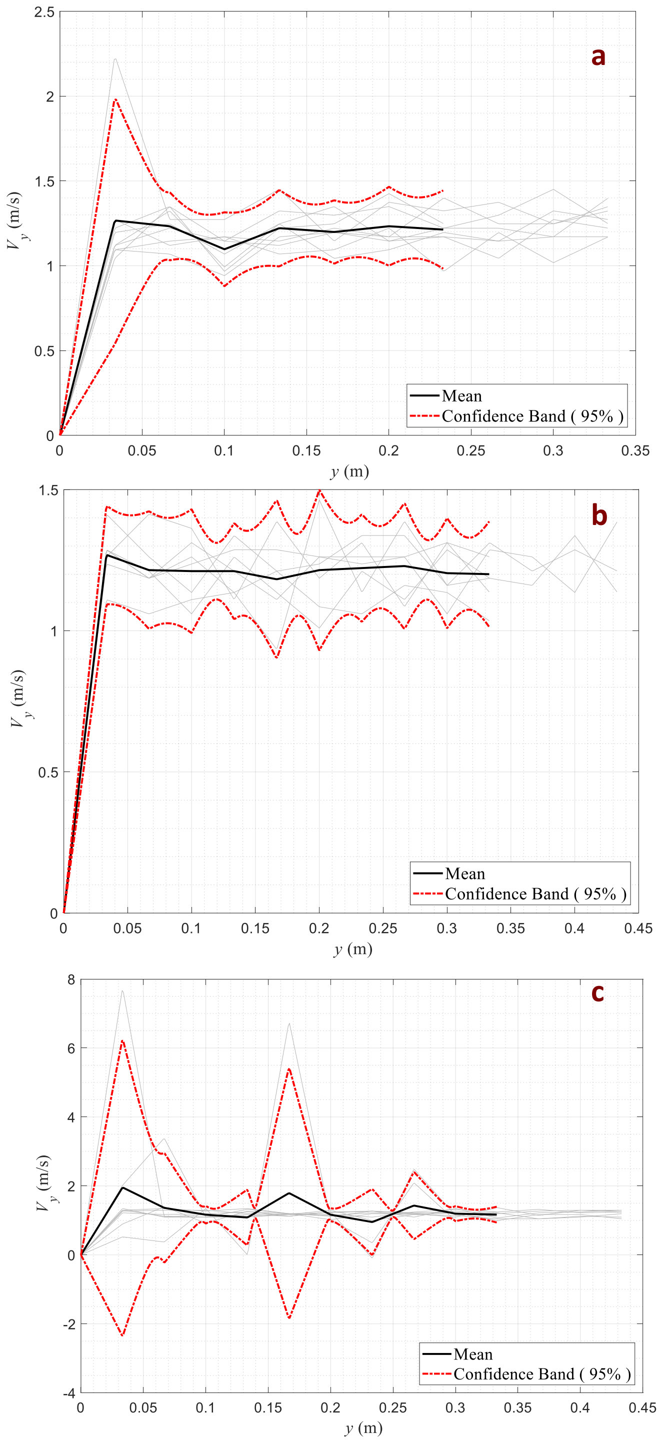

Figure 35 Settling velocity profile of TPU MPs with biofilm formation by a) *E. coli*, b) *E. faecalis* and c) *P. aeruginosa* in seawater column

As a summative assessment, mean settling velocities of biofilm formed MPs in freshwater are collected in Figure 36 and Figure 37. According to the results, settling velocity of PS particles increased 8.2 % due to biofilm formation by *E. coli* and 10.1% by *E. faecalis* and showed a 12.0% decrease by *P. aeruginosa* in freshwater. Biofilm formation by *E. faecalis* on TPU surface increased TPU settling velocity by 5.7% but, *E. coli* and *P. aeruginosa* biofilm formation reduced particle settling velocity by 4.1% and 0.96% in order. In the case of PET, biofilm formation by all species caused retardation of settling. *P. aeruginosa* biofilm formation significantly lowered the particle settling by almost 22%.

P. aeruginosa biofilm caused a decrease in settling velocities of all initially settling MPs in freshwater. The reason could be the sticky texture of *P. aeruginosa* culture medium after 72 hours of incubation. The highly viscous layer around MP surface due to EPS formation by *P. aeruginosa* could have slowed down the settling of the MPs. Myszka and Czaczyk (2009) proposed that EPS formation increases as the incubation time increases, where the starvation conditions take place. In this study, as previously discussed in section 4.1, *P. aeruginosa* culture exhibited death phase after 60^{th} hour of the experiment. This could have triggered EPS production by P. *aeruginosa*, resulting in highly viscous biofilm matrix. Further, the MPs covered with this biofilm matrix would be subjected to higher drag force in water columns than of pristine MPs and less EPS covered MPs. Lattermost, increased drag force acting upon MP particles would cause lower settling velocities as Stoke's law states (Tchobanoglous et al., 2014).

One other interesting result is the effect of biofilm formation by *E. coli* on the sinking behaviour of MPs in freshwater. Although it caused around 5% decrease in settling velocities of TPU and PET particles, PS settling velocity was increased by 8.2%.

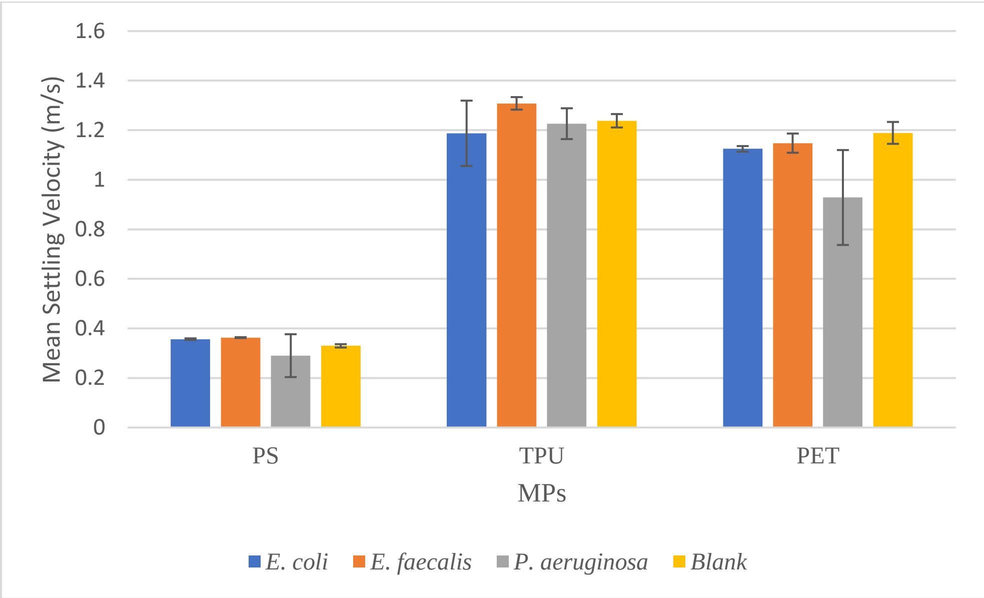

Figure 36 Summarizing results of MP settling velocities in freshwater after 72 hours of incubation in LB broth medium at 37°C, 80 rpm

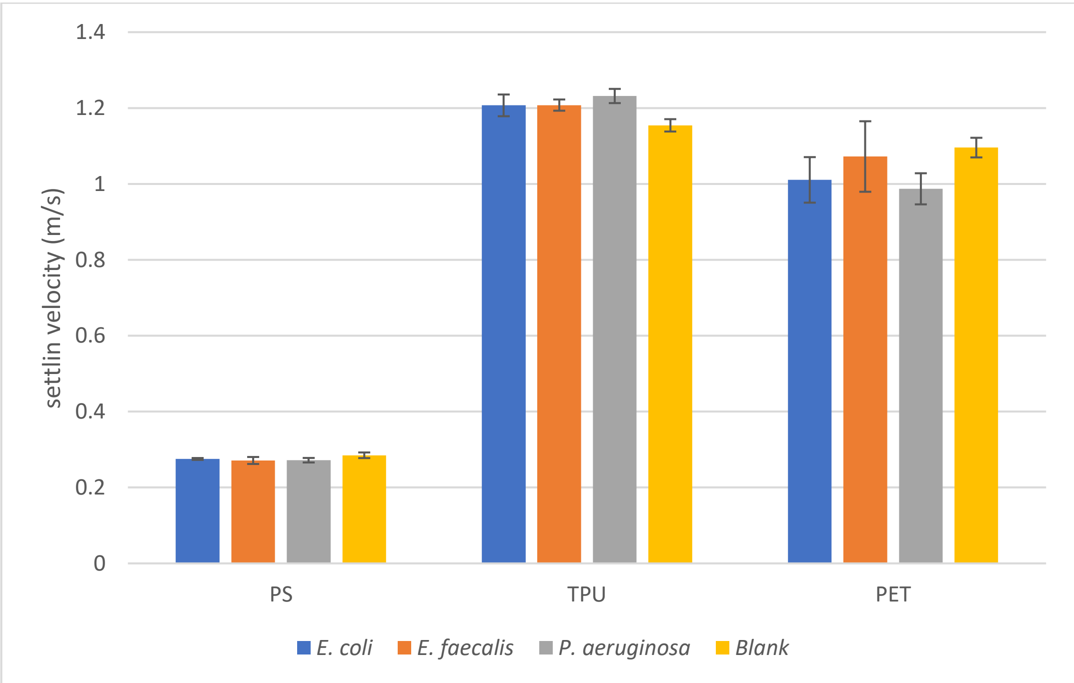

Figure 37 Summarizing results of MP settling velocities in seawater water after 72 hours of incubation in LB broth medium at 37°C, 80 rpm

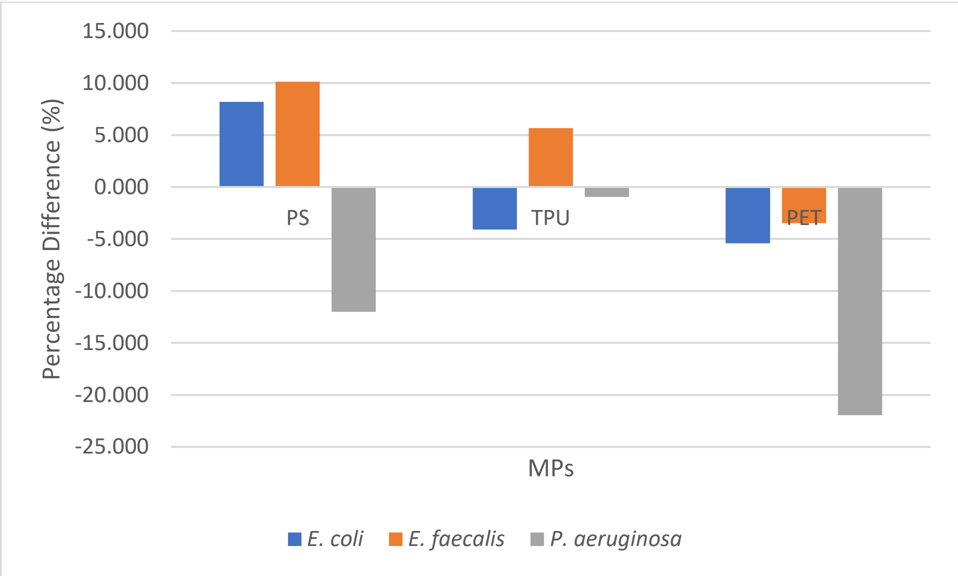

Figure 38 Percentage difference of settling velocities of MPs after biofilm formation with respect to settling velocities of pristine MPs in freshwater

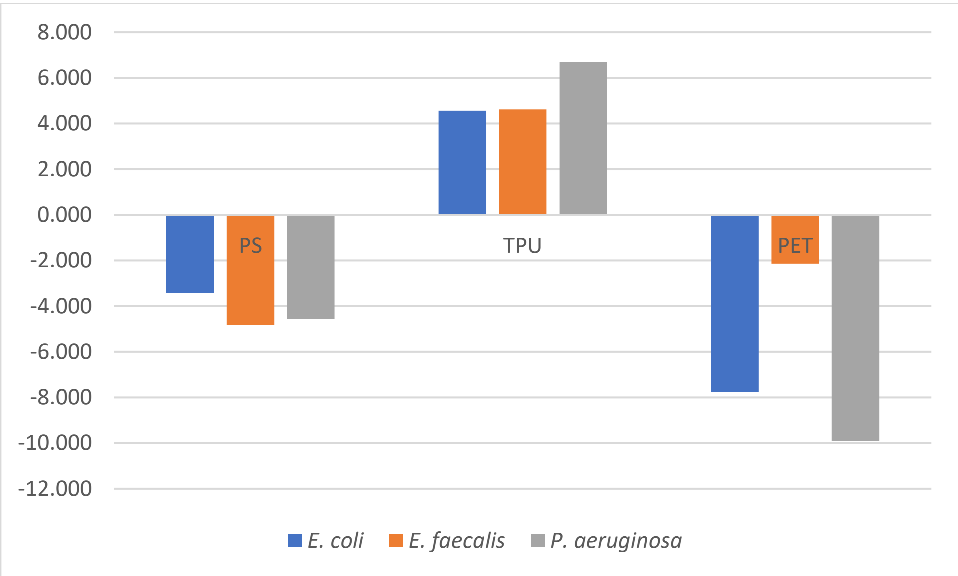

Figure 39 Percentage difference of settling velocities of MPs after biofilm formation with respect to settling velocities of pristine MPs in seawater

Table 11 Mean settling velocities of MPs with and without biofilm formation by different bacteria in different water columns

Settling column	Bacteria specie	Mean settling velocity ± σ (m/s)						
		PE	**HDPE**	**LDPE**	**PP**	**PS**	**TPU**	**PET**
Freshwater ($1.0 \ g/cm^3$)	*E. coli*	Floating	Floating	Floating	Floating	0.3567± 0.0031	1.1875± 0.1317	1.1247± 0.0113
	E. faecalis	Floating	Floating	Floating	Floating	0.3630± 0.0017	1.3081± 0.0253	1.1478± 0.0388
	P. aeruginosa	Floating	Floating	Floating	Floating	0.2901± 0.0866	1.2262± 0.0622	0.9283± 0.1915
	Pristine	Floating	Floating	Floating	Floating	0.3297 ± 0.0068	1.2381± 0.0270	1.1892± 0.0442
Seawater ($1.025 \ g/cm^3$)	*E. coli*	Floating	Floating	Floating	Floating	0.2752± 0.0025	1.2071± 0.0286	1.0107± 0.0600
	E. faecalis	Floating	Floating	Floating	Floating	0.2712± 0.0092	1.2079± 0.0148	1.0724± 0.0929
	P. aeruginosa	Floating	Floating	Floating	Floating	0.2719± 0.0060	1.2318± 0.0187	0.9872± 0.0410
	Pristine	Floating	Floating	Floating	Floating	0.2850± 0.0075	1.1545± 0.0163	1.0958± 0.0259
Wastewater ($1.05 \ g/cm^3$)	Pristine	Floating	Floating	Floating	Floating	0.26275± 0.0077	1.19586± 0.0313	1.10162± 0.0120

CHAPTER 5

CONCLUSIONS

Within the scope of the thesis, time dependent biofilm formation on MPs, HDPE, LDPE, PE, PET, PP, PS and TPU by pure cultures of bacteria was analyzed by *E. coli, E. faecalis, P. aeruginosa.* Biofilm formation was quantified gravimetrically and optically at 24th, 48th and 72th hours. SEM analysis was conducted for pristine MPs and biofilm formed MPs at the end of 72 hour period. The effect of biofilm formed on the settling velocities of MPs in freshwater and seawater was investigated by MATLAB code based on image tracking process. Also, a comparative assessment was done for the validation of the code by comparing the settling velocities obtained by the code with the theoretical settling velocities calculated based on Stoke's law for pristine MPs in freshwater, seawater and wastewater. The major outcomes of the thesis are given as follows,

- Amount of biofilm formed on MPs was changing with MP type, bacteria specie, and incubation period.
- Initially buoyant MPs did not settle down after biofilm formation by *E. coli, E. faecalis, P. aeruginosa* at 37°C in LB broth medium for 72 hours.
- Biofilm formation could either increase or decrease the settling of MPs therefore the hypothesis that biofilm increases the settling is not true.
- MPs are not uniform hence measuring their settling requires a methodology such as visual tracking rather than simply calculating theoretical settling velocity
- To our knowledge, this thesis is the first study to measure biologically weathered MP settling velocity by adopting MATLAB image tracking algorithm.

Limitations

- Due to the experimental convenience in image tracking studies, only primary MPs in the size range 2-3 mm with regular shape were studied in this thesis.
- The effects of the change of biofilms were not estimated in this study such as EPS produced by the strains.
- Settling velocities were measured by releasing only one particle at a time, but in real cases, multiple releases might occur.
- Wastewater medium used in this study does not fully comply with real wastewater.
- Biofilm measurement methods revealed results with high standard deviations, causing uncertainty in the analysis.

Future Recommendations

- Biofilm formation and its effects on MP transport should be studied extensively by experimenting on secondary and/or weathered MPs.
- Settling velocity measurements should be fully automatized by improving colour detection algorithms.
- Biofilm formation on MPs by microbial consortia should be studied to see the synergistic effect of different microbes.
- MP transport should be studied in turbulent flow conditions.
- Settling velocities of MPs should be measured by releasing a group of MPs at the same time, to observe the possible effects caused by agglomeration or repulsion among the particles.

REFERENCES

Andrady, A. L. (2011). Microplastics in the marine environment. *Marine Pollution Bulletin*, *62*(8), 1596–1605. https://doi.org/https://doi.org/10.1016/j.marpolbul.2011.05.030

Andrady, A. L. (2017). The plastic in microplastics: A review. *Marine Pollution Bulletin*, *119*(1), 12–22. https://doi.org/https://doi.org/10.1016/j.marpolbul.2017.01.082

Au, S. Y., Bruce, T. F., Bridges, W. C., & Klaine, S. J. (2015). Responses of Hyalella azteca to acute and chronic microplastic exposures. *Environmental Toxicology and Chemistry*, *34*(11), 2564–2572. https://doi.org/10.1002/etc.3093

Auta, H. S., Emenike, C. U., & Fauziah, S. H. (2017). Distribution and importance of microplastics in the marine environment: A review of the sources, fate, effects, and potential solutions. *Environment International*, *102*, 165–176. https://doi.org/10.1016/j.envint.2017.02.013

Barnes, D. K. A., Galgani, F., Thompson, R. C., & Barlaz, M. (2009). Accumulation and fragmentation of plastic debris in global environments. *Philosophical Transactions of the Royal Society of London. Series B, Biological Sciences*, *364*(1526), 1985–1998. https://doi.org/10.1098/rstb.2008.0205

Benjamin, M. M., & Lawler, D. F. (2013). *Water Quality Engineering: Physical / Chemical Treatment Processes*. John Wiley & Sons, Ltd.

Booth, A. M., Kubowicz, S., Jørgen, CJ Beegle-Krause Tor Nordam, S., Landsem, E., Throne-Holst, M., & Jahren, S. (2017). *Microplastic in global and Norwegian marine environments: Distributions, degradation mechanisms and transport*.

Boucher, J., & Friot, D. (2017). *Global, Primary Microplastics in the Oceans: A Sources, Evaluation of*. https://portals.iucn.org/library/sites/library/files/documents/2017-002-En.pdf

Bratovcic, A. (2019). *Degradation of Micro-and Nano-Plastics by Photocatalytic Methods*. *3*, 1–9. https://doi.org/10.18875/2577-7920.3.304

Carr, S. A., Liu, J., & Tesoro, A. G. (2016). Transport and fate of microplastic particles in wastewater treatment plants. *Water Research*, *91*, 174–182. https://doi.org/https://doi.org/10.1016/j.watres.2016.01.002

Carsten, L., Hansen, S. F., Magnusson, K., Norén, F., Hartmann, N. I. B., Jensen, P. R., Nielsen, T. G., & Brinch, A. (2015). *Microplastics Occurrence, effects and sources of releases to the environment in Denmark*.

Ceccarini, A., Corti, A., Erba, F., Modugno, F., La Nasa, J., Bianchi, S., & Castelvetro, V. (2018). The Hidden Microplastics: New Insights and Figures from the Thorough Separation and Characterization of Microplastics and of Their Degradation Byproducts in Coastal Sediments. *Environmental Science & Technology*, *52*(10), 5634–5643. https://doi.org/10.1021/acs.est.8b01487

Center, E. C. J. R. (2013). *Guidance on Monitoring of Marine Litter in European Seas*.

Chazotte, B. (2008). Labeling the Golgi Apparatus with BODIPY-FL-Ceramide (C5-DMB-ceramide) for Imaging. *CSH Protocols*.

Chubarenko, I., Bagaev, A., Zobkov, M., & Esiukova, E. (2016). On some physical and dynamical properties of microplastic particles in marine environment. *Marine Pollution Bulletin*, *108*(1), 105–112. https://doi.org/https://doi.org/10.1016/j.marpolbul.2016.04.048

Cole, M., Lindeque, P., Fileman, E., Halsband, C., & Galloway, T. S. (2015). The Impact of Polystyrene Microplastics on Feeding, Function and Fecundity in the Marine Copepod Calanus helgolandicus. *Environmental Science & Technology*, *49*(2), 1130–1137. https://doi.org/10.1021/es504525u

Colón-González, M., Méndez-Ortiz, M. M., & Membrillo-Hernández, J. (2004). Anaerobic growth does not support biofilm formation in Escherichia coli K-12. *Research in Microbiology*, *155*(7), 514–521. https://doi.org/10.1016/J.RESMIC.2004.03.004

Conley, K., Clum, A., Deepe, J., Lane, H., & Beckingham, B. (2019). Wastewater treatment plants as a source of microplastics to an urban estuary: Removal efficiencies and loading per capita over one year. *Water Research X*, *3*, 100030. https://doi.org/https://doi.org/10.1016/j.wroa.2019.100030

Da Costa, J. P., Nunes, A. R., Santos, P. S. M., Girão, A. V, Duarte, A. C., & Rocha-Santos, T. (2018). Degradation of polyethylene microplastics in seawater: Insights into the environmental degradation of polymers. *Journal of Environmental Science and Health, Part A*, *53*(9), 866–875. https://doi.org/10.1080/10934529.2018.1455381

De Tender, C. (2017). *Microbial community analysis in soil (rhizosphere) and the marine (plastisphere) environment in function of plant health and biofilm formation*. 254.

Dow. (n.d.). *FUSABOND^{TM} Functional Polymer*. Retrieved July 12, 2019, from https://www.dow.com/en-us/product-search/fusabondfunctionalpolymer

D.S., B. (1997). *Thermoplastics: Directory and Databook*. Chapman & Hall.

Duis, K., & Coors, A. (2016). Microplastics in the aquatic and terrestrial environment: sources (with a specific focus on personal care products), fate and effects. *Environmental Sciences Europe*, *28*(1), 1–25. https://doi.org/10.1186/S12302-015-0069-Y

DuPont. (2013). *DuPont Packaging & Industrial Polymers*. E.I. Du Pont de Nemours and Company, Inc. https://plasticker.de/recybase/docs/943_1393834372.pdf

Essel, R., Engel, L., Carus, M., & Ahrens, R. H. (2015). Sources of microplastics relevant to marine protection in Germany. *Texte*, *64*(2015), 656–660.

ExxonMobil. (2017). *ExxonMobilTM LDPE LD600BA*. https://exxonmobilchemical.ides.com/datasheet.aspx?I=58933&FMT=PDF&CULTURE=en-US&PS=PE&E=243991

Fauziah, S. H., Bhatti, M., Anuar, N., Anuar, N., Mohan, P., & Periathamby, A. (2018). Worldwide distribution and abundance of microplastic: How dire is the situation? *Waste Management & Research*, *36*, 0734242X1878573. https://doi.org/10.1177/0734242X18785730

Flint, S. (2002). Enterococcus Faecalis And Enterococcus Faecium. *Encyclopedia of Dairy Sciences*, 904–907. https://doi.org/10.1016/B0-12-227235-8/00144-9

Fulford, G., Forrester, P., & Jones, A. (1997). *Modelling with Differential and Difference Equations*. Cambridge University Press.

Galgani, F., Hanke, G., Werner, S., L, O., Nilsson, P., Fleet, D., Kinsey, S., RC, T., Van Franeker, J., Vlachogianni, T., Scoullos, M., Mira Veiga, J., Palatinus, A., Matiddi, M., Maes, T., Korpinen, S., A, B., H, L., Gago, J., & Liebezeit, G. (2013). *Guidance on Monitoring of Marine Litter in European Seas*.

GESAMP. (2015). *Sources, Fate and Effects of Microplastics in the Marine Environment: A Global Assessment*.

Gewert, B., Ogonowski, M., Barth, A., & MacLeod, M. (2017). Abundance and composition of near surface microplastics and plastic debris in the Stockholm Archipelago, Baltic Sea. *Marine Pollution Bulletin*, *120*(1), 292–302. https://doi.org/https://doi.org/10.1016/j.marpolbul.2017.04.062

Goral, K. D. (2020). *Physical Modeling Of Solid Spheres' Motion Under Solitary Wave Attack*. Middle East Technical University.

Goral, K. D., Guler, H. G., Baykal, C., & Yalciner, A. C. (2021). An experimental study on the motion of solid spheres under solitary wave attack. *Ocean Engineering*, *240*, 109946. https://doi.org/10.1016/J.OCEANENG.2021.109946

Graca, B., Szewc, K., Zakrzewska, D., Dołęga, A., & Szczerbowska-Boruchowska, M. (2017). Sources and fate of microplastics in marine and beach sediments of the Southern Baltic Sea—a preliminary study. *Environmental Science and Pollution Research*, *24*(8), 7650–7661. https://doi.org/10.1007/s11356-017-8419-5

Gündoğdu, S., Çevik, C., Güzel, E., & Kilercioğlu, S. (2018). Microplastics in municipal wastewater treatment plants in Turkey: a comparison of the influent and secondary effluent concentrations. *Environmental Monitoring and Assessment*, *190*(11). https://doi.org/10.1007/s10661-018-7010-y

Hale, R. (2016). *Technical Review of Microbeads/Microplastics in the Chesapeake Bay*.

Hamidian, A. H., Ozumchelouei, E. J., Feizi, F., Wu, C., Zhang, Y., & Yang, M. (2021). A review on the characteristics of microplastics in wastewater treatment plants: A source for toxic chemicals. *Journal of Cleaner Production*, *295*, 126480. https://doi.org/10.1016/j.jclepro.2021.126480

Harrison, J. P., Hoellein, T. J., Sapp, M., Tagg, A. S., Ju-Nam, Y., & Ojeda, J. J. (2018). *Microplastic-Associated Biofilms: A Comparison of Freshwater and Marine Environments BT - Freshwater Microplastics : Emerging Environmental Contaminants?* (M. Wagner & S. Lambert, Eds.; pp. 181–201). Springer International Publishing. https://doi.org/10.1007/978-3-319-61615-5_9

Hchaichi, I., Bandini, F., Spini, G., Banni, M., Cocconcelli, P. S., & Puglisi, E. (2020). Enterococcus faecalis and Vibrio harveyi colonize low-density polyethylene and biodegradable plastics under marine conditions. *FEMS Microbiology Letters*, *367*, 125. https://doi.org/10.1093/femsle/fnaa125

Hebner, T. S., & Maurer-Jones, M. A. (2020). Characterizing microplastic size and morphology of photodegraded polymers placed in simulated moving water conditions. *Environmental Science: Processes & Impacts*, *22*(2), 398–407. https://doi.org/10.1039/C9EM00475K

Hepsø, M. O. (2018). *Experimental weathering of microplastic under simulated environmental conditions*. Norwegian University of Science and Technology.

Hidalgo-Ruz, V., Gutow, L., Thompson, R. C., & Thiel, M. (2012). Microplastics in the Marine Environment: A Review of the Methods Used for Identification and Quantification. *Environmental Science & Technology*, *46*(6), 3060–3075. https://doi.org/10.1021/es2031505

Hidayaturrahman, H., & Lee, T.-G. (2019). A study on characteristics of microplastic in wastewater of South Korea: Identification, quantification, and fate of microplastics during treatment process. *Marine Pollution Bulletin*, *146*, 696–702. https://doi.org/https://doi.org/10.1016/j.marpolbul.2019.06.071

Horton, A. A., & Dixon, S. J. (2018). Microplastics: An introduction to environmental transport processes. *WIREs Water*, *5*(2), e1268. https://doi.org/10.1002/wat2.1268

Horton, A. A., Dixon, S. J., & Alice Horton, C. A. (2017). *Microplastics: An introduction to environmental transport processes*. https://doi.org/10.1002/wat2.1268

IDES. (2014). *Ramapet® N1*. http://www.eper.it/cgi-bin/file/830_ramapet n1.pdf

Irankhah, S., Abdi Ali, A., Reza Soudi, M., Gharavi, S., & Ayati, B. (2018). Highly efficient phenol degradation in a batch moving bed biofilm reactor: benefiting from biofilm-enhancing bacteria. *World Journal of Microbiology and Biotechnology*, *34*(11), 164. https://doi.org/10.1007/s11274-018-2543-3

ITTC. (2011). ITTC – Recommended Procedures: Fresh Water and Seawater Properties. *International Towing Tank Conference*.

Jiang, C., Yin, L., Wen, X., Du, C., Wu, L., Long, Y., Liu, Y., Ma, Y., Yin, Q., Zhou, Z., & Pan, H. (2018). Microplastics in Sediment and Surface Water of West Dongting Lake and South Dongting Lake: Abundance, Source and Composition. *International Journal of Environmental Research and Public Health*, *15*(10), 2164. https://doi.org/10.3390/ijerph15102164

Kataoka, T., Nihei, Y., Kudou, K., & Hinata, H. (2019). Assessment of the sources and inflow processes of microplastics in the river environments of Japan. *Environmental Pollution*, *244*, 958–965. https://doi.org/https://doi.org/10.1016/j.envpol.2018.10.111

Kesy, K., Oberbeckmann, S., Kreikemeyer, B., & Labrenz, M. (2019). Spatial Environmental Heterogeneity Determines Young Biofilm Assemblages on Microplastics in Baltic Sea Mesocosms. *Frontiers in Microbiology*, *10*, 1665. https://doi.org/10.3389/fmicb.2019.01665

Khatmullina, L., & Isachenko, I. (2017). Settling velocity of microplastic particles of regular shapes. *Marine Pollution Bulletin*, *114*(2), 871–880. https://doi.org/https://doi.org/10.1016/j.marpolbul.2016.11.024

Klein, S., Dimzon, I. K., Eubeler, J., & Knepper, T. P. (2018). Analysis, Occurrence, and Degradation of Microplastics in the Aqueous Environment. In M. Wagner & S. Lambert (Eds.), *Freshwater Microplastics : Emerging Environmental Contaminants?* (pp. 51–67). Springer International Publishing. https://doi.org/10.1007/978-3-319-61615-5_3

Kroukamp, O., Dumitrache, R. G., & Wolfaardt, G. M. (2010). Pronounced Effect of the Nature of the Inoculum on Biofilm Development in Flow Systems. *Applied and*

Environmental Microbiology, *76*(18), 6025–6031. https://doi.org/10.1128/AEM.00070-10

Kubowicz, S., & Booth, A. M. (2017). Biodegradability of Plastics: Challenges and Misconceptions. *Environmental Science and Technology*, *51*(21), 12058–12060. https://doi.org/10.1021/acs.est.7b04051

Labauve, A. E., & Wargo, M. J. (2012). Growth and Laboratory Maintenance of Pseudomonas aeruginosa. *Curr Protoc Microbiol*. https://doi.org/10.1002/9780471729259.mc06e01s25

Lassen;HansenNorwegian, C., Agency, E., , Steffen Foss; Magnusson, Kerstin;Hartmann, N. B. ; R. J., & Pernille; Nielsen, Torkel Gissel; Brinch, A. (2015). *Microplastics Occurrence, effects and sources of releases to the environment in Denmark*.

Leiser, R., Jongsma, R., Bakenhus, I., Möckel, R., Philipp, B., Neu, T. R., & Wendt-Potthoff, K. (2021). Interaction of cyanobacteria with calcium facilitates the sedimentation of microplastics in a eutrophic reservoir. *Water Research*, *189*, 116582. https://doi.org/10.1016/J.WATRES.2020.116582

Liu, F., Nord, N. B., Bester, K., & Vollertsen, J. (2020). Microplastics removal from treated wastewater by a biofilter. *Water (Switzerland)*, *12*(4). https://doi.org/10.3390/W12041085

Long, Z., Pan, Z., Wang, W., Ren, J., Yu, X., Lin, L., Lin, H., Chen, H., & Jin, X. (2019). Microplastic Abundance, Characteristics, and Removal in Wastewater Treatment Plants in a Coastal City of China. *Water Research*, *155*. https://doi.org/10.1016/j.watres.2019.02.028

Lucas, N., Bienaime, C., Belloy, C., Queneudec, M., Silvestre, F., & Nava-Saucedo, J.-E. (2008). Polymer biodegradation: Mechanisms and estimation techniques – A review. *Chemosphere*, *73*(4), 429–442. https://doi.org/https://doi.org/10.1016/j.chemosphere.2008.06.064

lyondellbasell. (2019). *Clyrell RC213M*. https://www.lyondellbasell.com/en/polymers/p/Clyrell-RC213M/331a4307-a5fe-47a9-92f4-9aad8ceace24

Magni, S., Binelli, A., Pittura, L., Avio, C. G., Della Torre, C., Parenti, C. C., Gorbi, S., & Regoli, F. (2019). The fate of microplastics in an Italian Wastewater Treatment Plant. *Science of The Total Environment*, *652*, 602–610. https://doi.org/https://doi.org/10.1016/j.scitotenv.2018.10.269

Magnusson, K., & Norén, F. (2014). Screening of microplastic particles in and down-stream a wastewater treatment plant. *IVL Swedish Environmental Research Institute*, *C 55*(C), 22.

Mahon, A. M., O'Connell, B., Healy, M. G., O'Connor, I., Officer, R., Nash, R., & Morrison, L. (2017). Microplastics in Sewage Sludge: Effects of Treatment. *Environmental Science & Technology*, *51*(2), 810–818. https://doi.org/10.1021/acs.est.6b04048

McGivney, E., Cederholm, L., Barth, A., Hakkarainen, M., Hamacher-Barth, E., Ogonowski, M., & Gorokhova, E. (2020). Rapid Physicochemical Changes in Microplastic Induced by Biofilm Formation. *Frontiers in Bioengineering and Biotechnology*, *8*, 205. https://doi.org/10.3389/fbioe.2020.00205

Murphy, F., Ewins, C., Carbonnier, F., & Quinn, B. (2016a). Wastewater Treatment Works (WwTW) as a Source of Microplastics in the Aquatic Environment. *Environmental Science and Technology*, *50*(11), 5800–5808. https://doi.org/10.1021/acs.est.5b05416

Murphy, F., Ewins, C., Carbonnier, F., & Quinn, B. (2016b). Wastewater Treatment Works (WwTW) as a Source of Microplastics in the Aquatic Environment. *Environmental Science & Technology*, *50*(11), 5800–5808. https://doi.org/10.1021/acs.est.5b05416

Myszka, K., & Czaczyk, K. (2009). Characterization of Adhesive Exopolysaccharide (EPS) Produced by Pseudomonas aeruginosa Under Starvation Conditions. *Current Microbiology*, *58*, 541–546. https://doi.org/10.1007/s00284-009-9365-3

National Institutes of Health. (2019). *Microplastics*. https://toxtown.nlm.nih.gov/sources-of-exposure/microplastics

Nayar, K. G., Sharqawy, M. H., Banchik, L. D., & Lienhard V, J. H. (2016). *Seawater Thermophysical Properties Library*. http://web.mit.edu/seawater/2017_MIT_Seawater_Property_Tables_r2b.pdf

Nielsen, J., Pedersen, N., Peydaei, A., Baudu, E., Gurevich, L., Fojan, P., Wimmer, R., Jonge, N., & Fernando, E. (2019). *Potential for biodegradation of microplastics in thermophilic anaerobic digesters*.

Paço, A., Duarte, K., da Costa, J. P., Santos, P. S. M., Pereira, R., Pereira, M. E., Freitas, A. C., Duarte, A. C., & Rocha-Santos, T. A. P. (2017). Biodegradation of polyethylene microplastics by the marine fungus Zalerion maritimum. *Science of The Total Environment*, *586*, 10–15. https://doi.org/https://doi.org/10.1016/j.scitotenv.2017.02.017

Peixoto, D., Pinheiro, C., Amorim, J., Oliva-Teles, L., Guilhermino, L., & Vieira, M. N. (2019). Microplastic pollution in commercial salt for human consumption: A review. *Estuarine, Coastal and Shelf Science*, *219*, 161–168. https://doi.org/10.1016/J.ECSS.2019.02.018

Peng, G., Xu, P., Zhu, B., Bai, M., & Li, D. (2018). Microplastics in freshwater river sediments in Shanghai, China: A case study of risk assessment in mega-cities. *Environmental Pollution*, *234*, 448–456. https://doi.org/https://doi.org/10.1016/j.envpol.2017.11.034

Percival, S. L., & Williams, D. W. (2014). Escherichia coli. *Microbiology of Waterborne Diseases: Microbiological Aspects and Risks: Second Edition*, 89–117. https://doi.org/10.1016/B978-0-12-415846-7.00006-8

Prata, J. C., da Costa, J. P., Lopes, I., Duarte, A. C., & Rocha-Santos, T. (2020). Environmental exposure to microplastics: An overview on possible human health effects. *Science of the Total Environment, 702*, 134455. https://doi.org/10.1016/j.scitotenv.2019.134455

Ragusa, A., Svelato, A., Santacroce, C., Catalano, P., Notarstefano, V., Carnevali, O., Papa, F., Rongioletti, M. C. A., Baiocco, F., Draghi, S., D'Amore, E., Rinaldo, D., Matta, M., & Giorgini, E. (2021). Plasticenta: First evidence of microplastics in human placenta. *Environment International*, *146*, 106274. https://doi.org/10.1016/j.envint.2020.106274

Rajala, K., Grönfors, O., Hesampour, M., & Mikola, A. (2020). Removal of microplastics from secondary wastewater treatment plant effluent by coagulation/flocculation with iron, aluminum and polyamine-based chemicals. *Water Research*, *183*, 116045. https://doi.org/10.1016/J.WATRES.2020.116045

Ramsperger, A. F. R. M., Stellwag, A. C., Caspari, A., Fery, A., Lueders, T., Kress, H., Löder, M. G. J., & Laforsch, C. (2020). *Structural Diversity in Early-Stage Biofilm Formation on Microplastics Depends on Environmental Medium and Polymer Properties*. https://doi.org/10.3390/w12113216

Rodrigues, D. A., Almeida, M. A., Teixeira, P. A., Oliveira, R. T., & Azeredo, J. C. (2009). Effect of Batch and Fed-Batch Growth Modes on Biofilm Formation by Listeria monocytogenes at Different Temperatures. *Current Microbiology*, *59*(4), 457–462. https://doi.org/10.1007/s00284-009-9460-5

Rodríguez-Chueca, J., Morales, M., Mosteo, R., Ormad, M. P., & Ovelleiro, J. L. (2013). Inactivation of Enterococcus faecalis, Pseudomonas aeruginosa and Escherichia coli present in treated urban wastewater by coagulation-flocculation and photo-Fenton processes. *Cite This: Photochem. Photobiol. Sci*, *12*, 864. https://doi.org/10.1039/c3pp25352j

Roland Essel, Linda Engel, M. C. (2015). *Sources of microplastics relevant to marine protection in Germany*.

Rosato, A., Barone, M., Negroni, A., Brigidi, P., Fava, F., Xu, P., Candela, M., & Zanaroli, G. (2020). Microbial colonization of different microplastic types and biotransformation of sorbed PCBs by a marine anaerobic bacterial community. *Science of The Total Environment*, *705*, 135790. https://doi.org/10.1016/J.SCITOTENV.2019.135790

Rummel, C., Jahnke, A., Gorokhova, E., Kühnel, D., & Schmitt, M. (2017). Impacts of Biofilm Formation on the Fate and Potential Effects of Microplastic in the Aquatic

Environment. *Environmental Science & Technology Letters*, *4*. https://doi.org/10.1021/acs.estlett.7b00164

Sadara. (2019). *High Density Polyethylene*. https://www.sadara.com/ProductsHome/Products/Polyethylene/HDPE?prodfamily=HDPE&Bl=Polyethylene

Sanchez, W., Bender, C., & Porcher, J.-M. (2013). Wild gudgeons (Gobio gobio) from French rivers are contaminated by microplastics: Preliminary study and first evidence. *Environmental Research*, *128*. https://doi.org/10.1016/j.envres.2013.11.004

Sangale, M. K. (2012). A Review on Biodegradation of Polythene: The Microbial Approach. *Journal of Bioremediation and Biodegradation*, *03*(10). https://doi.org/10.4172/2155-6199.1000164

Sekiguchi, T., Saika, A., Nomura, K., Watanabe, T., Watanabe, T., Fujimoto, Y., Enoki, M., Sato, T., Kato, C., & Kanehiro, H. (2011). Biodegradation of aliphatic polyesters soaked in deep seawaters and isolation of poly(ε-caprolactone)-degrading bacteria. *Polymer Degradation and Stability*, *96*(7), 1397–1403. https://doi.org/https://doi.org/10.1016/j.polymdegradstab.2011.03.004

Semcesen, P. O., & Wells, M. G. (2021). Biofilm growth on buoyant microplastics leads to changes in settling rates: Implications for microplastic retention in the Great Lakes. *Marine Pollution Bulletin*, *170*, 112573. https://doi.org/10.1016/J.MARPOLBUL.2021.112573

Setälä, P., Hakala, O., Kautto, P., Lehtiniemi, M., Raitanen, E., Sillanpää, M., Talvitie, J., & Äystö, L. O. (2017). *Microplastics - a growing environmental risk* (p. OP-). Finnish Environment Institute. http://hdl.handle.net/10138/177568

Shafiei, S., Melville, B. W., Shamseldin, A. Y., Beskhyroun, S., Adams, K. N., Professor, A., & Teaching Fellow, P. (2016). Measurements of tsunami-borne debris impact on structures using an embedded accelerometer. *Journal of Hydraulic Research*, *54*(4), 435–449. https://doi.org/10.1080/00221686.2016.1170071

Simon, M., van Alst, N., & Vollertsen, J. (2018). Quantification of microplastic mass and removal rates at wastewater treatment plants applying Focal Plane Array (FPA)-

based Fourier Transform Infrared (FT-IR) imaging. *Water Research*, *142*, 1–9. https://doi.org/10.1016/j.watres.2018.05.019

STAP. (2011). *Marine Debris as a Global Environmental Problem*.

Straub, S., Hirsch, P. E., & Burkhardt-Holm, P. (2017). Biodegradable and Petroleum-Based Microplastics Do Not Differ in Their Ingestion and Excretion but in Their Biological Effects in a Freshwater Invertebrate Gammarus fossarum. *International Journal of Environmental Research and Public Health*, *14*(7), 774. https://doi.org/10.3390/ijerph14070774

Sundt, P. S. P.-E. S. F. (2014). *Sources of microplastic pollution to the marine environment*.

Sun, J., Dai, X., Wang, Q., van Loosdrecht, M. C. M., & Ni, B. J. (2019). Microplastics in wastewater treatment plants: Detection, occurrence and removal. *Water Research*, *152*, 21–37. https://doi.org/10.1016/j.watres.2018.12.050

Talvitie, J., Heinonen, M., Pääkkönen, J. P., Vahtera, E., Mikola, A., Setälä, O., & Vahala, R. (2015). Do wastewater treatment plants act as a potential point source of microplastics? Preliminary study in the coastal Gulf of Finland, Baltic Sea. *Water Science and Technology*, *72*(9), 1495–1504. https://doi.org/10.2166/WST.2015.360

Talvitie, J., Mikola, A., Koistinen, A., & Setälä, O. (2017). Solutions to microplastic pollution – Removal of microplastics from wastewater effluent with advanced wastewater treatment technologies. *Water Research*, *123*, 401–407. https://doi.org/https://doi.org/10.1016/j.watres.2017.07.005

Talvitie, J., Mikola, A., Setälä, O., Heinonen, M., & Koistinen, A. (2017). How well is microlitter purified from wastewater? – A detailed study on the stepwise removal of microlitter in a tertiary level wastewater treatment plant. *Water Research*, *109*, 164–172. https://doi.org/10.1016/j.watres.2016.11.046

Tarafdar, A., Lee, J. U., Jeong, J. E., Lee, H., Jung, Y., Oh, H. bin, Woo, H. Y., & Kwon, J. H. (2021). Biofilm development of Bacillus siamensis ATKU1 on pristine short chain low-density polyethylene: A case study on microbe-microplastics interaction.

Journal of Hazardous Materials, *409*, 124516. https://doi.org/10.1016/J.JHAZMAT.2020.124516

Tchobanoglous, G., Stensel, H. D., Tsuchihashi, R., & Burton, F. (2014). *Wastewater Engineering: Treatment and Source Recovery* (5th ed., Vols. 1 & 2). Mc Graw Hill Education.

ter Halle, A., Ladirat, L., Martignac, M., Mingotaud, A. F., Boyron, O., & Perez, E. (2017). To what extent are microplastics from the open ocean weathered? *Environmental Pollution*, *227*, 167–174. https://doi.org/https://doi.org/10.1016/j.envpol.2017.04.051

Thompson, R. C., Moore, C. J., vom Saal, F. S., & Swan, S. H. (2009). Plastics, the environment and human health: Current consensus and future trends. *Philosophical Transactions of the Royal Society of London. Series B, Biological Sciences*, *364*, 2153–2166. https://doi.org/10.1098/rstb.2009.0053

Tofa, T. S. (2018). *Degradation of Microplastic Residuals in Water by Visible Light Photocatalysis*. KTH ROYAL INSTITUTE OF TECHNOLOGY.

Turner, S., Horton, A. A., Rose, N. L., & Hall, C. (2019). A temporal sediment record of microplastics in an urban lake, London, UK. *Journal of Paleolimnology, 61*(4), 449–462. https://doi.org/10.1007/s10933-019-00071-7

UNEP. (2016). *Marine plastic debris and microplastics – Global lessons and research to inspire action and guide policy change.*

Urbanek, A. K., Rymowicz, W., & Mirończuk, A. M. (2018). Degradation of plastics and plastic-degrading bacteria in cold marine habitats. *Applied Microbiology and Biotechnology*, *102*(18), 7669–7678. https://doi.org/10.1007/s00253-018-9195-y

Urbanek, A. K., Rymowicz, W., Strzelecki, M. C., Kociuba, W., Franczak, Ł., & Mirończuk, A. M. (2017). Isolation and characterization of Arctic microorganisms decomposing bioplastics. *AMB Express*, *7*(1), 148. https://doi.org/10.1186/s13568-017-0448-4

van Cauwenberghe, L., & Janssen, C. R. (2014). Microplastics in bivalves cultured for human consumption. *Environmental Pollution*, *193*, 65–70.

Verla, A. W., Enyoh, C. E., Verla, E. N., & Nwarnorh, K. O. (2019). Microplastic–toxic chemical interaction: a review study on quantified levels, mechanism and implication. *SN Applied Sciences, 1*(11), 1400. https://doi.org/10.1007/s42452-019-1352-0

Wagner, M., & Lambert, S. (2018a). *Freshwater microplastics: emerging environmental contaminants?*

Wagner, M., & Lambert, S. (2018b). *Freshwater Microplastics - The Handbook of Environmental Chemistry 58* (p. 302). https://doi.org/10.1007/978-3-319-61615-5

Wang, Z., Dou, M., Ren, P., Sun, B., Jia, R., & Zhou, Y. (2021). Settling velocity of irregularly shaped microplastics under steady and dynamic flow conditions. *Environ Sci Pollut Res Int., 28*(44). https://doi.org/10.1007/s11356-021-14654-3/Published

Wardrop, D., Bott, C., Criddle, C., Hale, R., McDevitt, J., Morse, M., & Rochman, C. M. (2016). Technical Review of Microbeads / Microplastics in the Chesapeake Bay. *STAC Publication 16-002*, *April*, 1–21.

Weast, R. C. (1972). *Handbook of Chemistry and Physics* (53rd ed.). Chemical Rubber Pub.

Welden, N. A. C., & Cowie, P. R. (2016). Environment and gut morphology influence microplastic retention in langoustine, Nephrops norvegicus. *Environmental Pollution*, *214*, 859–865. https://doi.org/https://doi.org/10.1016/j.envpol.2016.03.067

Wilkes, R. A., & Aristilde, L. (2017). Degradation and metabolism of synthetic plastics and associated products by Pseudomonas sp.: capabilities and challenges. *Journal of Applied Microbiology*, *123*(3), 582–593. https://doi.org/10.1111/jam.13472

Willis, K. A., Eriksen, R., Wilcox, C., & Hardesty, B. D. (2017). Microplastic Distribution at Different Sediment Depths in an Urban Estuary. *Frontiers in Marine Science*, *4*, 419. https://doi.org/10.3389/fmars.2017.00419

Woodall, L. C., Sanchez-Vidal, A., Canals, M., Paterson, G. L. J., Coppock, R., Sleight, V., Calafat, A., Rogers, A. D., Narayanaswamy, B. E., & Thompson, R. C. (2020). The deep sea is a major sink for microplastic debris. *Royal Society Open Science*, *1*(4), 140317. https://doi.org/10.1098/rsos.140317

Wu, W., Jin, Y., Bai, F., & Jin, S. (2015). Pseudomonas aeruginosa. *Molecular Medical Microbiology: Second Edition*, *2–3*, 753–767. https://doi.org/10.1016/B978-0-12-397169-2.00041-X

Zhang, X., Chen, J., & Li, J. (2020). The removal of microplastics in the wastewater treatment process and their potential impact on anaerobic digestion due to pollutants association. *Chemosphere*, *251*, 126360. https://doi.org/https://doi.org/10.1016/j.chemosphere.2020.126360

Zhang, Y., Kang, S., Allen, S., Allen, D., Gao, T., & Sillanpää, M. (2020). Atmospheric microplastics: A review on current status and perspectives. *Earth-Science Reviews*, *203*, 103118. https://doi.org/https://doi.org/10.1016/j.earscirev.2020.103118

Zheng, S., Bawazir, M., Dhall, A., Kim, H.-E., He, L., Heo, J., & Hwang, G. (2021). Implication of Surface Properties, Bacterial Motility, and Hydrodynamic Conditions on Bacterial Surface Sensing and Their Initial Adhesion . In *Frontiers in Bioengineering and Biotechnology* (Vol. 9). https://www.frontiersin.org/article/10.3389/fbioe.2021.643722

Zhu, L., Zhao, S., Bittar, T. B., Stubbins, A., & Li, D. (2020). Photochemical dissolution of buoyant microplastics to dissolved organic carbon: Rates and microbial impacts. *Journal of Hazardous Materials*, *383*, 121065. https://doi.org/https://doi.org/10.1016/j.jhazmat.2019.121065

Ziajahromi, S., Neale, P. A., Rintoul, L., & Leusch, F. D. L. (2017). Wastewater treatment plants as a pathway for microplastics: Development of a new approach to sample wastewater-based microplastics. *Water Research*, *112*, 93–99. https://doi.org/10.1016/J.WATRES.2017.01.042

Zumstein, M. T., Schintlmeister, A., Nelson, T. F., Baumgartner, R., Woebken, D., Wagner, M., Kohler, H.-P. E., McNeill, K., & Sander, M. (2018). Biodegradation of synthetic polymers in soils: Tracking carbon into CO_2 and microbial biomass. *Science Advances*, *4*(7), eaas9024. https://doi.org/10.1126/sciadv.aas9024

APPENDICES

A. CODES USED IN SETTLING VELOCITY ANALYSIS

In this section, MATLAB codes for the settling velocity measurements are presented.

cutCodFun.m (Cuts videos into frames)

```
 function cutCodeFun(videoName,outputFolderName)


startTime=0;
%
%
v=VideoReader(videoName,'CurrentTime',startTime);
fr=v.FrameRate;
i=1;
mkdir(outputFolderName);
for i=1:v.NumFrames
      img=readFrame(v);
      filename=[sprintf('%03d',i) '.png'];
      fullname=fullfile(outputFolderName,filename);
      imwrite(img,fullname);
end
%
end
```

pre_RotDist.m (Calibrates the distance)

```
clear
clc
close all

% This code is written for image processing using "color detection by
hue"
% approach by H. G. Guler.

% Read the image and decide rotation angle (rot) by trial and error.
% If you would like to check distance, you may change dist to 1.


% INPUTS
inputFolderName='images';
imageName='001.png';
rot=0;
dist=1; % 1: distance check, 0: no distance check
%
curDir=pwd;
fullname=fullfile(curDir,inputFolderName,imageName);
simg=imread(fullname);

J = imrotate(simg,rot,'bilinear','crop');
figure(1)
imshow(J);
if dist==1
    imdistline()
end
```

SettlingVidAnlys_v1_Manual.m (Tracks particle position at certain time)

```
clear
clc
close all

% INPUTS

rot=0;                % from pre_rotDist.m
calibRatio=40*0.02/982.62;      % from pre_rotDist.m, cm/numPixels
frameRate=1/30;          % from pre_cutCode.m

startnumber=001; %Starting number of the images
endnumber=150; %Ending number of the images
sampling=10;   %Sampling division

outputPrefix=['repetNum5']; % outputs are written as time vs y
coordinates (meters)


inputFolderName='images';

fontName='Calibri';
```

SettlingVidAnlys_v1_Manual.m (continued)

```
fontSize=22;
fontSize2=20;

% Basics
curDir=pwd;
refHeight=1;      % height of the test setup (m)


% Read Images from /curDir/INPUTFOLDERNAME

j=1;
for i=startnumber:sampling:endnumber

    imagenumber(j)=i;

    if imagenumber(j)<0
        manualoverride=strcat('00',num2str(imagenumber(j)),'.png');
    elseif imagenumber(j)<100 || imagenumber(j)==sampling
        manualoverride=strcat('0',num2str(imagenumber(j)),'.png');
    else
        manualoverride=strcat(num2str(imagenumber(j)),'.png');
    end

    if imagenumber(j)>sampling

    dummy = imread(fullfile(curDir,inputFolderName,manualoverride));
    dummy = imrotate(dummy,rot,'bilinear','crop');
```

```
    imgs{j,1} = dummy;
    time(j,1)=(i-1)*frameRate;

    j=j+1;

    end

end

for i = 1:length(imgs)

    close
    %Sanity check Graph
    figure1=figure('Position', [0, 0, 1080, 1920]);
    %Plots the image
    image( imgs{i,1} );
    xlabel('Pixels','FontSize',fontSize,'FontName',fontName);
    ylabel('Pixels','FontSize',fontSize,'FontName',fontName);
    set(gca,'FontSize',fontSize2);
    set(gca,'FontName',fontName);
    titleName=sprintf('t= %.2f sec',time(i,1));
    title(titleName,'FontSize',fontSize+2,'FontName',fontName);
    fprintf('Image Number= %.0f \n',imagenumber(i));

    datacursormode on
    cursorobj = datacursormode(figure1);

   pause

    % Export cursor to workspace
    pos = getCursorInfo(cursorobj);
    yCenter(i) = pos.Position(1,2);

end

results=[time refHeight-yCenter(:).*calibRatio]
resultsName=sprintf('%s.dat',outputPrefix)
resultsPath=fullfile(curDir,resultsName)
writematrix(results,resultsPath)
```

Settling Analysis.m (Measures settling velocity)

```
clc
clear all
close all

startIndex=1; %Start of trial no
trialno=1; %Number of trials
y_dist=0.; %Cut-off distance for the analysis (m)
framerate=30; %Framerate for velocity and acceleration analysis
confidence=95; %Confidence Band limit for plot
confidence1=1.96; %Confidence Band std multiplier
color=[0.7 0.7 0.7]; %Color of plot
plotsize=[100 100 1000 700]; %Boundaries of the plot

fpassplot=0; %Plot frequency plot (1:on 0:off)
fpass=3;% High pass for eliminating camera oscilations
crt=pwd;
printt=0; %Save the figures to current folder

startws=0.25/0.001; %Settling velocity measurement start point
endws=0.35/0.001; %Settling velocity measurement end point

for i=startIndex:trialno

    trial=num2str(i);

    subdomain=strcat(crt,'\',trial);

    datastr=strcat('repetNum',trial,'.dat');

    cd(subdomain);
    trialdlm=dlmread(datastr); %Specific name of the data file
    time{i}=trialdlm(:,1);
    ydirection{i}=trialdlm(:,2);


end
cd(crt);
%%

for i=startIndex:trialno

    for j=1:length(time{i})

        if j==1
            time{i}(j,1)=0;
        else
            time{i}(j,1)=(j-1)/framerate;
        end

    end

end
```

```
% %% Frequency Analysis
%
% for i=startIndex:trialno
%
% coeff_eta=fft(ydirection{1,i})/length(ydirection{1,i});
% real_coeff=real(coeff_eta);
% imag_coeff=imag(coeff_eta);
% T0_coeff=time{1,i}(end);
% delta_coeff=T0_coeff/(length(coeff_eta)-1);
% fs_coeff=1/delta_coeff;
% f_nyquist=fs_coeff/2;
% df_coeff=1/T0_coeff;
% f_coeff(1)=0;
% for j=1:length(coeff_eta)-1
%
%     f_coeff(j+1)=j/T0_coeff;
% end
%
% j=round(f_nyquist/df_coeff)+1;
%
% for z=round(f_nyquist/df_coeff)+2:length(coeff_eta)
%
%     coeff_eta(z)=conj(coeff_eta(j));
%     j=j-1;
% end
% for j=1:length(coeff_eta)
%
%     c_coeff(j)=(real_coeff(j)^2+imag_coeff(j)^2)^(1/2);
%     amp_coeff(j)=2*c_coeff(j);
%     Sf(j)=1/2*amp_coeff(j)^2/df_coeff;
% end
%     Sf_Total{i}=Sf;
%     f_coeff_Total{i}=f_coeff;
%dummyy=highpass(ydirection{1,i},fpass,framerate,'ImpulseResponse','iir';
%
%    dummyy=ydirection{1,i}-dummyy;
%
%    ydirection{1,i}=dummyy;
% end

%% Velocity Analysis and Graph

for i=startIndex:trialno

    dummyy=[];
```

Settling Analysis.m (continued)

```
 dummyy=ydirection{1,i};
    vlcy=[];

    vlcy(1)=0;

    for j=1:length(dummyy)-1
```

```
        vlcy(j+1,1)=(dummyy(j+1)-dummyy(j))/(1/framerate);

     end

     velocityy{i}=vlcy;

end

ydist=0:0.001:y_dist;

  for i=startIndex:trialno


 velocityyy{i}=-interp1(time{i},velocityy{i},ydist);

  end

 for i=1:length(ydist)

 yvelocityStore{i}(1)=0;

     for j=startIndex:trialno

      yvelocityStore{i}=[yvelocityStore{i};velocityyy{j}(i)];

      end

 yvelocityStore{i}(1)=[];

 mean_vy(i)=mean(yvelocityStore{i});
 std_vy(i)=std(yvelocityStore{i});

 end


for i=startIndex:trialno

  Ws(i)=mean(velocityyy{i}(round(startws):round(endws)));

end

writematrix(Ws','Ws.dat');

%% W_s Plot

figure('rend','painters','pos',plotsize,'DefaultAxesFontSize',15);
figure(1);

for i=startIndex:trialno

   plot(ydist,velocityyy{i},'Color',color);
   hold on

end
```

```
   grid on
   grid minor
   xlabel('{\it y} (m)','FontSize',18,'Fontname','times');
   ylabel('{\it V_y} (m/s)','FontSize',18,'Fontname','times');

f1=plot(ydist,mean_vy(1:length(ydist)),'k',ydist,(mean_vy(1:length(ydist)
)+confidence1*std_vy(1:length(ydist))),'r-
.',ydist,(mean_vy(1:length(ydist))-
confidence1*std_vy(1:length(ydist))),'r-.','LineWidth',2);
   legend(f1,{'Mean',sprintf('Confidence Band ( %g%%
)',confidence)},'FontSize',18,'Fontname','times','Location','southeast');
%%
if fpassplot==1

   figure('rend','painters','pos',plotsize,'DefaultAxesFontSize',15);
   figure(2);

    for i=startIndex:trialno

      plot(f_coeff_Total{i},Sf_Total{i});
      hold on

    end
     title('Varience Density Spectrum');
     xlabel('Frequency (Hz)','FontSize',15);


   ylabel('S_n','FontSize',15);
     grid on
end
%%
if printt==1
    print('-f1','1.emf','-dmeta');
end

meanWs=mean(Ws)
stdWs=std(Ws)

%% Paper_data

data.time=time;
data.ydirection=ydirection;

save('data','data');
```